

**MODELING THE BANK EROSION OF SELECTED REACH OF
JAMUNA RIVER**

MAHMOOD KHAN

Student No: 0412162047P



**Department of Water Resources Engineering
Bangladesh University of Engineering and Technology
Dhaka, Bangladesh
May 2015**

**MODELING THE BANK EROSION OF SELECTED REACH OF
JAMUNA RIVER**

A thesis Submitted to
The Department of Water Resources Engineering
of
Bangladesh University of Engineering and Technology
In partial fulfillment of the requirement
for the degree
of
**MASTER OF SCIENCE IN WATER RESOURCES
ENGINEERING**

by
Mahmood Khan
Student No: 0412162047P

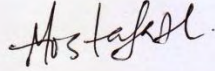


Department of Water Resources Engineering
Bangladesh University of Engineering and Technology
Dhaka, Bangladesh

May 2015

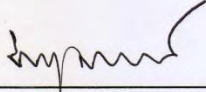
CERTIFICATE OF APPROVAL

The thesis titled “**Modeling the Bank Erosion of Selected Reach of Jamuna River**” submitted by Mahmood Khan, Roll No: 0412162047P, Session: April 2012 has been accepted as satisfactory in partial fulfillment of the requirements for the degree of **Masters of Science In Water Resources Engineering** on 02 May, 2015.



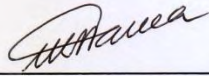
Dr. Mohammad Mostafa Ali
Associate Professor
Department of WRE, BUET, Dhaka
(Supervisor)

Chairman



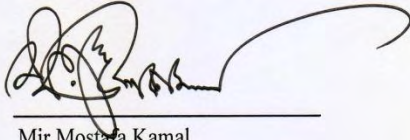
Dr. Md. Sabbir Mostafa Khan
Professor and Head
Department of WRE, BUET, Dhaka

Member
(Ex-Officio)



Dr. Umme Kulsum Navera
Professor
Department of WRE, BUET, Dhaka

Member



Mir Mostafa Kamal
Director,
River Engg. Division, IWM
House # 496, Road # 32
New DOHS, Mohakhali Dhaka-1206.

Member
(External)

May 2015



DECLARATION

It is hereby declared that this thesis work or any part of it has not been submitted elsewhere for the award of any degree or diploma.

mahmood khan

Mahmood Khan

Signature of the Candidate

ACKNOWLEDGEMENT

First of all, the author would like to express his gratefulness to the Almighty ALLAH (SWT), the Creator of universe for His sheer blessings.

The author acknowledges his deepest gratitude to his supervisor Dr. Mohammad Mostafa Ali, Associate Professor, Department of Water Resources Engineering, BUET for providing an interesting idea for the thesis and encouraging to work with it. His cordial supervision, valuable suggestions and in-depth expertise contributed greatly to this thesis.

The author is also grateful to Dr. Md. Sabbir Mostafa Khan, Professor and Head, Department of Water Resources Engineering, BUET, Dr. Umme Kulsum Navera, Professor, Department of Water Resources Engineering, BUET and Mr. Mir Mostafa Kamal, P.Eng, Director, River Engineering Division, IWM, who are the members of the board of Examiners.

The author would like to thank his parents for their encouragement and inspiration. The author is grateful for their guidance and blessings.

The author would like to express his sincere gratitude and appreciation to all of his colleagues and friends for their help, support and inspiration.

Author is in debt to Institute of Water Modelling (IWM), for providing necessary data, information and modelling tools to carry out this research work.

ABSTRACT

Stream being a dynamic system changes its course to attain stability. In this continuous process of attainment of stability planform, morphology and other features of streams change to cope with it. In some reaches the changes are insignificant over a short period of time while in some reaches changes are so dramatic to bring about avulsion. The effects of such changes are eventually noticed in planform and the most common outcome of such adaptation is bank erosion. In this study, an attempt has been made to analyze the bank erosion of a selected reach of the Jamuna River by preparing a morphological model of this river. The selected reach covers about 160km reach of Jamuna River, from downstream of Teesta offtake to Sirajganj.

In this study five vulnerable reaches along five districts (Gaibandha, Bogra, Sirajganj, Jamalpur and Tangail) were identified for incorporating bank protection structures. Revetment was introduced in the model along those vulnerable reaches to evaluate the feasibility of revetments as bank protection measures. Having selected the five reaches to carry out the study the model has been simulated through two flood events; flood events with return period 2.33-year (2005 flood year) and 100-year (1998 flood year). Response of Jamuna River in the vicinity of proposed revetments with respect to these flood events have been evaluated and compared with that from the model of the base condition. Impact assessment of these flood events have been carried out in terms of near bank velocity, bed level changes and bank erosion.

In general near bank velocity reduces after the introduction of revetments along the erosion prone reaches. Oblique flow was noticed in some of the erosion prone reaches rendering the reaches more susceptible to bank erosion. The proposed structure-induced bed scour may vary from 0.8m to 10 m. In general, revetment type of bank protection works executes satisfactory performance to restrain the possible bank erosion along the selected reach of Jamuna River. Based on the results of the two-dimensional morpho-dynamic model MIKE21C, the river bank protection work structures proposed in this study do not cause significant changes in the short term (one flood season) hydro-morphology of the Jamuna River. Besides a correlation between average discharge prevailing during monsoon and shear stress applied by the erosive action of flow, was established. The correlation accounts for hydraulic erosion only, i.e. erosion due to geotechnical failures or other

reasons cannot be estimated by this correlation. The correlation was later used to estimate the extent of erosion of the respective reaches for another hydrologic event (2013), which was found to be satisfactory for four out of five reaches.

Table of Contents

Contents	Page no.
DECLARATION	Error! Bookmark not defined.
ACKNOWLEDGEMENT	vi
ABSTRACT	vii
LIST OF TABLES	xiii
List of Figures	xiv
CHAPTER 1	1
INTRODUCTION	1
1.1 General	1
1.2 Background of the Study	1
1.3 Objectives of the Study	3
1.4 Structure of the Thesis	3
CHAPTER 2	5
LITERATURE REVIEW AND STUDY AREA	5
2.1 General	5
2.2 Studies on Mechanics of Bank Erosion	5
2.3 Studies on Causes of Bank Erosion	6
2.4 Previous Studies on Bank Erosion Processes	6
2.5 Laboratory experiments regarding bank erosion	7
2.6 Application of Numerical Model in Bank Erosion Study	8
2.7 Bank Erosion in context of Bangladesh	10
2.8 Study Area	12
2.8.1 Jamuna River System	13
2.8.2 Catchment Characteristics	13
2.8.4 Topography of Catchment Area	15
2.8.5 Sediment Characteristics	17
2.8.6 Hydraulic Characteristics of Jamuna	17
2.8.7 Bank Erosion of Jamuna River	18
2.8.8 Major River Training Works along Jamuna River	19
Chapter 3	21
THEORY AND METHODOLOGY	21
3.1 General	21

3.2	Mechanics of River Banks	21
3.2.1	Bank Erosion	21
3.2.2	Weakening of Resistance to Erosion	21
3.2.3	Bank Stability with respect to Mass Failure	22
3.2.4	Basal End-point Control	22
3.2.5	Vegetation Effects	22
3.2.6	Bank Advance	23
3.3	River Bank Erosion Processes	23
3.3.1	Process of Bank Toe Erosion	23
3.3.2	Process of River Bank Failure	24
3.4	River Bank Protection Measures	28
3.5	Morphological Variables	28
3.5.1	Independent Variables	29
3.5.2	Dependent Variables	30
3.6	Sediment Transport in Rivers and Channels	31
3.6.1	Sediment Transport	32
3.6.2	Sediment Loads	32
3.7	Sediment Transport Equations	33
3.7.1	Engelund Hansen Equation (1967)	34
3.7.2	Van Rijn's Equation (1984)	34
3.8	Mathematical Modeling	35
3.9	MIKE 21C	36
3.9.1	Governing Flow Equation of MIKE 21C	37
3.9.2	Morphological Model of MIKE 21C	38
3.9.3	Bank Erosion Model of MIKE 21C	38
3.10	Methodology	39
3.10.1	Collection of Data	39
3.10.2	Hydrological and Morphological Analysis of Collected Data	39
3.10.3	2-D morphological Model Set-up for the Study Area	40
3.10.4	Selection of Different Flood Events by Frequency Analysis	41
3.10.5	Identification of Vulnerable Reaches for introducing bank protection measures	41
	CHAPTER 4	42
	DATA ANALYSIS & MODEL DEVELOPMENT	42
4.1	General	42

4.2	Data Collection	42
4.2.1	Water Level	42
4.2.2	Discharge	43
4.2.3	Bathymetry Data	44
4.2.4	Satellite Image	46
4.2.5	Bankline Data	46
4.2.6	Sediment Data	46
4.3	Data Analysis	46
4.3.1	Hydrological Analysis	46
4.3.1.5	Determination of Flood Event for Bankfull Discharge Event	53
4.4	Morphological Analysis	54
4.5	Model Development for the Study Area	58
4.5.1	Model Setup	58
4.5.2	Generation of Computational Grid	58
4.5.3	Generation of Model Bathymetry	60
4.5.4	Model Calibration	61
4.5.5	Model Validation	64
4.5.6	Calibration of Bank Erosion	66
4.5.7	Selection of Erosion Prone Reaches for Bank Protection	69
	CHAPTER 5	70
	RESULTS AND DISCUSSIONS	70
5.1	General	70
5.2	Results and Discussions	70
5.2.1	Near Bank Velocity	70
5.2.2	Changes in Bed Level for proposed revetments	74
5.2.3	Bank Erosion	78
5.3	Correlation between Average discharge and flow induced shear stress	86
5.4	Summary	91
	CHAPTER 6	92
	CONCLUSIONS AND RECOMMENDATIONS OF THE STUDY	92
6.1	General	92
6.2	Conclusions of the Study	92
6.3	Recommendations of the Study	93
	References	94

LIST OF TABLES

Table	Title	Page no.
Table 2.1	Summary of hydraulic characteristics of the Jamuna River (Source: IWM, 2012)	18
Table 4.1	Available water level data for the study area	43
Table 4.2	Available Discharge Data for the Study Area	46
Table 4.3	Available Sediment Data for the Study Area	46
Table 4.4	Yearly maximum Discharge of Jamuna River from 1956-2012	49
Table 4.5	Peak flows of Jamuna River at Bahadurabad for selected return periods using different distribution	50
Table 4.6	Goodness of fit test among three distributions	51
Table 4.7	Peak flow according to Log Normal three parameters distribution	52
Table 4.8	Comparison of different bankfull discharge predictors	53
Table 4.9	List of images	55
Table 4.10	Summary of the parameters used for the model domain	62
Table 5.1	Summary results for different reaches	91

List of Figures

Figure	Title	Page no.
Figure 2.1	River Systems of Bangladesh (source: IWM)	11.
Figure 2.2	Extent of the Study Area	14
Figure 2.3	Catchment of GBM Basin (Source: CEGIS, 2007)	15
Figure 2.4	Brahmaputra-Jamuna River System within Bangladesh Territory (Source: IWM, 2012)	16
Figure 3.1	Continuous and abrupt bank retreat processes	24
Figure 3.2	Different types of the riverbank failure in cohesive and composite soils (Thorne et al., 1981)	26
Figure 3.3	Schematic illustration of modes of cantilever failure (Thorne and Tovey, 1981). Top: shear failure; middle :beam failure and bottom: tensile failures	27
Figure 3.4	Postulated bank erosion process in dense non-cohesive soils in respect to dynamics of the flow regime	29
Figure 3.5	Flow Chart of methodology applied in this study	40
Figure 4.1	Location of discharge and water level station within the study area	44
Figure 4.2	Transect line of bathymetric survey for the study area in Jamuna River	45
Figure 4.3	Available Sediment Data for the Study Area	46
Figure 4.4	Maximum, minimum and average water level at Bahadurabad station of Jamuna River	47
Figure 4.5	Maximum, minimum and average water level at Aricha station of Jamuna River	48
Figure 4.6	Yearly Maximum discharges at Bahadurabad station of Jamuna River	49
Figure 4.7	Gumbel Distribution	50
Figure 4.8	Log-Pearson Distribution	51
Figure 4.9	Log-Normal Distribution	51

Figure 4.10	Sediment rating curve of Jamuna River at Bahadurabad station during 1968-2002	54
Figure 4.11	Delineated bank lines of Jamuna River for several years	57
Figure 4.12	Computational grid cells in the study area	59
Figure 4.13	Model bathymetry of the study area for post-monsoon 2011	60
Figure 4.14	Boundary conditions for the year 2012	61
Figure 4.15	Water Level Calibration at Sirajganj Station for the year 2012	63
Figure 4.16	Sediment transport rate Calibration at Sirajganj Station for the year 2012	64
Figure 4.17	Boundary Conditions used in the model for the year 2013	65
Figure 4.18	Comparison of Observed and Model simulated water level for 2013	66
Figure 4.19	Comparison of Sediment transport rate at Sirajganj Station for the year 2013	67
Figure 4.20	Comparison of model simulated and digitized banklines for 2012 at Gaibandha, Jamalpur and Bogra	68
Figure 4.21	Comparison of model simulated and digitized banklines for 2012 at Bogra, Sirajganj and Tangail	69
Figure 4.22	Selected Erosion prone reaches for introducing bank protection	72
Figure 5.1	Simulated velocity contour of the Jamuna during peak of the monsoon near Reach-1 under base condition for average flood event (2005)	72
Figure 5.2	Simulated velocity contour of the Jamuna during peak of the monsoon near Reach-1 with proposed revetment for average flood event (2005)	73
Figure 5.3	Simulated velocity contour of the Jamuna during peak of the monsoon near Reach-1 under base condition for 100 year flood event (1998)	73

Figure 5.4	Simulated velocity contour of the Jamuna during peak of the monsoon near Reach-1 with proposed revetment for 100 year flood event (1998)	74
Figure 5.5	Simulated bathymetry under base condition at Reach-1 at the end of monsoon for average flood event (2005)	74
Figure 5.6	Simulated bathymetry with proposed revetment at Reach-1 at the end of monsoon for average flood event (2005)	76
Figure 5.7	Simulated bathymetry with proposed revetment near Reach-1 at the end of monsoon for 100 year flood event (1998)	76
Figure 5.8	Simulated bathymetry with proposed revetment near Reach-1 at the end of monsoon for 100 year flood event (1998)	77
Figure 5.9	Model generated accumulated bank erosion along the right bank of the Jamuna in the vicinity of Reach-1 for average flood event (2005)	77
Figure 5.10	Model generated accumulated bank erosion along the right bank of the Jamuna in the vicinity of Reach-1 for extreme flood event (1998)	78
Figure 5.11	Model generated accumulated bank erosion along the right bank of the Jamuna in the vicinity of Reach-2 for bankfull event (2011)	79
Figure 5.12	Model generated accumulated bank erosion along the right bank of the Jamuna in the vicinity of Reach-2 for average flood event (2005)	79
Figure 5.13	Model generated accumulated bank erosion along the right bank of the Jamuna in the vicinity of Reach-2 for extreme flood event (1998)	80
Figure 5.14	Model generated accumulated bank erosion along the right bank of the Jamuna in the vicinity of Reach-3 for bankfull event (2011)	80
Figure 5.15	Model generated accumulated bank erosion along the right bank of the Jamuna in the vicinity of Reach-3 for average flood event (2005)	81
Figure 5.16	Model generated accumulated bank erosion along the right bank of the Jamuna in the vicinity of Reach-3 for extreme flood event (1998)	81

Figure 5.17	Model generated accumulated bank erosion along the right bank of the Jamuna in the vicinity of Reach-3 for bankfull event (2011)	82
Figure 5.18	Model generated accumulated bank erosion along the right bank of the Jamuna in the vicinity of Reach-4 for average flood event (2005)	82
Figure 5.19	Model generated accumulated bank erosion along the right bank of the Jamuna in the vicinity of Reach-4 for extreme flood event (1998)	83
Figure 5.20	Model generated accumulated bank erosion along the right bank of the Jamuna in the vicinity of Reach-4 for bankfull event (2011)	83
Figure 5.21	Model generated accumulated bank erosion along the right bank of the Jamuna in the vicinity of Reach-5 for average flood event (2005)	84
Figure 5.22	Model generated accumulated bank erosion along the right bank of the Jamuna in the vicinity of Reach-5 for extreme flood event (1998)	84
Figure 5.23	Model generated accumulated bank erosion along the right bank of the Jamuna in the vicinity of Reach-4 for bankfull event (2011)	85
Figure 5.24	Correlation between τ_a and average discharge at Gaibandha (Reach-1)	87
Figure 5.25	Correlation between τ_a and average discharge at Bogra (Reach-2)	87
Figure 5.26	Correlation between τ_a and average discharge at Sirajganj (Reach-3)	88
Figure 5.27	Correlation between τ_a and average discharge Jamalpur (Reach-4)	88
Figure 5.28	Correlation between τ_a and average discharge Tangail (Reach-5)	89
Figure 5.29	Correlation between τ_a and average discharge Tangail (Reach-5)	89
Figure 5.30	Comparison of predicted and observed bank erosion rates at the selected reaches	90

CHAPTER 1

INTRODUCTION

1.1 General

Stream being a dynamic system changes its course to attain stability. In this continuous process of attainment of stability planform, morphology and other features of streams change to cope with it. In some reaches of streams the changes are insignificant over a short period of time while in some reaches changes are so dramatic to bring about avulsion. The effects of such changes are eventually noticed in planform and the most common outcome of such adaptation is bank erosion. Excessive erosion causes problems like desertification, decline in productivity, sedimentation in waterways and ecological collapse due to loss of nutrient rich upper soil layers. These adverse influences of stream bank erosion led it to be the need of the time to study on mechanism of bank erosion, bank protective measures, hazards of bank erosion etc in the field of water resources engineering. Two dimensional morphological numerical model is a well-established modern tool to understand the physical processes underlying the bank erosion phenomena and to predict its probable extents and impacts. This study will lead to a profound insight to the bank erosion scenario of the selected reach of Jamuna River, a morphologically highly active river in Bangladesh.

1.2 Background of the Study

Riverbank erosion is a recurrent and highly unpredictable phenomenon prevailing all over the world. Missouri River and Mississippi River in America, Gordon River in Australia, Danube River in Europe, Nile River in Africa, Mekong River in Asia have several erosion prone reaches offering a great challenge to the water resources engineers and planners. Bangladesh is no exception to this.

The major river systems of Bangladesh are morphologically extremely dynamic resulting in continuous erosion and accretion processes. Consequently river bank erosion has become a common phenomenon along with the major and minor rivers of Bangladesh. About 5% of the total flood plain of the country is affected by bank erosion while 94

upazillas out of 489 upazillas experience this calamity each year [BWDB, 2004]. But the scale and frequency of erosion varies from river to river due to characteristics of bank materials, water level variation, planform, near bank flow velocities and supply of water and sediment into the river [FAP 24]. The bank erosion process along the Ganges is controlled mainly by its wandering planform characteristics. In the braiding reaches, the river can erode along both banks, as can be seen in the reaches downstream of the Hardinge Bridge [CEGIS, 2010]. Maximum bank erosion, however, occurs in the meandering reaches, where the outer bend can still migrate laterally within the corridor. In the period 1984-93, the maximum observed rate was 665 m/year. Along the right and left bank of the Ganges, erosion rates are 56m and 20m per year respectively [CEGIS, 2007]. Bank erosion in the Padma River is governed by the planform characteristics of a wandering river. The braided reach of the river is eroding along both banks, while the meandering reaches erode only at the outer banks. The average width of the river varied from 5.7 km in 1984 to 7.1 km in 1993, corresponding to a widening rate of 159 m/year; left and right bank erosion rates were 121 m and 38m per year respectively. Rajbari, Faridpur, Manikganj, Dhaka, Munshiganj, Shariatpur districts along the Padma River are prone to bank erosion. Average bank erosion rates along the right and left banks of the Upper Meghna River were found to be 9m and 7m per year respectively. The Lower Meghna experiences prominent erosion at downstream reaches of Chandpur. During 1984 – 1993 the scenario was the worst with erosion rate as high as 824 m/year [CEGIS 2010]. The other major river Jamuna is also characterized by substantial bank erosion during or soon after flood.

Most of the stretches of Jamuna River have been suffering from bank erosion. According to Coleman two types of bank erosion generally occur in the Jamuna River, liquefaction of flowage of material and shearing away of bank materials [FAP-24]. The most common process of bank failure in the Jamuna River is due to shearing, caused by flow attacking the bank or over-steepening the bank by a thalweg approaching the bank. Besides, the unconsolidated bank materials of Jamuna River have accelerated its susceptibility to erosion. The rate of erosion varies from several tens of meters to kilometers per year. From year to year the amount of erosion varies within a range of several thousand hectares. The maximum lateral extent of erosion can be as high as 2,000 m/year [CEGIS, 2007]. On one occasion along the left bank near Daulatpur at 15km upstream of Aricha, the lateral extent was more than 2,000 m/y for the two years, 1987-1989. There were a

number of locations where the lateral extent of erosion was between 1500 to 2000 m/yr. The rate of erosion is about 40 to 50% higher along the left bank than that of the right bank [Naznin, 2010]. The rate of erosion along the left bank is much more sensitive to the annual maximum discharge than that along the right bank. The rate of erosion along different reaches of the right bank is sensitive to the presence of perennial (main) flanking channels. But the rate of erosion along the left bank is not sensitive to the presence of such flanking channels [CEGIS 2007].

In the field of water resources engineering, mathematical modeling is an established widely used tool that represents the physical scenario by means of mathematical equations and predicts future behavior based on it. In this study a two dimensional morphological model MIKE 21C has been used to understand the bank erosion process of Jamuna River.

1.3 Objectives of the Study

The main objective of the study is to understand the bank erosion process of Jamuna River. Following are the specific objectives:

1. To analyze the planform changes of Jamuna River using satellite images in order to assess erosion prone reaches.
2. To develop a two-dimensional morphological model for the selected reaches of Jamuna River using MIKE 21C.
3. To simulate bank erosion process and compare results with satellite images.
4. To study bank erosion process under different hydrologic conditions.

1.4 Structure of the Thesis

The thesis has been organized under seven chapters which are described as below:

- | | |
|-----------|---|
| Chapter 1 | describes background and objectives of the study |
| Chapter 2 | reveals previous studies related to this study and the study area |
| Chapter 3 | describes the theories regarding the thesis work and a brief description of the methodology |

- Chapter 4 shows relevant analyses of collected data and development of 2D morphological model using MIKE 21C
- Chapter 5 demonstrates the results in terms of bed level, velocity and bank erosion for different simulations
- Chapter 6 shows conclusions drawn from this study and recommendations for further study

CHAPTER 2

LITERATURE REVIEW AND STUDY AREA

2.1 General

To meet the challenges offered by bank erosion several studies have been done on this topic all over the world. Besides many laboratory experiments, numerical modeling have been carried out to study mechanisms and impacts of bank erosion. In Bangladesh quite a good number of studies have already been conducted on planform changes, hydrodynamics and morphology, hydrology, bank erosion etc. Most of the studies were carried out on the major rivers like Ganges, Padma, Meghna and Jamuna. Jamuna River with its dynamic nature has addressed the cream attention of the researchers, government and associated organizations. Literatures available on bank protection or erosion mitigation measures have also been reviewed. The gist of the relevant studies in connection with the present study will be discussed in the following articles.

2.2 Studies on Mechanics of Bank Erosion

Fischenich (1989) reported that fluvial erosion generally occurs in one of the three ways: hydraulic forces remove erodible bed or bank material, geotechnical instabilities or a combination of the two forces. Bank erosion occurs when flowing water exerts a tractive force that exceeds for the particular stream bank material. Hydraulic force is generally characterized by a lack of vegetation, high boundary velocities and no mass soil wasting at the toe of the slope. Geotechnical failures that are unrelated to hydraulic failures are usually a result of bank moisture problems. Moisture can affect the ability of bank materials to withstand stresses. Failures are often the result of shear strength of bank materials being exceeded. Characteristics of geotechnical failure may vary but mass wasting of soil at the toe of the bank is often one indicator. Another common cause of failure is the combination of hydraulic and geotechnical forces. For example bed degradation due to over-steepening of banks which can result in a geotechnical failure of mass wasting. Erosion due to hydraulic forces is usually related to flow velocities and its direction. Human actions are often responsible. Any unusual destruction of bank vegetation promotes hydraulic failures.

2.3 Studies on Causes of Bank Erosion

Leopold (1994) stated three causes of bank erosion which include shear caused by high velocity flow against banks, seepage forces and frost action. He stated that the most common cause of bank erosion is shear stress on stream bank by fast moving water during peak flows. However in many rivers shear stress is not important as an erosion mechanism since bank materials are softened, granulated, crumbled or slumped due to seepage action or frost. The loose materials become a pile of debris ready to be moved downstream during the next high flow. After a flood peak has passed water drains through the soil to the stream bank, causing slumping or other erosion. If it is during the winter, flow from the floodplain to the stream bank is slow and provides a source of water to any ice crystals growing on the bank surface. As an ice crystal grows a granule of bank material can be held at its tip. When the ice crystal melts the granular material falls to the base of the bank and thus gets ready to be washed during the next high flow.

2.4 Previous Studies on Bank Erosion Processes

Mossleman E. (1989) carried out a study to analyze bank erosion process. They analyzed a real case study of an actively retreating bank of Cecina River in Italy. On the basis of field activity data and numerical modeling they revealed that bank erosion is the result of interaction of several factors such as rainfall infiltration, vertical geotechnical characteristics, groundwater hydrodynamics, river hydrodynamics and morphodynamics, mass wasting, weathering-weakening and seepage. From information collected by monitoring activity and numerical simulation it was showed that in case of alternate lateral bar channels, higher shear stresses at the bank toe are experienced mainly at the beginning and at the end of flow events, when discharges are low and flows are mainly concentrated at low water bed. This could explain interactions with mass failure processes and timing of bank collapse.

Lawler K. et al. (1997) conducted a study on bank erosion events and processes in the Upper Severn Basin to examine river bank retreat rates, individual erosion events and processes that drive them. Traditional erosion network pins were used to deliver information on patterns of downstream change in erosion rates. In addition novel Photo-Electric Erosion Pin (PEEP) monitoring system was deployed to generate near continuous data on the temporal distribution of bank erosion and accretion. Erosion dynamics data

were combined with detailed information on bank material properties and spatial change in channel hydraulics derived from direct field survey, to assess the relationship between flow properties and bank erosion rates. Results show that bank erosion rates generally increase downstream, but relate more strongly to discharge than to reach mean shear stress, which peaks near the basin head. Downstream changes in erosion mechanisms and boundary materials are especially significant. Examples of sequences of bank erosion events show how the PEEP system can (a) quantify the impact of individual, rather than aggregated, forcing events (b) reveal the full complexity of bank response to given driving agents, including delayed erosion events and (c) establish hypotheses of process control in bank erosion systems. These findings have important implications for the way in which bank erosion problems are researched and managed. The complex responses demonstrated have special significance for the way in which bank erosion processes and channel-margin sediment injections should be handled in river dynamics model.

2.5 Laboratory experiments regarding bank erosion

University of Minnesota (1991) carried out theoretical and experimental studies on bank erosion. Emphasis was placed on a physically based model of bank erosion into which various kinds of bank protection measures can be imbedded. The experiment consisted of two parts. The first one was devoted to an experimental study of the problem. The process of bank erosion of coarse material was studied. The channel was allowed to erode until an equilibrium state was attained. It was shown that sufficient density of distributed drag elements can substantially slow or stop the bank erosion. When fine, suspendable material was added to the water, this material tended to settle out preferentially in the near bank field of retarded velocity due to distributed drag. As a result, not only could bank erosion be prevented, but eroded banks could be reconstructed by means of deposition from suspension. The second part of the study was devoted to a theoretical and numerical model of bank erosion and its prevention, in parallel with the experiments. The Finite Element Method was used to model the flow and sediment transport field, as well as describe the time evolution of the channel.

Throne C. (1991) conducted a study on bank retreat that usually occurs as a combination of fluvial attack of intact bank material plus mass failure under gravity, followed by basal clean out of failed material. This research illustrated how geomorphic controls triggered by erosion resistant materials in the flood plain sediments encountered at the outer bank

of a meander can alter the rate, direction and pattern of planform development of whole reaches of the river. The findings have important implications for the prediction of river response to changes in regime. The morphology of the channel has been shown to be function of the boundary materials present in the bank materials as well as of the gross basin parameters which determine the topography and the hydrological and sedimentary inputs to the river.

2.6 Application of Numerical Model in Bank Erosion Study

Mosselman (1998) included a bank erosion mechanism and provisions to account for the associated planform changes and input of bank erosion products in a two-dimensional, depth-averaged model of river morphology. The model is applied to a reach of the meandering gravel-bed River Ohrře (Eger) in the former state of Czechoslovakia. The agreement with observations is poor, but this can be ascribed to shortcomings in the flow and bed topography sub models rather than to shortcomings in the bank erosion sub model. Better results are expected when a three- dimensional flow model, equations for sediment mixtures and a bank accretion mechanism are included. This inclusion will have to be preceded by fundamental research on bank accretion mechanisms and on hiding and exposure effects in the relationship for the influence of gravity pull on sediment transport direction.

Bahar et al. (2002) experimented on two types of eroded bank; near-water-surface and under-water-surface for the Yoshino River. Flow field of the near-water-surface eroded bank was examined through physical bank model experiment and numerical analysis. In this paper, the flow fields near and inside of the both eroded banks were investigated. They showed that the flow properties of the near-water-surface and under-water-surface eroded bank shapes were different, which signified two different erosion mechanism of the bank shapes. The numerical model, which was used to simulate near-water-surface eroded bank flow fields, could not reproduce the flow field of under-water-surface eroded bank because of its confined flow inside the eroded bank. A 2D numerical model was developed incorporating SIMPLE method for the under-water-surface eroded bank. This model could reproduce the flow fields of successive model eroded banks of near-water-surface and under-water-surface for two different erosion stages.

Fathi et al (2012) conducted study on river channel change simulation of Khoske Rud Farsan River and bank erosion process using a numerical depth-averaged model, CCHE-

2D. They revealed that Numerical models can be applied to simulate bank erosion by computing all the involved, physical processes, such as main and secondary flow, sediment transport processes and mass failure. The capabilities for simulating the secondary flow effects on suspended sediment and bed load sediment transport have been developed and implemented to the CCHE2D model. The bank surface erosion and mass failure mechanisms have been also developed with the eroded bank materials being transported as bed load. The mesh stretching technique was used to dynamically vary the mesh and handle the moving boundary (banks) problem. Several sets of experimental data were used to validate the developed sediment transport capabilities in curve channels with good agreements. Bank erosion capabilities were tested using a field case of Khoshke Rudd River, Iran. Calculated channel bed change in the period of 2004-2010 was compared with the measured data with reasonable agreement. The computed bank erosion in one reach of the river is also compared with the bank erosion estimated using the difference of 2004 and 2010 DEM data.

Hiroshi and Fujita (2012) applied numerical approach on Khushiro River in Japan to study the bank erosion process of rivers in wetland. In this study, mathematical model of bank erosion process for banks with both the cohesive and non-cohesive layers is developed. Furthermore, the model is installed into the horizontal two dimensional channel deformation models. The governing equations of the channel deformation model are written in boundary fitted moving general coordinate system. Hence, the shape of numerical grids is changed with bank erosion. The results indicate that the horizontal shift speed of banks changes with time very much. When the bottom layer with non-cohesive material is not exposed to the flow, the speed of bank erosion is very slow. However, when bed near the bank is eroded with time and bottom non-cohesive layer starts to be exposed to flow, the bank erosion rate increases rapidly. The calculated horizontal shape of bank lines is not so smooth and local curvature of bank lines becomes small, when bank is composed of both cohesive and non-cohesive materials. We can also observe a lot of vegetation on banks in wetlands. Those roots suppress the bank erosion velocity and work like cohesive sediment in the model. These results indicate that meandering rivers which have high sinuosity are easy to be formed in wetlands and it is difficult to observe braided channels in wetlands.

Eric (2011) studied bank erosion in alluvial rivers with non-cohesive soil in case of unsteady flow. So far the theory of bank failure in non-cohesive soils is limited to the

avalanche of loose, not compacted, fully saturated discrete grains, applicable mainly to gravel banks. However, the field investigation under this study indicated that undercutting of the riverbank, slip failure of the submerged zone of the bank, as well as cantilever failure of the overhang are the dominant processes in non-cohesive dense (sandy) soils under unsteady flow conditions. These processes have been modeled in the present work by an innovative method, which has been validated by field measurements. The results showed that the method enhanced the simulation accuracy up to six times in comparison to the earlier methods.

Jagers (2003), in his Ph.D. thesis modeled planform changes of braided rivers. He carried out his study with Jamuna River in Bangladesh. A multi-layer perception network has been trained to predict bank erosion based on a limited amount of geometrical information: the location (distance and direction) relative to the nearest channel, the local width of the nearest channel, and the fraction of water in the neighborhood. Based on these data the neural network was able to learn a number of simple rules, such as: erosion is more likely along wide channels. The second part of the study has, therefore, focused on the formation of new channels as a result of cutoffs. Two-dimensional depth-averaged morphological simulations of sharp bends have been carried out to improve the understanding of the processes involved. An additional sensitivity analysis has shown that the numerical aspects have not significantly influenced the outcome of the simulations. In all simulations, the cutoff channel started forming at the upstream end, which agrees with the observations of the Jamuna River.

2.7 Bank Erosion in context of Bangladesh

The major river systems (Figure 2.1) of Bangladesh are morphologically extremely dynamic resulting in continuous erosion and accretion processes. Consequently river bank erosion has become a common phenomenon along with the major and minor rivers of Bangladesh. About 5% of the total flood plain of the country is affected by bank erosion while 94 upazillas out of 489 upazillas experience this calamity each year. But the scale and frequency of erosion varies from river to river due to characteristics of bank materials, water level variation, planform, near bank flow velocities and supply of water and sediment into the river (BWDB, 2004).



Figure 2.1 River Systems of Bangladesh (source: IWM)

CEGIS (2010) conducted a study on long term erosion processes of Ganges River. During 1973-2009 about 75,680 ha of land was eroded both in India and Bangladesh along the river from the international boundary of Bangladesh at Nawabganj to the confluence with the Jamuna at Rajbari. On the other hand, accretion was 29,946 ha during the same period along the same reach. However inside the territory of Bangladesh, erosion-accretion is in a net balance. Most of the erosion takes place along the right bank of the Ganges where there is no cohesive bank material. The rate of erosion in this river is less susceptible to

flood discharge. It has been found that a 20% increase in annual peak discharge increases annual erosion by 5%.

Naznin et. al.(2013) conducted a study on river bank erosion of Meghna River at Chandpur using GIS and remote sensing approach. The study has undertaken to study the trends of riverbank erosion at Chandpur district. Data analysis of the last three decades from 1980-2010 showed that average erosion rate was 495.03 sq meter/year and from three study locations Haimchar upazila is more vulnerable for erosion. From the period 1980 to 1990, the erosion rate was high in Chandpur. Recently in the decade of 2002 to 2010, deposition rate is higher than the erosion rate. In the last 30 years total eroded area on the left bank of the Meghna was 14851 sq meters and total deposition was 10940 sq meters. The river course shows an overall migration of the left bank is northwestward and southeastward direction.

CEGIS (2007) carried out a study on long term bank erosion processes of Jamuna River. The very high widening rate of the river in 1970s and 1980s, apparently punctuated the westward migration for a short period, but in the recent years westward migrations seems to be restored. From 1970s the mean annual rate of erosion increased and reached its maximum in 1980s. In 1990s and in recent years, erosion along the river has been decreasing rapidly. The reduction in mean annual rate of erosion is about two and a half fold. It has been observed that the annual rate of erosion was at maximum during the two very large floods in 1988 and 1998. The rate of erosion is about 40 to 50% higher along the left bank than that of the right bank. The annual rate of erosion increases with the annual maximum flood discharge. The main flanking channels contribute about 75% of erosion along the right bank, whereas, this type of channel contributes only 40% of erosion along the left bank. The life span of meandering bends of the main channel varies widely from one year to several years. The average life span of such channels along the right bank is 4 to 5 years, whereas it is about 3 to 4 years for the channels along the left bank. Probably due to the variation in consolidation, the characteristics of the bank erosion process differ from the left bank to the right bank.

2.8 Study Area

The study area covers the reach of Jamuna River from immediate downstream of outfall of Teesta River to 20 km upstream of Ganges-Jamuna-Padma confluence, covering about 150km reach of as shown in Figure 2.2. In this study area, various important hydraulic

structures like East Guide Bund and West Guide Bund of Bangabandhu Bridge, Sirajganj Hard Point and Bhuapur Hard Point are situated. From various previous studies, different features of study area is tried to focus in the following paragraph.

2.8.1 Jamuna River System

The Brahmaputra, the largest river in Bangladesh, originates at the snout of a glacier in the Kailas Range of the Himalayas, south of the Gunkyud Lake in southwestern Tibet. The river rises at an elevation of about 5300 m (Goswami, 1998) and then flows 1100 km eastward across the Tibetan Plateau as Tsangpo River, before turning south to cross the east-west trending ranges of the Himalayas (Figure 2.2). Within Bangladesh, the length of the Jamuna River up to the confluences with the Ganges River at Aricha is approximately 240 km along the right bank and 220 km along the left bank (CEGIS, 2007).

Sometime between 1776 and 1830, the course of the Brahmaputra River shifted from the east of Madhupur block to the west, and the river in its new course took the name Jamuna. The term „avulsion“ may be used to describe this shift as the change in channel alignment was achieved by a abandonment of one course and adoption of a new one some distance away rather than by a progressive shift (Bristow, 1999).

2.8.2 Catchment Characteristics

The Brahmaputra-Jamuna drains the northern and eastern slopes of the Himalayas, and has a catchment area of 5, 83,000 sq.km. 50.5 percent of which lie in China, 33.6 percent in India, 8.1 percent in Bangladesh and 7.8 percent in Bhutan (Figure 2.3). The catchment area of Jamuna River in Bangladesh is about 47,000 sq. km. The average annual discharge is about 19,200 m³/sec, which is nearly twice that of the Ganges. The Brahmaputra River is characterized by high intensity flood flows during the monsoon season, June through September. There is considerable variation in the spatio-temporal distribution of rainfall with marked seasonality. Precipitation varies from as low as 120 cm in parts of Nagaland to above 600 cm in the southern slopes of the Himalayas. In Bangladesh territory rainfall varies from 280 cm at Kurigram to 180 cm at Ganges-Brahmaputra confluence (FAP 2).

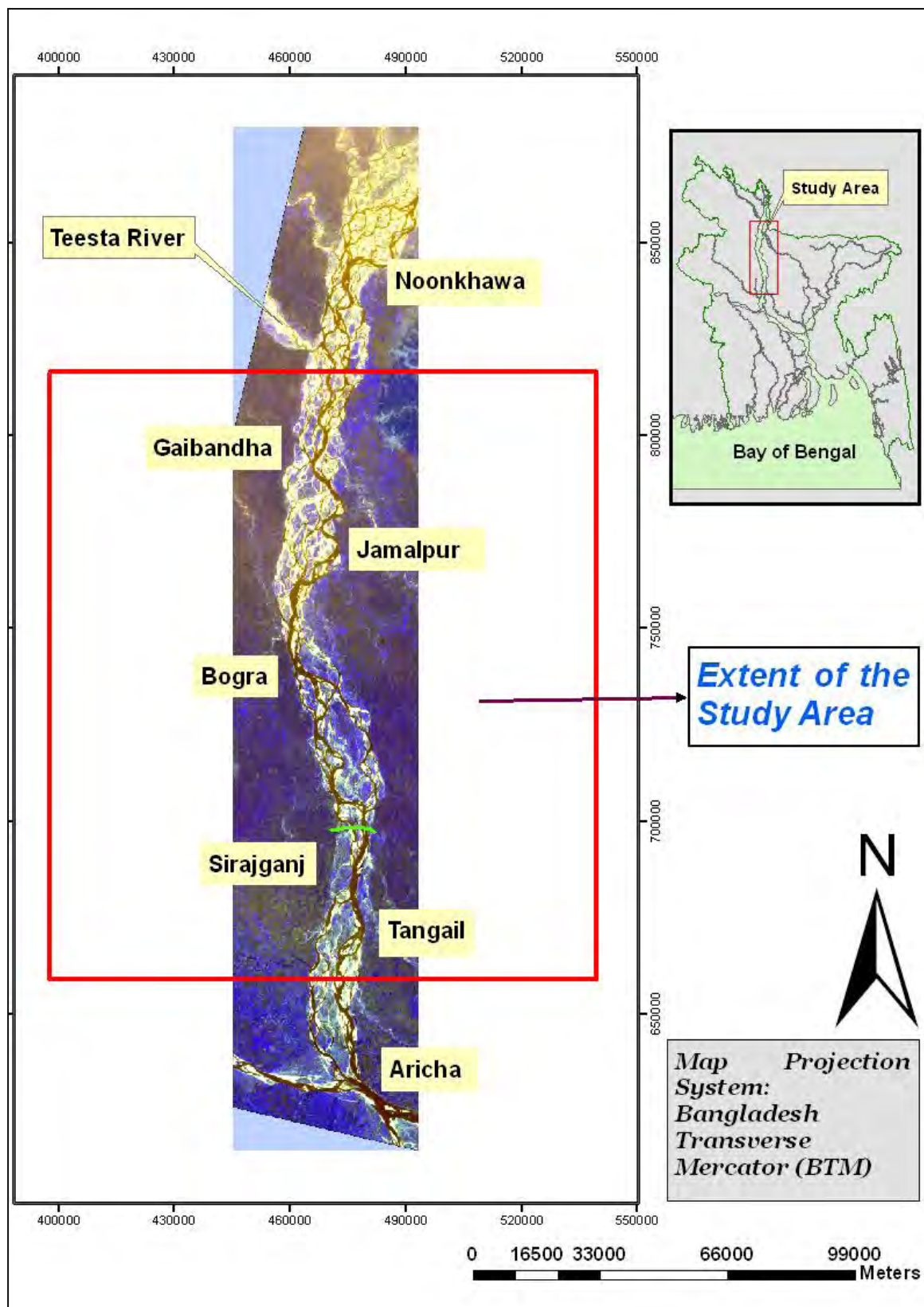


Figure 2.2 Extent of the Study Area



Figure 2.3 Catchment of GBM basin (Source: CEGIS, 2007)

Monsoon rains from June to September accounts for 60-70% of the annual rainfall. These rains that contribute a large portion of the runoff in the Brahmaputra and its tributaries are primarily controlled by the position of a belt of depressions called the monsoon trough extending from northwest India to the head of the Bay of Bengal. Deforestation in the Jamuna watershed has resulted in increased siltation levels, flash floods, and soil erosion. Occasionally, massive flooding causes huge losses to crops, life and property. Periodic flooding is a natural phenomenon which is ecologically important because it helps maintain the lowland grasslands and associated wildlife. Periodic floods also deposit fresh alluvium replenishing the fertile soil of the Jamuna River Valley.

2.8.4 Topography of Catchment Area

Topographically, the study area is part of alluvial plains (low land) formed by the sediments of river and its tributaries and distributaries. In the context of physiography, the study area belongs to region: floodplains and sub-region: Jamuna floodplain. The sub-region can be again subdivided into the Bangali-Karatoya floodplain, Jamuna-Dhaleshwari floodplain, and diyaras and chars. The soil and topography of chars and diyaras vary considerably. Some of the largest ones have point bars. The elevation between the lowest and highest points of these accretions may be as much as 5m. The difference between them and the higher levees on either bank can be up to 6m. Some of the ridges are shallowly flooded but most of the ridges and all the basins of this floodplain

region are flooded more than 0.91m deep for about four months (mid-June to mid-October) during the monsoon. Land elevation of the study area varies from 13mPWD to 18mPWD.

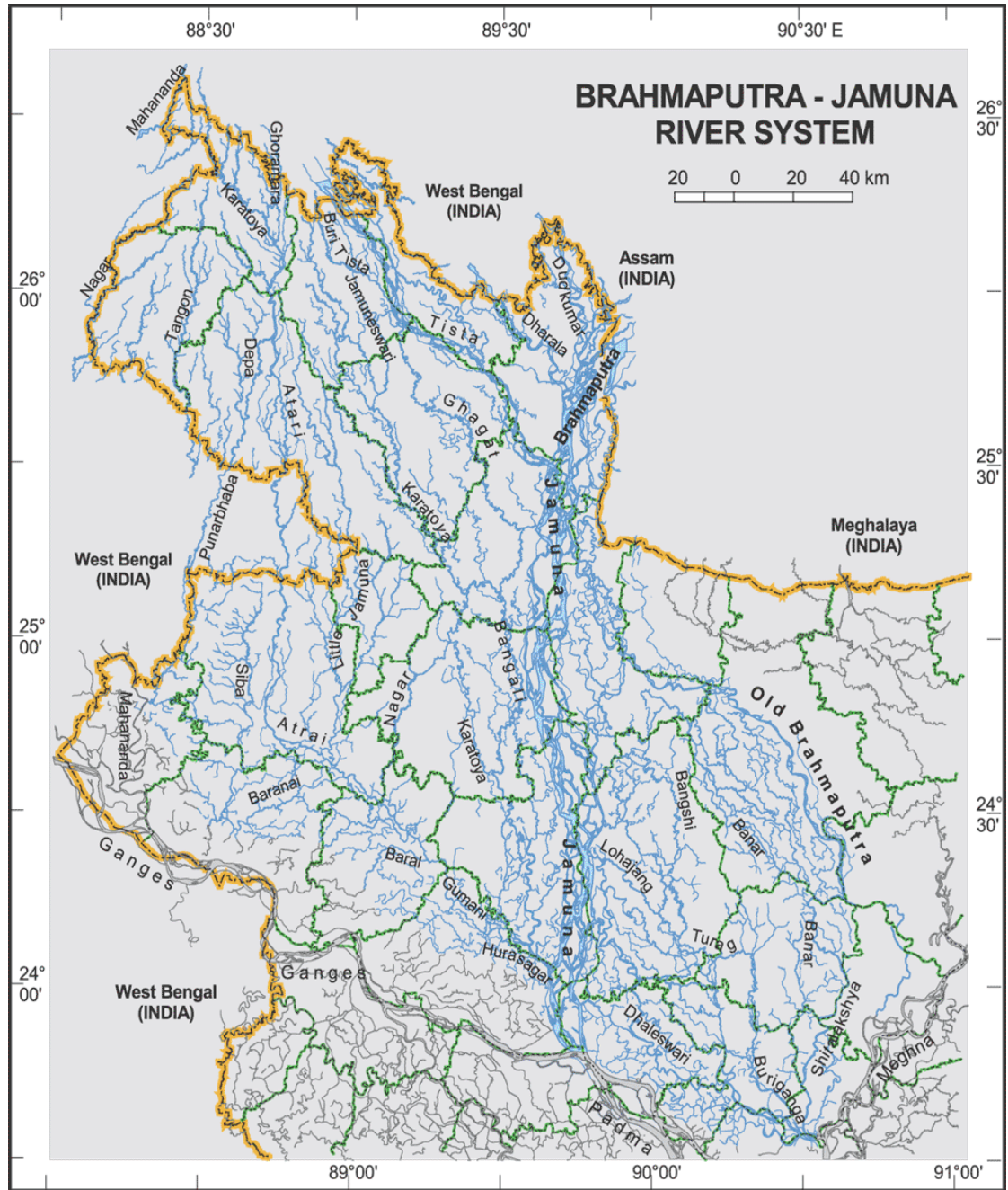


Figure 2.4 Brahmaputra-Jamuna River System within Bangladesh Territory (Source: IWM, 2012)

2.8.5 Sediment Characteristics

The Jamuna River catchment supplies enormous quantities of sediment from the actively uplifting mountains in the Himalayas, the erosive foothills of the Himalayan Foredeep and the great alluvial deposits stored in the Assam Valley. Consequently, the Jamuna River carries a heavy sediment load, estimated to be over 650 million tonnes annually (Coleman, 1969). Most of this is in the silt size class (suspended load) but around 15 to 25 percent is sand (bed load). This sand is deposited along the course of the river and the clay fraction is transported to the delta region. The banks of the Jamuna River consist of fine cohesionless, silty sand. The composition of the bank materials is remarkably uniform. For the Jamuna River the angle of internal friction is approximately 30° [FAP-24]. It is however dependent on the mica contents. Because of the varying location of the river branches, much of the sediment has been eroded and accreted many times. The sand size sediment is relatively uniformly graded. The range of d_{50} values vary between 0.21 mm and 0.14 mm [FAP 24].

2.8.6 Hydraulic Characteristics of Jamuna

The Jamuna is the lowest reach of the Brahmaputra River in Bangladesh. It is a large braided sand-bed river; the number of braids (during low flows) varies between 2 to 3. The average discharge during floods is about $50,000 \text{ m}^3/\text{s}$ and the maximum width during floods is more than 15km. The bed material is quite uniform. The valley slope in Bangladesh decreases gradually from 0.10 to 0.06 m/km (FAP24). The width of the river varies from 3 km to 18 km but the average width is about 10 km. Width/depth ratios for individual channels vary from 50:1 to 500:1. The gradient of the river in Bangladesh is 0.000085, decreasing to 0.00006 near the confluence with the Ganges. The river has a total annual sediment flow of about 650 million tons. The Chezy value varies from 60. to $90 \text{ m}^{0.5}/\text{s}$ while the eddy viscosity varies from 0.80 to $4.0 \text{ m}^2/\text{s}$ [FAP-24]. The characteristics of the Jamuna River have been summarized in Table 2.1. According to an extensive sampling carried out by FAP 1 (1991), bank material seems to be quite uniform and consists of fine sand. The little variation in bank material composition in downstream direction is due to old clayey deposits.

Table 2.1: Summary of hydraulic characteristics of the Jamuna River
(Source: IWM, 2012)

Description	Parameter
Maximum total discharge	100,000 m ³ /s
Dominant discharge	38,000 m ³ /s
Average depth (main channel)	8 m
Average depth above chars during floods	1-2 m
Chezy coefficient (average)	70 m ^{1/2} /s
Chezy coefficient (floods)	90 m ^{1/2} /s
Average velocity during floods	2 m/s

2.8.7 Bank Erosion of Jamuna River

Pahlowan (2015) conducted a study on erosion hazards of Jamuna River. The net land change was found to be 107 km² indicating the overall loss of land. Discharge continuously changes the size of different bars and the area of active channel during study period. These bars trigger the bank erosion and the accretion rate of Jamuna River. By using this information compiled with other data like short-term intense rainfall in the catchment area of Jamuna river will serve to taking up a long-term prediction for erosion and accretion.

CEGIS (2013) carried out a study on erosion pattern of Jamuna River. The land eroded along Jamuna River was 2408 ha in 2012, living space of about 24000 people based on the average population density along the flood plain. About 1284 ha land and 216 settlement were found to be vulnerable. The predicted maximum erosion of land was in Sirajganj, the second and third ones are Kurigram and Jamalpur respectively.

Hasnat (2013) conducted a study on erosion scenario of Jamuna River. The erosion along right bank of Jamuna River was 900 ha, of which about 86 ha comprised settlements. Around 7 km of embankments were eroded along that bank. Erosion along left bank was much higher than that of right bank due to the presence of highly erodible bank materials

along the left bank. Around 1515 ha of land of which 329 ha were settlements eroded along left bank.

2.8.8. Major River Training Works along Jamuna River

Structures on the Right Bank of the Jamuna River:

Sirajganj Hard Point

The hard point at Sirajganj was constructed in connection with Jamuna Multipurpose Bridge Project. The hard point is about 2.50km in length and is located at about 7.00km upstream from the bridge. The construction of the hard point was completed in 1997-98 at a cost of about Tk. 3123.7 million (including repair works). The hard point serves the purpose of protecting Sirajganj town as well as guiding the Jamuna flow towards the bridge. No serious damage is reported so far despite the fact that a threatening condition has been prevailing at its upstream termination for a few years due to large bank erosion immediately upstream of the hard point [CEGIS 2007].

West Guide Bund

Before the construction of Jamuna Bridge the width of the river at bridge location was about 10km. The width was constricted to 4.8km for the construction of the bridge. There was a char in the river at the bridge location dividing the river into two channels. The west guide bund was constructed on this char and the west channel was closed by the approach road. The length of the approach road is 16.94km. The guide bund is about 3.2km long. The construction of the guide bund was completed in 1997-98 at a cost of about Tk. 7139.4 million. No serious damage is reported so far except in 2007 monsoon depression in the underwater slope at the upstream tip was noticed at sporadic locations. The following hydraulic design parameters were used for design of the guide bund [CEGIS 2007]:

Structures on the Left Bank of The Jamuna River

Bhuapur Hard Point

It is a BBA (erstwhile JMBA) structure constructed in connection with the construction of Jamuna Bridge. The length of the hard point is 1700m. The construction was completed in 1997-98 at a cost of Tk.422.0 million. No serious damage to the hard point is reported

so far. At present the left bank channel is somewhat away from the hard point [CEGIS 2007].

East Guide Bund

The east guide bund of Jamuna Bridge was constructed along the left bank margin of the river. The length of the guide bund is about 3.1km. The guide bund was constructed in 1997-98 at a cost of about Tk. 6789.0 million. The approach road of east guide bund is 14.76km. No serious damage to the hard point is reported so far. In 2007 monsoon noticeable bank erosion took place at the upstream of the hard point although the left bank channel is relatively weak now in terms of flow area [CEGIS 2007]. The following hydraulic design parameters were used for design of the guide bund:

Chapter 3

THEORY AND METHODOLOGY

3.1 General

Bank erosion process is one of the most challenging issues that water resources engineers deal with. Many theories regarding the mechanisms of bank erosion are the upshot of extensive research carried out by analytical methods, laboratory experiments and numerical modeling. The purpose of this chapter is to give a brief description of the related theories regarding bank erosion processes. Moreover, various mathematical equations and formulas of MIKE21C are also explained in the following section.

3.2 Mechanics of River Banks

The fundamental processes concerned with the mechanics of bankline movement are bank erosion, weakening of resistance to erosion, bank stability with respect to mass failure, basal endpoint control and effects of vegetation, seepage effects and bank advance.

3.2.1 Bank Erosion

Water flowing in an alluvial river exerts forces of drag and lift on the boundaries that tend to detach and entrain surface particles. To remain in place boundary sediment must be able to supply an internally derived force capable of resisting the erosive forces applied by the flow. The origin of the resisting forces varies according to the grain size, the size distribution and the nature of electrochemical bonding that may exist between particles. Erodibility of bank may vary spatially over relatively short distances. In case of non-cohesive bank materials the forces resisting erosion are generated primarily due to the immersed weight of the particles.

3.2.2 Weakening of Resistance to Erosion

The erodibility of bank soils can be increased markedly by the process of weakening and weathering. The processes responsible for loosening and detaching grains and aggregates are closely associated with soil moisture condition at and beneath the bank surface.

Changes in the moisture and freezing and thawing can significantly influence the erodibility of riverbank. Swelling and shrinkage of soils during repeated cycles of wetting and drying can contribute to cracking that significantly increases erodibility and reduces soil shear strength. Temporal variability in the erodibility of bank soils due to the operation of weakening processes means that the effectiveness of a given flow event in eroding a bank depends not only on the magnitude and duration of a particular event but also on antecedent conditions.

3.2.3 Bank Stability with respect to Mass Failure

Fluvial erosion drives bank retreat directly by removing material from the bank face, but it also often causes bank retreat by triggering mass instability. The stability of a bank with regard to mass failure depends on the balance between gravitational forces, which tend to move soil down slope, and forces of friction and cohesion, which resist movement. Failure of the bank occurs when scour of the bed next to bank toe increases the bank height, or when undercutting increases the bank angle.

3.2.4 Basal End-point Control

Although fluvial erosion processes and geotechnical failures are controlled by different aspects of bank geomorphology, they are actually linked. The key to characterizing this link lies in recognizing that mass wasting delivers the failed material to the toe of the slope, or basal area, but does not entirely remove it from the bank profile. The removal of failed materials from the basal area depends primarily on its entrainment by current and wave action, following by fluvial transport downstream. The concept of basal endpoint control explains how medium to long term retreat rate of bank is controlled by the rate of sediment entrainment and removal from the toe.

3.2.5 Vegetation Effects

The role of vegetation in affecting bank erosion and width adjustment is complex and poorly understood. Although vegetation generally reduces soil erodibility, its impact on bank stability with respect to mass failure may be either positive or negative. Hence depending on the geomorphic context and dominance of either fluvial processes or mass

failure, vegetation may produce either a net increase or decrease in the rate of bankline shifting.

3.2.6 Bank Advance

Bank advance occurs through sediment deposition, a process that tends to narrow the channel. Bank advance occurs in a variety of different geomorphic settings and sediments may be deposited from bed load, suspended bed material load, wash load or a combination of all three transport processes. Despite this diversity, however, processes of bank advance have a common result; new flood plain deposits are created as bank advances. This suggests that bank advance should more broadly viewed as one of several processes that create new floodplains.

3.3 River Bank Erosion Processes

Evolution of the riverbank in non-cohesive soils can be considered to involve three main processes, namely, bank-toe erosion, riverbank erosion as well as distribution of failed bank materials.

3.3.1 Process of Bank Toe Erosion

Bank-toe (basal area) erosion is linked to the bank failure through the concept of basal endpoint control (Carson and Kirkby, 1972; Thorne, 1982; Thorne,1991). According to this concept, bank-toe erosion occurs if the rate of removal of sediment from bank-toe exceeds the rate of materials supplied from bank erosion process, sediment feeding from upstream as well as across the channel. In this case fluvial erosion of the basal area of the bank causes both the bank height and the slope of the bank to increase to the extent that eventually riverbank mass failure occurs (Figure 3.1). Bank-toe aggradation and berm formation occur when the sediment feeding to this zone exceeds the removal rate of the sediment at the bank-toe and it contributes to the stabilization of the river bank (Thorne,1982). Bank-toe erosion in non-cohesive soils begins by detachment and entrainment of individual particles, when fluid forces (lift and drag) exceed resisting forces (friction and inter-locking due to compaction).

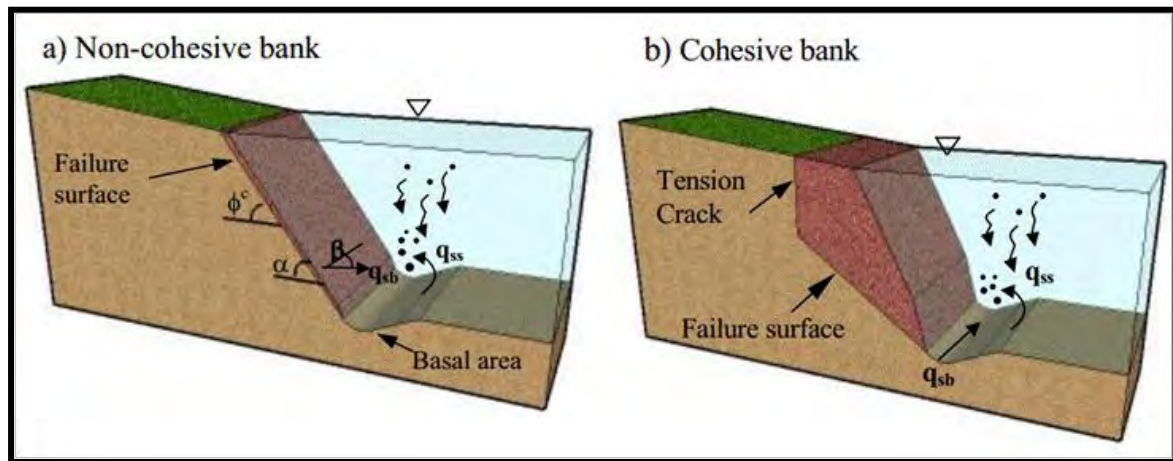


Figure 3.1 Continuous and abrupt bank retreat processes

3.3.2 Process of River Bank Failure

Bank failure is a complex process depending on the geotechnical properties of bank material, stratigraphy and geometry of the bank (Thorne, 1991), as well as dynamics of the flow regime in the river and bank. Riverbanks may be broadly classified on the basis of material and stratigraphy as non-cohesive, cohesive and layered (Thorne et al., 1997). In riverbanks composed of non-cohesive soils, shear strength increases faster with depth than does shear stress, so that critical conditions are more likely to occur at shallow depths. In cohesive soils, shear stress increases more rapidly than shear strength with increasing depth so that critical surfaces tend to be located deep within the bank (Terzaghi and Peck, 1948).

In non-cohesive materials failure occurs by dislodgment and avalanche of individual particles or shear failure along shallow, planar or very slightly curved slip surfaces (Thorne, 1991; ASCE Task Committee, 1998). In cohesive soils, deep-seated failure occurs along a rotational (circular) failure surfaces (Fig. 3.2a) in high, mildly sloped (less than 60°) stream banks, while planar failure (Fig. 3.2b) occurs often in steep banks, with the failed block sliding down into the channel (Thorne, 1982). During the process of temporal incision of channels, planar failures often occur earlier than rotational failures in the adjustment sequences when banks are lower (Simon, 1989) and it can occur along any critical failure surface irrespective of whether this plane passes through the bank-toe. This type of failure is a consequence of bank-toe erosion and generation of

a near vertical tension crack (Lohnes and Handy, 1968; Thorne et al., 1981).

Cantilever failure (Fig. 3.2c) prevails on composite banks when erosion of the erodible underlying layer by flow generates undercutting to the extent that triggers this type of failure (Thorne and Lewin, 1979; Thorne and Tovey, 1981; Pizzuto, 1984). Three modes of cantilever failure, namely shear, beam and tensile failure have been addressed by Thorne and Tovey (1981). Beam failure occurs in cohesive soils in the form of rotation of the overhang block around its neutral axis forward towards the river. This failure occurs along a vertical plane, where 90% of the failure surface over neutral axis is in tension and the rest in compression (Pizzuto, 1984).

Shear failure occurs when the block fails along a vertical plane without rotation, which is the most commonly observed type of cantilever failure (Thorne and Tovey, 1981). This happens when the weight of the block exceeds the shear strength along the failure plane. Tensile failure occurs if a weak plane exists along the horizontal plane in cohesive soils or due to saturation of the lower soil (Pizzuto, 1984). Riparian vegetation roots can increase the stability of the overhang and tensile failure can occur below vegetation roots, leaving root-bounded overhangs, which fail subsequently by shear or beam failure (ASCE Task Committee, 1998).

Pizzuto (1984) addressed the influence of the side grown roots on enhancement of tensile strength of the soil and its resistance against cantilever failure. Fibrous roots of vegetation in soil build a reinforced composite material, which increases the shear strength. Pollen (2004) found that the force required for pulling out the vegetation element is almost equal to their tension failure. Further information on the topic is given by Cancienne et al (2008).

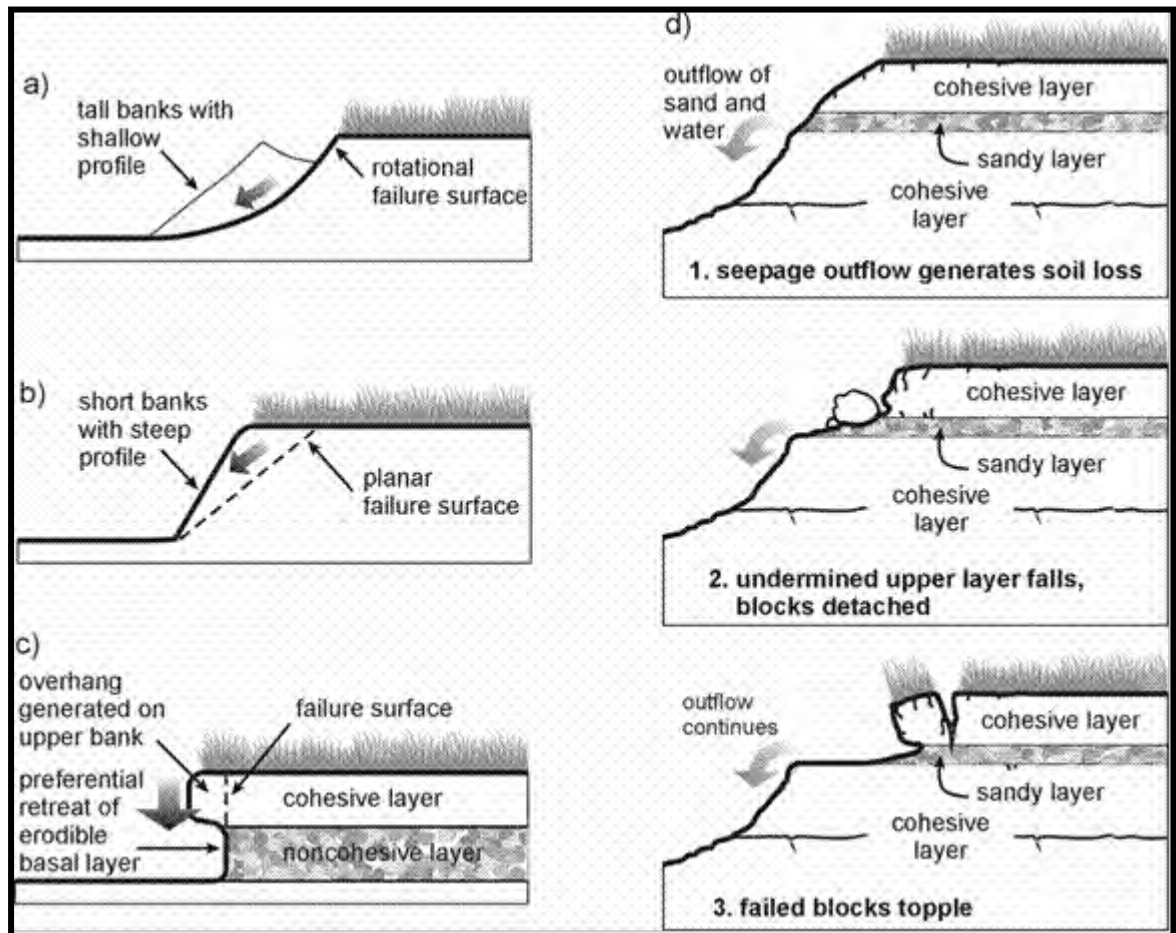


Figure 3.2 Different types of the riverbank failure in cohesive and composite soils (Thorne *et al.*, 1981).

Cantilever failure can also occur in dense non-cohesive soils covered with vegetation. Further research is needed to find out if cantilever failure mechanisms are identical to those in cohesive soils. Moreover, the parameters that affect the stability of the overhang needed to be studied systematically. Additionally, failure slopes can be different in these two soil types, since tension cracks are not normally present in non-cohesive soils.

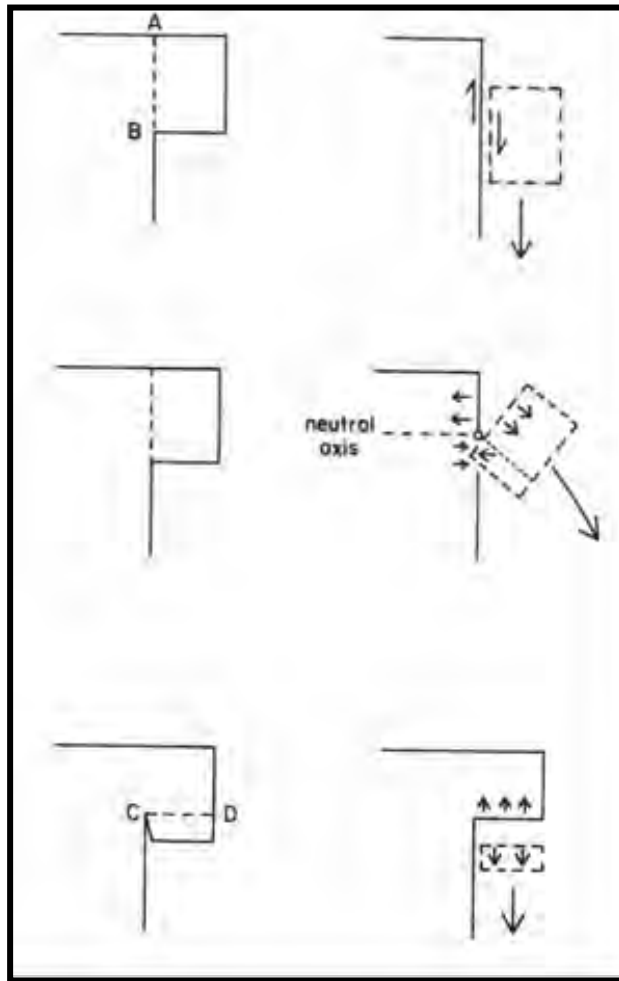


Figure 3.3 Schematic illustration of modes of cantilever failure (Thorne and Tovey, 1981). Top: shear failure; middle :beam failure and bottom: tensile failure

Dynamics of the flow regime in the river, comprising water rise and drop during rising and falling limb of the hydrograph, respectively, as well as fluctuation of water table in the riverbank have a significant effect on the process of bank failure. The latter process is manifest in pore water pressure. Pore water pressure is defined as the pressure of water filling the voids in soil. The effect of pore water pressure on the mechanical properties of soil has been first presented by Terzaghi (1936). In fully saturated soils all soil pores are filled with water, and a part of stress is born by the water in soil body. Hence the effective stress is the difference between the total normal stress and pore water pressure.

In unsaturated soils, however, the voids (pores) are partly occupied by water and partly by air. Water adheres to the surface of soil particles leaving the rest of the voids

occupied by the air. The pore water pressure is less than pore air pressure in unsaturated zone (due to the surface tension). Since the gauge air pressure is zero (in equilibrium with atmosphere), the pore water pressure above the water table is negative. The difference between air pressure and pore water pressure is called matric suction. Matric suction is a positive quantity. Measurement of matric suction can be made using tensiometer (Fredlund and Rahardjo, 1993). The presence of matric suction in unsaturated soils increases the shear strength of the materials which is often manifested in steeper bank slopes than those indicated by the angle of repose (Simon et al., 2000).

3.4 River Bank Protection Measures

In general, three relevant concepts of erosion counter measures are in existence:

- River training measures, which are instream structures that are intended to influence the flow conditions or channel properties downstream of the location of the measure (active measures), e.g., bottom vanes, floating screens bandalling.
- Structures, which are constructed as a protrusion from the river bank to decrease the hydraulic impacts in front of the area to be protected (partly active or partly passive measures), e.g., groynes and spur.
- Structures to protect the bankline directly without active interference with the water flow to reduce its erosive strength before attacking the bank slope (passive measures), e.g., revetments.

It should always be kept in mind that whatever bank protection measure is carried out, the succeeding river response will certainly call for compensatory measures in the following years. Therefore, adaptation and supplementary measures must always be seen as an inseparable element of the protection measures.

3.5 Morphological Variables

Rivers being a very dynamic systems are one of the most sensitive and dynamic components of the physical landscape and are influenced by a variety of interconnected factors. Each river responds to a number of independent inputs, the river characteristics being the resulting dependent outputs. Lane (1957) established the major factors affecting alluvial stream channel forms. The independent variables of the river catchment are

determined by the climate and the geology of the basin, but not directly; also the vegetation, the weathering process and human interference play a role. The dependent variables in a particular river reach are the river characteristics which comprises of both river morphology and hydraulics.

3.5.1 Independent Variables

Factors result in variables like discharge, sediment volumes, sediment characteristics and valley slope. These factors are:

- Climate: precipitation, temperature, evaporation humidity
- Hydrology: water levels and discharge versus major river shifts
- Topography: relief versus sediment concentrations
- Geology: tectonics, faults, soil types and sedimentary yields
- Base-level changes: sea level rise versus sedimentary structure
- Human interference: deforestation, sediment transport

The climatic factor is an important geo morphological control of a river system. It governs the amount of precipitation and consequently the surface runoff and river discharge to determine the extent and intensity of basin denudation and indirectly the sediment yield. Hydrological factors like water level and discharge important parameters which may change the characteristics of river behavior. River basin areas of various topographies such as hilly, mountainous and coastal relief offer different sediment yield in the form of sediment amount, sediment size and shape etc. Geology and climate do not determine the discharges and the sediment transport rates in a river system directly. There are the role of the vegetation and the weathering process. The geology in combination with the climate determines the rate of weathering and this again has a significant influence on the growth of the vegetative cover. However, each independent variable is different for different river reaches; e.g. a more downstream reach usually has

to carry more sediment. Hence for all independent variables at the river reach level it holds that they are a function of the longitudinal coordinate. Otherwise, the sediments transported in a river are distinguished as far as their origin and their mode of transport is concerned. In line with this the total volume of sediment that has to be transported is divided in bed material and wash load.

3.5.2 Dependent Variables

The dependent variables are classified into primary dependent variables and secondary dependent variables as follows:

Primary Dependent Variables

The primary dependent variables are the combination of morphological characteristics and hydraulic characteristics of a river reach. The offtakes and confluences are nodes of a river system and considered to belong to the primary dependent characteristics. The primary dependent variables are:

- ***Dependent morphological characteristics:***
 - Number of channels, n
 - Average width of channel(s) B_b , where the index b stands for bank full conditions
 - - sinuosity p of the river channel(s)
 - - typical wave length of the curved channels L
 - - total width B_t , occupied by the river channel(s)
 - - bankfull depth h_b of the river channel(s)
 - - slope of the river bank

- ***Dependent hydraulic characteristics:***
 - Average water depth in the main channel;
 - -“Wet” width either in the main channel or including the floodplain;
 - - Inundation depth of the floodplain;
 - - the roughness coefficient of the main channel and of the

- floodplain;
- the average velocity.

Secondary Dependent Variables

The secondary dependent variables in a particular river reach are more detailed, local and dynamic in nature. These are:

- bars
- bifurcations
- scour holes
- bank erosion
- cutoffs

The dependent variables are linked to the independent variables through relationships of river mechanics. There is no single-valued relationship between the imposed variables and the dependent characteristics. The excess flow strength leads to bed degradation when banks are fixed. This bed degradation increases the water depth and reduces the longitudinal slope until the flow strength reaches a value which matches the transport of the sediment supplied from upstream. When the banks are erodible there are three additional modes of adjustment. Firstly, the river can become wider. Secondly, the longitudinal slope can be reduced by increasing the sinuosity through the expansion of meander loops. Thirdly, new channels can be carved in the floodplain at discharges above bank full, which leads to an anabranches system. The vertical responses of rivers with fixed banks are rather unambiguous, but the distribution of horizontal response over the three modes of adjustment depends on the initial state of the river and the time series of discharge and sediment supply during the transition to new equilibrium.

3.6 Sediment Transport in Rivers and Channels

An important aspect of fluvial processes is the movement of sediment in rivers and channels, to which river morphology and river channel changes are closely related (Kamal, 2009). The sediment cycle begins with the erosion of soil and rock in a watershed and transport of that material by surface runoff or by mass wasting. The

transport of sediment through a river system consists of multiple erosional and depositional cycles, as well as progressive physical breakdown of the material. Many sediment particles are intermittently stored in alluvial deposits along the channel margin or floodplain, and ultimately re-entrained via bank and bed erosion.

3.6.1 Sediment Transport

Whenever water flows in a channel (natural or artificial), it tries to scour its bed and erode its bank. Silt or gravels or even larger boulders are detached from its bed or banks. These detached particles are carried downstream by the moving water. This phenomenon is known as sediment transport.

The transport of sediment through the stream system depends on the sediment supply (size and quantity) and the ability of the stream to transport that sediment supply.

3.6.2 Sediment Loads

The term load, as used in sediment transport, may refer to the sediment that is in motion in a stream. It is also used to denote the rate at which sediment is moved, for example, cubic feet per second or tons per day.

There are two common classification of the load in a stream. The first classification is based on origin (bed-material load and wash load) and the later is based on transport mechanism (bed load and suspended load).

Wash load: Composed of particle smaller than the bed material and is supplied mainly from the erosion of the catchment.

Bed-material load: Consists of the fractions of the same size as the bed material and may originate not only from channel bottom or bank but also from the catchment.

Bed load: The sediment in almost continuous contact with the bed, carried forward by rolling, sliding or hopping.

Suspended load: Sediment which is maintained in suspension by turbulence in the flowing water for considerable periods of time without contact with the stream bed.

3.7 Sediment Transport Equations

The sediment transport process in river flow can be represented as a quasi-steady process. Therefore, the available bed-load transport formulae and suspended load transport formulae can be applied for transport rate predictions.

Many theories have been put forward to provide the framework for sediment transport prediction. Numerous theoretical and semi-empirical approaches have been developed for the calculation of sediment transport rates, for example, Einstein (1950), Yalin (1963), Bagnold (1966), Engelund-Hansen (1967), Ackres and White (1973), Yang (1973), Van Rijn (1984), Hossain (1985) – mainly based on observation on laboratory experimental flumes and small streams. Most of the formula can be represented by following form:

$$\Phi_s = f(\theta) \quad (3.19)$$

where ϕ_s and θ are known as transport parameter and Shields parameter respectively. These are expressed as:

$$\Phi_s = \frac{q_s}{D^{3/2} \sqrt{g\Delta}} \quad (3.20)$$

$$\theta = \frac{\mu h s}{\Delta D} \quad (3.21)$$

where, q_s is sediment transport per unit width (m^2/s), D is the effective sediment size, Δ is the relative density of sediment, g is the acceleration due to gravity, u is the averaged flow velocity and s is the slope.

Mainly stage, discharge, velocity, water surface and bed slope, shear stress, mean particle diameter and stream power control the sediment movement of any channel. Only a single equation cannot incorporate all these variables and predicts the sediment load. For this reason, different equations have been put forward on the basis of different independent variables. Out of many available empirical formulas the following three well known equations have been selected for the present study.

3.7.1 Engelund Hansen Equation (1967)

Engelund-Hansens' (1967) equation is based on the shear stress approach. In developing the equation Engelund-Hansen's relied on data from experiment in a specific series of test in a large flume. The sediment used in this flume had mean diameter of 0.19mm, 0.27 mm, 0.45 mm and 0.93 mm.

The equation can be written as:

$$g_s = 0.05\gamma_s V^2 \sqrt{D_{50}/g(\gamma_s/\gamma - 1) (\tau_o/(\gamma_s - \gamma) D_{50})^{3/2}} \quad (3.22)$$

where,

g_s = Sediment transport per unit time per unit width

γ_s = Specific weight of sediment particles

γ = Specific weight of water

τ_o = Bed shear stress

D_{50} = Median diameter of bed material

V = Average flow velocity

g = Acceleration due to gravity

This equation is dimensionally homogeneous and any consistent set of units can be used.

3.7.2 Van Rijn's Equation (1984)

A simplified method was given by Van Rijn for calculating suspended sediment transport.

This method is based on computer computations in combination with a roughness predictor. Using regression analysis, the computational results for a depth range of 1 to 20 m, a velocity range of 0.5 to 2.5 m/s and a particle range of 100 to 2000 μm were

represented by a simple power function, as follows:

$$q_{s,}/u \ h = (0.012 (u - u_{cr}) / (s - 1))^2 * g \ d_{50}^{0.5} * (d_{50}/h) * (1/D^*)^{0.6} \quad (3.23)$$

in which

$q_{s,}$ = volumetric suspended load transport (m^2/s)

u_{cr} = critical depth-averaged velocity according to Shields

h = water depth

u = depth-averaged velocity

Equation 3.3 only requires u , h and d_{50}

as input data and can be used to get a first estimate of the suspended load transport.

It is assumed that the instantaneous bed-load transport rate is related to the instantaneous T parameter, as follows

$$q_b = 0.1 (s - 1)^{0.5} * g^{0.5} * d_{50}^{1.5} * D^{*-0.3} * T_m^{2.1} \quad (3.24)$$

In which

$T_m = (\tau_{b,} - \tau_{b,cr}) / \tau_{b,cr}$ = instantaneous shear stress parameter

$\tau_{b,} = \mu \tau b$ = instantaneous effective bed shear stress

D^* = dimensionless particle parameter

When the bed load transport and the suspended load transport are known, the total load transport of bed material can be determined by summation of Equation 3.2 and 3.3.

$$q_t = q_b + q_s \quad (3.25)$$

3.8 Mathematical Modeling

Many modeling packages are available which can simulate hydrodynamic as well as morphological characteristics of a river. Moreover, modeling packages are so advanced that it can now simulate intervention phenomenon on river through control structure.

There are few softwares available that can simulate the flow through control structures and sediment transport with bed level changes in river systems. There are mainly HEC-RAS, MIKE 11, MIKE 21C, Delft 3D, SMS etc.

3.9 MIKE 21C

MIKE 21C is a special module of the MIKE 21 software package based on a curvilinear (boundary-fitted) grid, which makes it suitable for detailed hydrodynamic and morphological simulations of rivers and channels, where an accurate description of banklines is required. The numerical grid is created by means of a user-friendly grid generator. Areas of special interest can be resolved using a higher density of grid lines at these locations. The MIKE21C is particularly suited for river morphological studies and includes modules to describe:

- a) Flow hydrodynamics, i.e. water levels and flow velocities are computed over a curvilinear or a rectangular computational grid covering the study area by solving the vertically integrated St. Venant equations of continuity and conservation of momentum.
- b) Helical flow (secondary currents) which is developing in channel bends due to curved streamlines is included. The time and space lag in the development of the helical flow is also described.
- c) Sediment transport, based on various model types (e.g. Van Rijn, Meyer-Peter and Müller, Engelund-Hansen, Engelund-Fredsoe, Yang, or user-defined empirical formulas). The effect of helical flow, gravity on a sloping river bed, shapes of velocity and concentration profiles are taken into account in separate bed load and suspended load sub-models based on the theories by Galappatti. Graded sediment descriptions can be applied as well by defining a number of different sediment fractions, which are treated separately by the sediment transport module
- d) Alluvial resistance due to bed material and bed forms (calculation of skin friction from the grain sizes and form drag friction from the bed forms).
- e) Scour and Deposition: Large-scale movement of bed material is computed. The continuity equation for sediment is solved for determining changes in bed elevations at each grid cell at every time-step. The effect of supply limited sediment layers can be incorporated as well. This is used for simulating for

instance downstream migration of fine material on a coarse riverbed, or for representing non-erodible (protected) riverbed areas in the modelling domain

3.9.1 Governing Flow Equation of MIKE 21C

By introducing the simplification of three dimensional Navier Stokes theorems the three dimensional flow pattern of river can be reduced to two dimensional equations of conservations of mass and conservation of momentum in the two horizontal directions. Three directional (secondary flow) effects are maintained in the depth averaged model by introducing helical flow component in the flow equation.

Flow model is valid for the shallow, gently varying topography and mildly curved wide river channels with small Froude numbers. The flow equations solved in the curvilinear hydrodynamic model of MIKE 21C are:

$$\frac{\delta p}{\delta t} + \frac{\delta}{\delta s} \left(\frac{p^2}{h} \right) + \frac{\delta}{\delta n} \left(\frac{pq}{h} \right) - 2 \frac{pq}{hR_n} + \frac{p^2 - q^2}{hR_s} + gh \frac{\delta H}{\delta s} + \frac{g}{C^2} \frac{p\sqrt{p^2 + q^2}}{h^2} = RHS \quad (3.26)$$

$$\frac{\delta q}{\delta t} + \frac{\delta}{\delta s} \left(\frac{pq}{h} \right) + \frac{\delta}{\delta n} \left(\frac{q^2}{h} \right) + 2 \frac{pq}{hR_s} - \frac{q^2 - p^2}{hR_n} + gh \frac{\delta H}{\delta n} + \frac{g}{C^2} \frac{q\sqrt{p^2 + q^2}}{h^2} = RHS \quad (3.27)$$

$$\frac{\delta H}{\delta t} + \frac{\delta p}{\delta s} + \frac{\delta q}{\delta n} - \frac{q}{R_s} + \frac{p}{R_n} = 0 \quad (3.28)$$

where

s,n Coordinates in the curvilinear coordinate system

p,q Mass fluxes in the s and n direction

H Water Level

h Water Depth

g Acceleration of Gravity

C Chezy roughness coefficient

Rs,Rn Radius of curvature of s and n line

RHS the right hand side in the force balance, which contains Reynolds stresses, Coriolis force and atmospheric pressure.

These equations are solved by an implicit finite differential technique with variables (water flux density p and Q in two horizontal directions and water depth H) defined on a space staggered computational grid.

3.9.2 Morphological Model of MIKE 21C

A morphological model of MIKE 21C is a combined sediment transport and hydrodynamic model (DHI 2009). The hydrodynamic flow field is updated continuously according to changes in bed bathymetry.

Morphological model is a uncoupled model. In uncoupled model, the solution of hydrodynamics is solved at a certain time step prior to solution of the sediment transport equations. Subsequently, a new bed level is computed and the hydrodynamic model proceeds with the next time step.

Sediment Continuity Equation

Following calculation of sediment transport of bed material (bed load and suspended load), the bed level change can be computed from the equation:

$$(1 - n) \frac{\partial z}{\partial t} + \frac{\partial S_x}{\partial x} + \frac{\partial S_y}{\partial y} = \Delta S_e \quad (3.29)$$

Where

- S_x Total sediment transport in x-direction
- S_y Total sediment transport in y-direction
- n Bed porosity
- z Bed level
- t Time
- x, y Cartesian coordinated system
- ΔS_e Lateral sediment supply from bank erosion

MIKE 21C morphological model solves the sediment continuity equation implicitly.

3.9.3 Bank Erosion Model of MIKE 21C

The sediment transport model can include bank erosion in the continuity equation:

$$E_b = -\alpha * (\partial z / \partial t) + \beta * S/h + \gamma \dots \dots \dots (3.30)$$

Where

E_b = Bank erosion rate in m/s

Z = Local bed level

S = Near bank sediment transport

h = local sediment transport

α, β, γ calibration coefficients specified in the model

Observed bank erosion rates are used to calibrate the coefficients α and β . The recommended range of α is 0 to 20 while that for β is 0 to 1. A constant value of γ can be used for the model.

3.10 Methodology

Modeling of any physical phenomenon is an iterative development of a process. Model refinements are based on the availability and quality of data, hydrological understanding and scopes of the project. The general approach that has been followed in the current study can be summarized in the flowchart given in Figure 3.5. A brief description of the methodology and approaches are provided in this section to achieve the study objectives.

3.10.1 Collection of Data

Historical water level and discharge data of Jamuna River have been collected from IWM and BWDB. Recent data on river cross section, sediment transport within the study area and satellite images have also been collected from CEGIS. All the collected data were then compiled, processed and analyzed to the required extent for use in the model development and application. The detail description of data collection is discussed in next chapter.

3.10.2 Hydrological and Morphological Analysis of Collected Data

Based on the historical water level and discharge data, hydrological analysis have been done to understand the hydrological condition of the study area.

Planform analysis, bankline shifting etc have been carried out by using different satellite images (Chapter 4).

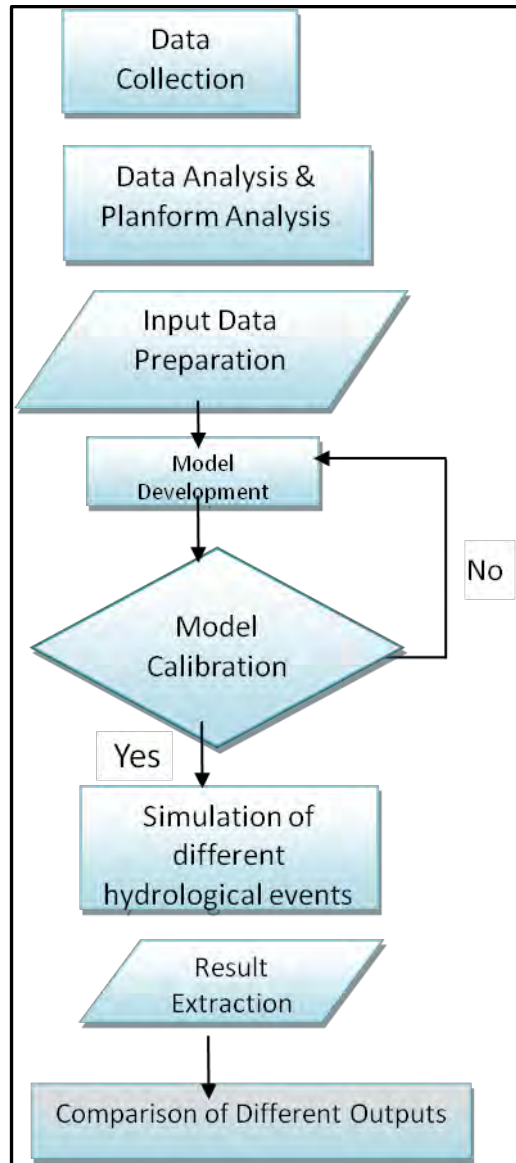


Figure 3.5 Flow Chart of methodology applied in this study

3.10.3 2-D morphological Model Set-up for the Study Area

Morphological assessment has been carried out with the aid of two-dimensional (2D) morphological model to resolve the governing physical processes to a sufficient degree of detail. A 2D model has been setup for 160 km reaches of Jamuna River. The model is based on the bathymetric data of post-monsoon 2011. The model is calibrated for both hydrodynamic and morphological conditions for the hydrological monsoon of 2012. The

model is also validated for hydrological monsoon of 2013 using the same calibrated parameters.

3.10.4 Selection of Different Flood Events by Frequency Analysis

After calibration and validation, this model has been finally used for different option simulations for different flood events. These hydrological flood events have been selected by frequency analysis using HYMOS software tool. For frequency analysis, historical discharge data of Jamuna River at Bahadurabad station were used and finally two different hydrological years have been selected.

3.10.5 Identification of Vulnerable Reaches for introducing bank protection measures

Based on model simulations five vulnerable reaches located in five different reaches under five districts have been selected to study the response of bank protection works along these reaches. In this regard revetments were incorporated in the model and the model was simulated for two different hydrological events.

CHAPTER 4

DATA ANALYSIS & MODEL DEVELOPMENT

4.1 General

In order to develop the mathematical morphological model, various kinds of data of recent and previous years have been collected and compiled. These data also form the basis for further analysis and interpretation of the model results leading to accurate assessment of hydro-morphological condition of the study area. According to the modelling requirements, a significant amount of data includes water level, discharge, cross-section, sediment data, satellite images and other relevant information like bank characteristics etc have been collected. This chapter describes a brief discussion about the collected data.

4.2 Data Collection

Quality data are prerequisite for reliable model setup, model results and to have understanding on the existing physical processes. To determine the present hydraulic and morphological conditions and to develop a mathematical model of Jamuna River, various data have been collected from different sources. A brief description of data is given below:

4.2.1 Water Level

Water level data at different locations are required for calculating the river slope, defining water level of different flood events as well as providing boundary of two-dimensional model and to calibrate the model. Therefore, historical water level data at Bahadurabad, Sirajganj and Aricha station of Jamuna River have been collected and analyzed to get an idea about the amount of water is flowing at this location. The duration of collected data are listed in Table 4.1. For calibration purpose, water level of Sirajganj station at Jamuna River during 2012 has been used.

Table 4.1 Available water level data for the study area

Station Name	Station ID	River Name	Easting (BTM)	Northing (BTM)	Duration	Source
Noonkhawa	SW45.0L	Jamuna	482190.1	865430.9	1990-2013	BWDB
Bahadurabad	SW46.9L	Jamuna	470050.2	782401.8	1990-2013	BWDB
Sirajganj	SW49.0R	Jamuna	472517.9	705832.151	1990-2013	BWDB
Aricha	SW 50.6L	Jamuna	496245.3	758008.5	1990-2013	BWDB

4.2.2 Discharge

Discharge data is needed to investigate the hydrological characteristics of the river and to provide boundary for the two-dimensional morphological model. Available discharge data for the Jamuna River is listed below (Table 4.2):

Table 4.2 Available Discharge Data for the Study Area

Station Name	Station ID	River Name	Easting (BTM)	Northing (BTM)	Duration	Source
Bahadurabad	SW46.9L	Jamuna	470050.2	782401.8	1956-2013	BWDB & IWM

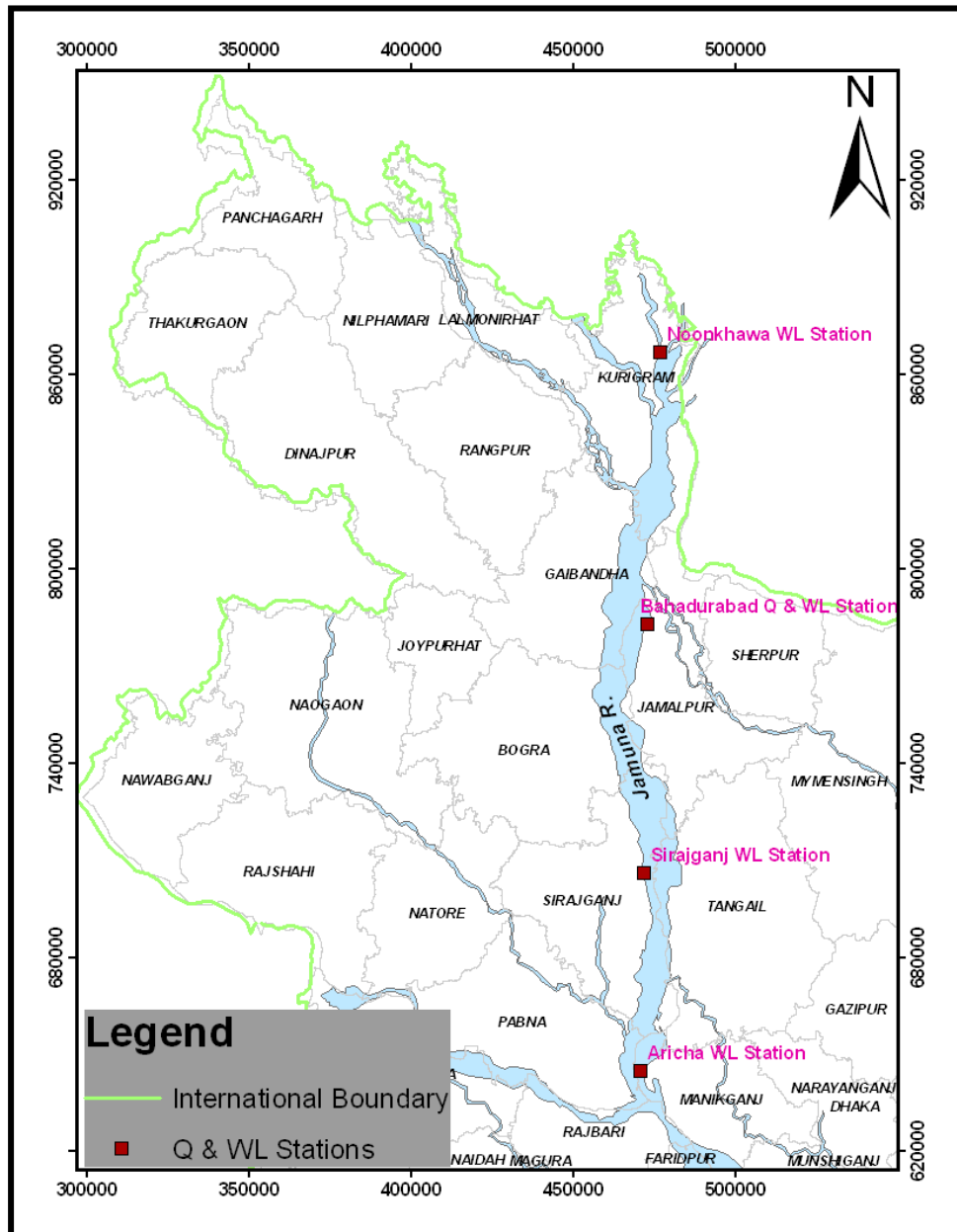


Figure 4.1 Location of discharge and water level station within the study area

4.2.3 Bathymetry Data

The post-monsoon 2011 bathymetry data of Jamuna River have been collected from IWM. These surveyed bathymetry data covers the entire 240km reach of Jamuna River from Noonkhawa at upstream to Aricha at downstream. Figure 4.2 shows the transect lines of bathymetry data within this reach. The spacing between the transect line is about 1km.

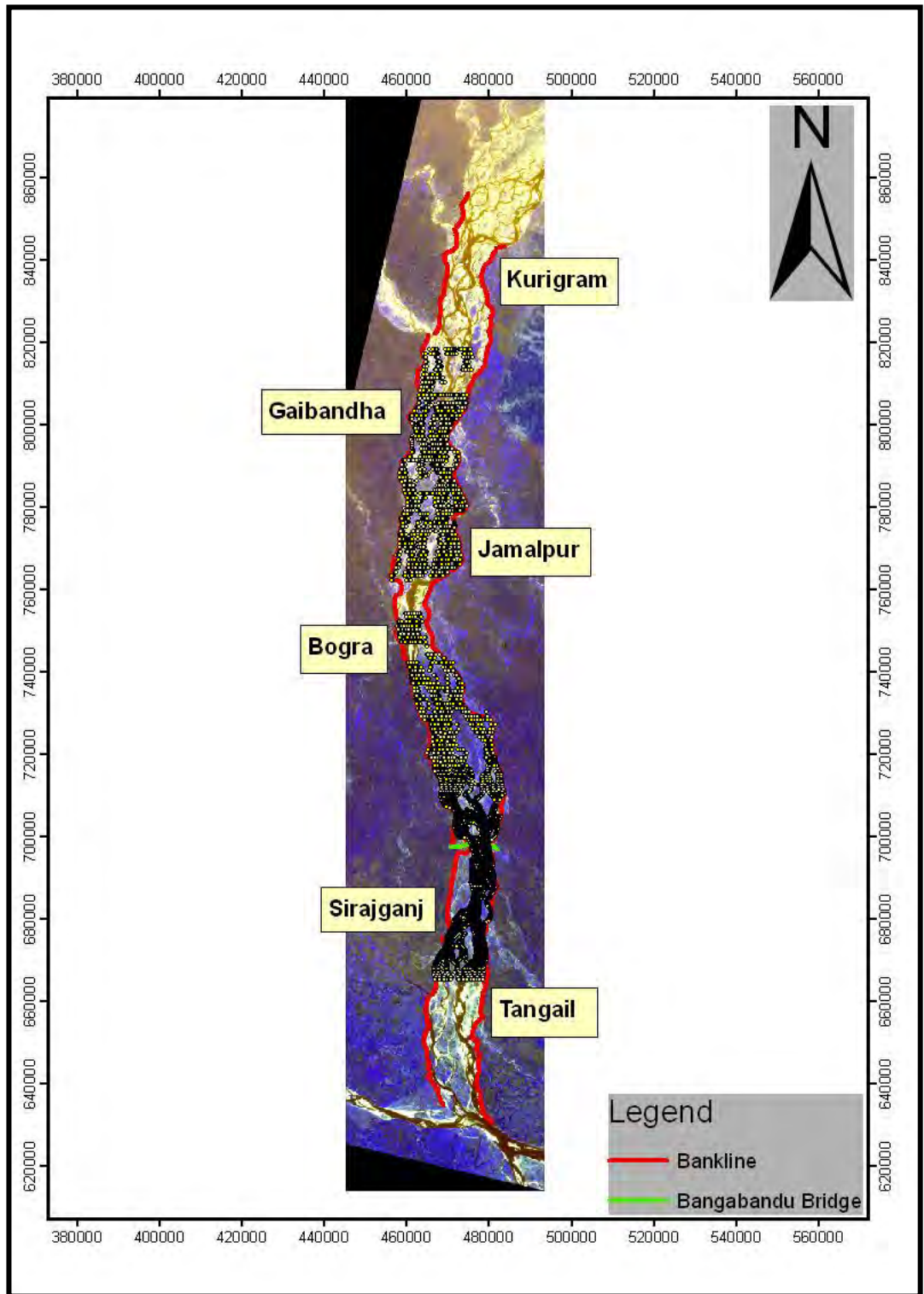


Figure 4.2 Transect line of bathymetric survey for the study area in Jamuna River

4.2.4 Satellite Image

The satellite images of Jamuna River of 2001, 2003, 2005, 2007, 2009 to 2013 have been collected from CEGIS for planform analysis and to delineate the bank lines for assessment of bankline shifting.

4.2.5 Bankline Data

Bankline data of Jamuna River have been collected for September 2011 (Figure 4.2) to generate the computational grid of the model.

4.2.6 Sediment Data

Sediment and other pertinent data were used in the model as input. The collected sediment data of the Jamuna includes suspended sediment and bed sample data.

Table 4.3 Available Sediment Data for the Study Area

Suspended Sediment Data			Bed Sample Data	
Station	Data Period	Source	Year of Sampling	Source
Bahadurabad	1966-70, 1976-82, 1983-88 and 1993-	BWDB and FAP 24	1993-96	FAP 24

4.3 Data Analysis

4.3.1 Hydrological Analysis

4.3.1.1 Water Level

Yearly maximum, minimum and average water level data of Jamuna River at Bahadurabad, Sirajganj and Aricha stations have been plotted as shown in Figure 4.3 to Figure 4.5 respectively.

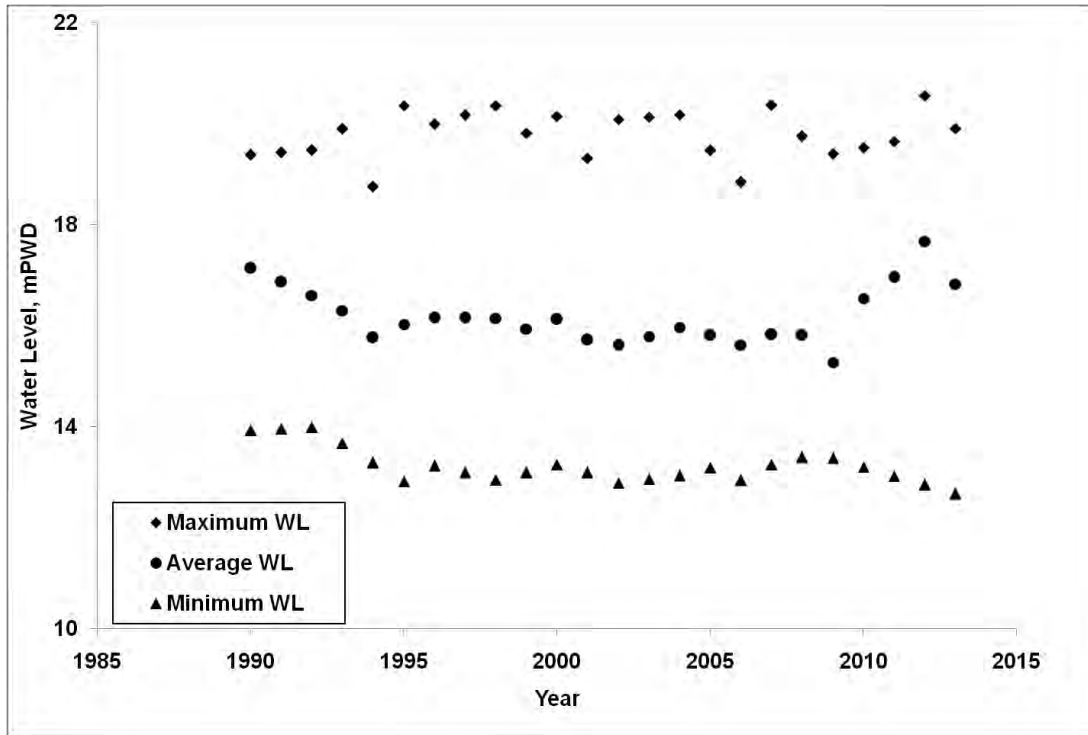


Figure 4.3 Maximum, minimum and average water level at Bahadurabad station of Jamuna River

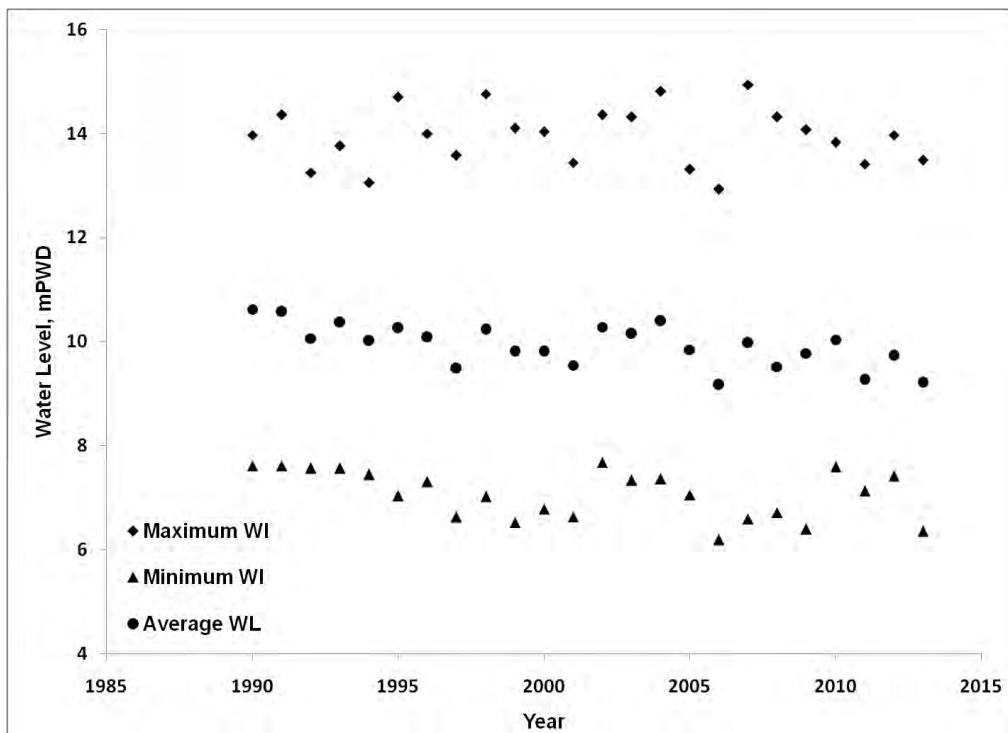


Figure 4.4 Maximum, minimum and average water level at Siajganj station of Jamuna River

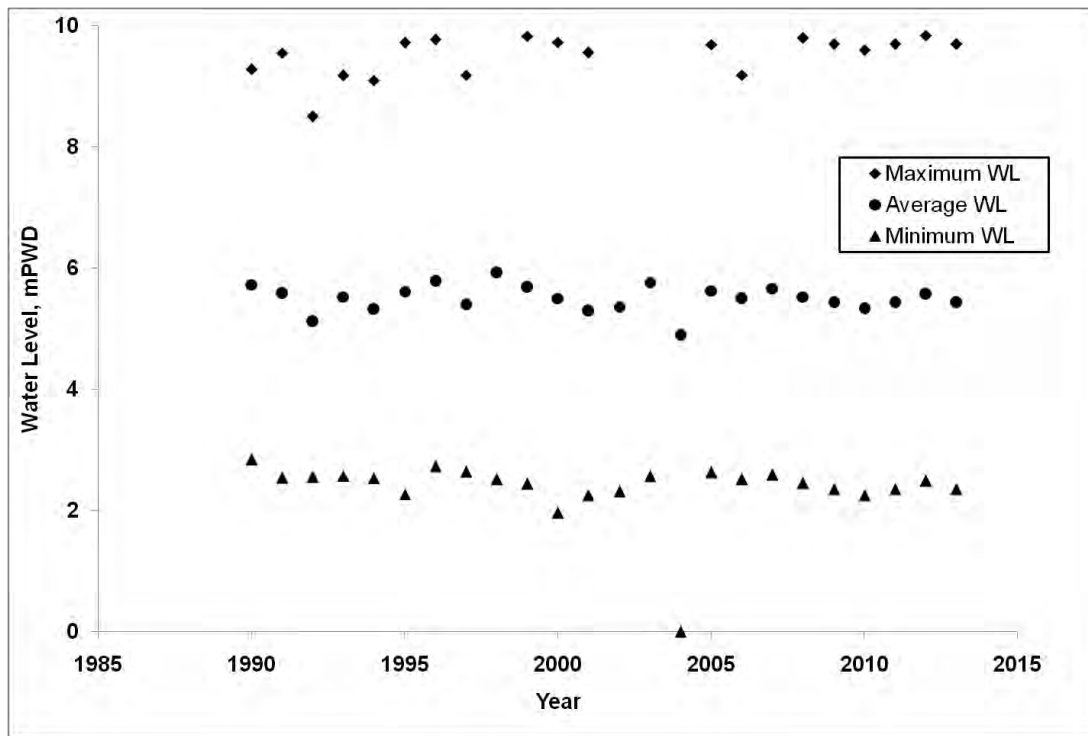


Figure 4.5 Maximum, minimum and average water level at Aricha station of Jamuna River

4.3.1.2 Discharge

Historical discharge data of Jamuna River at Bahadurabad station that have been collected from IWM are analyzed and plotted in Figure 4.6. From this figure, it is evident that maximum discharge occurred in the year 1998.

4.3.1.3 Frequency Analysis of Discharge Data

Using the maximum discharge shown in Table 4.4 the frequency analysis has been made with the tool HYMOS, Table 4.5 shows the discharge of different return periods for different distribution methods.

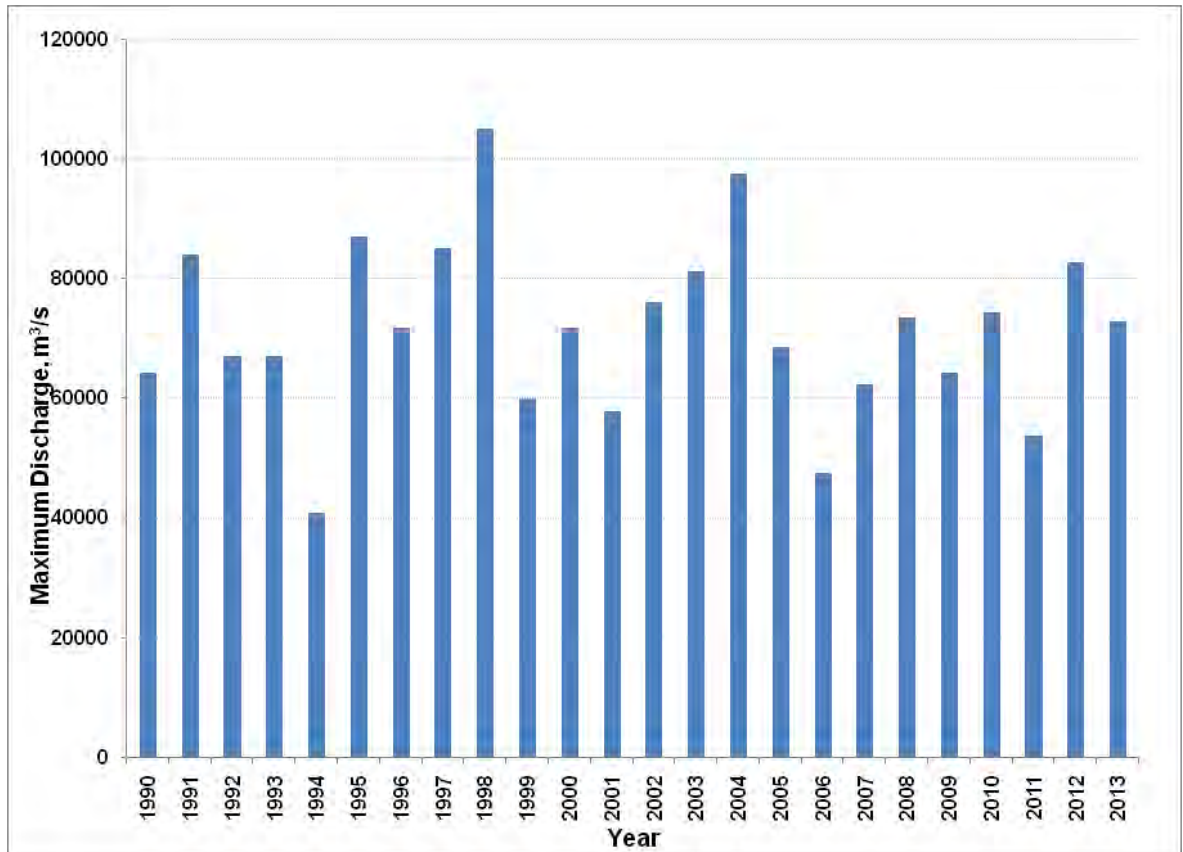


Figure 4.6 Yearly Maximum discharges at Bahadurabad station of Jamuna River

Table 4.4 Yearly maximum Discharge of Jamuna River from 1956-2012

Year	1950s	1960s	1970s	1980s	1990s	2000s	2010s
0		64800	75000	61200	64300	71907	74339
1		53800		66500	84100	57803	53864
2		69400	66600	55900	67000	76093	82746
3		56400	67300	56200	67000	81365	72838
4		63100	91100	76800	40900	97709	
5		64200	52200	63700	87000	68565	
6	60400	68900	65600	43100	71747	47626	
7	62500	69600	66600	73000	85090	62379	
8	71300	62300	56600	98300	103249	73509	
9	68500	56000	66100	70700	60047	64217	

Table 4.5 Peak flows of Jamuna River at Bahadurabad for selected return periods using different distribution

Probability Distribution	Return Period in year					
	2.33	5	10	25	50	100
Gumbel (EV1)	68688	78976	87356	97944	105799	113596
Log Pearson-3	69940	77974	84929	93264	99213	104990
Log Normal	69136	78013	84456	91902	97050	101923

Frequency analysis has been made based on the probability plots and goodness of fit tests (Chi square test and K-S test). The following Probability Plots in Figure 4.7 to Figure 4.9 show the Probability values using Gumbel, Log Pearson three parameters and Log Normal distribution respectively. From these figures it is seen that the confidence level of log-normal distribution is less variable among the three distributions.

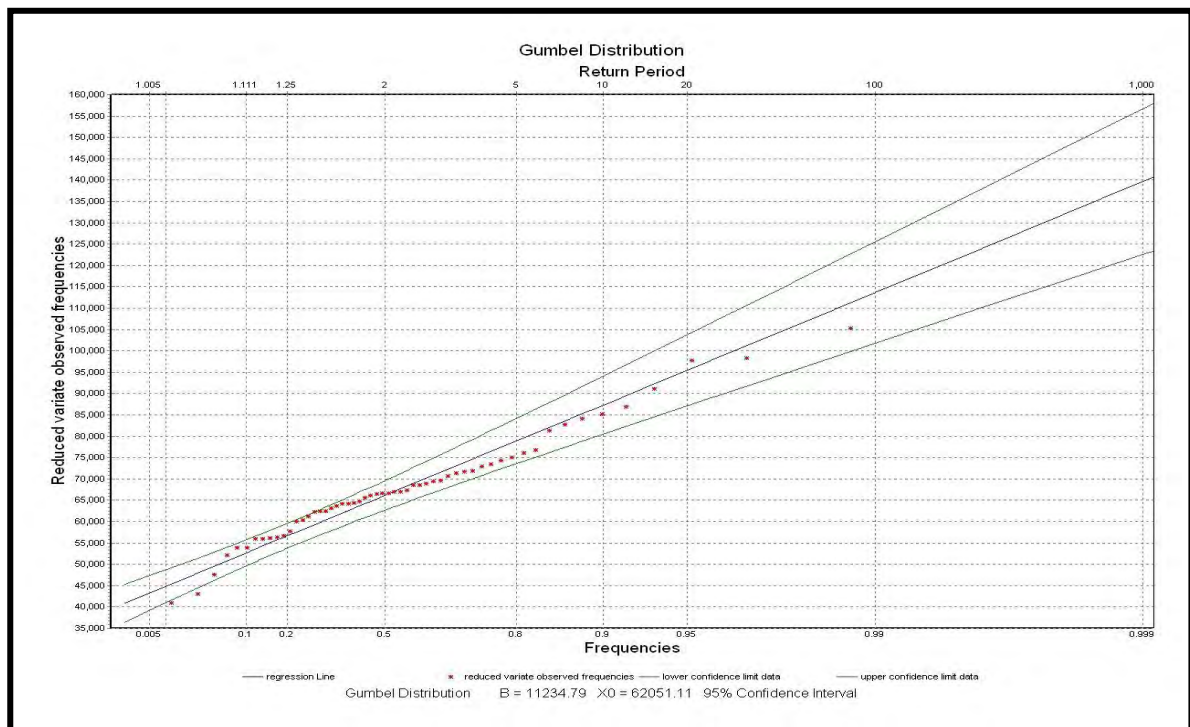


Figure 4.7 Gumbel Distribution of discharge data at Bahadurabad station

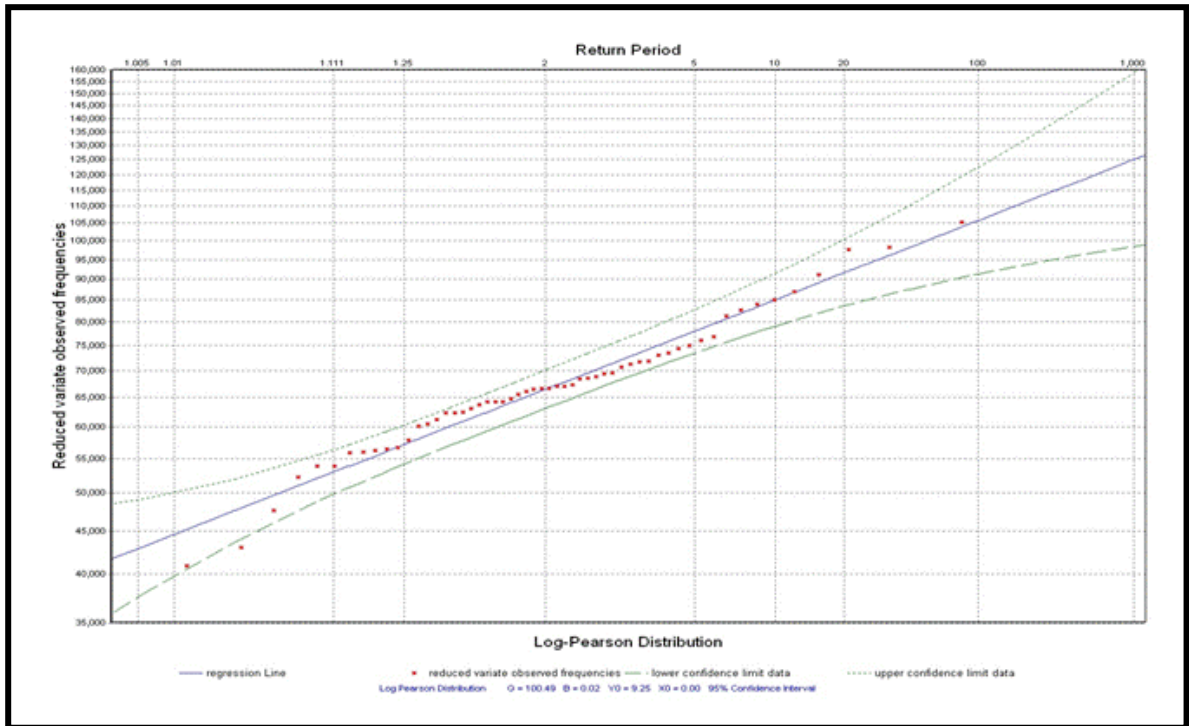


Figure 4.8 Log-Pearson Distribution of discharge data at Bahadurabad station

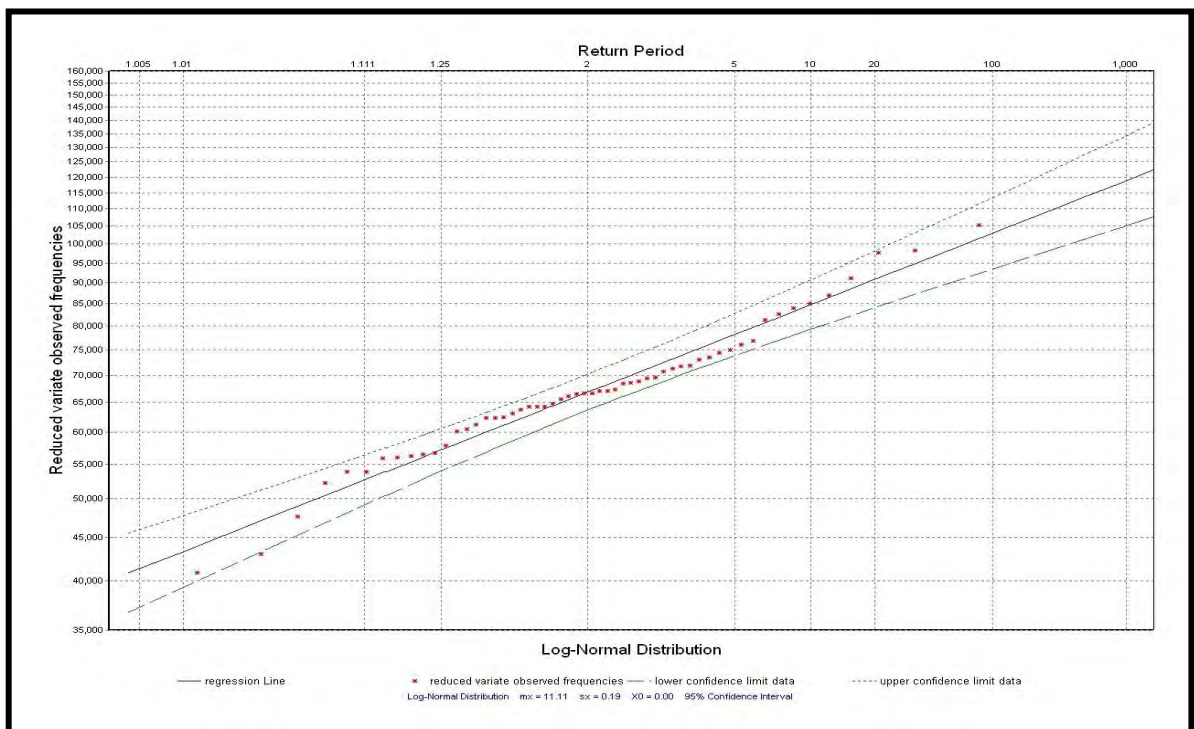


Figure 4.9 Log-Normal Distribution of discharge data

To select the best fit among the three distributions Chi square test and Kolmogorov-Smirnov (K-S) test has been made. The values of Chi Square and Kolmogorov-Smirnov test variates are presented in Table 4.6.

Table 4.6 Goodness of fit test among three distributions

Test	Gumbel	Log-Pearson	Log-Normal
Chi Square	11.655	9.42	8.54
Variate of K-S Test	0.118	0.096	0.085

From Table 4.6 it is seen that chi square is minimum for Log Normal distribution. Again It is know that if Chi square is equal to zero the theoretical and observed frequencies agree exactly; while if chi square is greater than zero they do not agree exactly and the larger the value of Chi square the greater is discrepancy between the observed and expected frequencies. Again the variate of K-S is also found minimum for Log-normal distribution.

4.3.1.4 Determination of Flood Events for Selected Probability Distribution

Among the Gumbel, Log Pearson three parameters and Log Normal distribution the chi square value is found minimum for the Log Normal distribution. Considering the two goodness of fit test the Log Normal three parameters has been selected to estimate the flood discharges for the selected return periods. Table 4.7 gives the peak flow according to Log Pearson three parameters distribution for two return periods and corresponding year that experienced equivalent flood discharges.

Table 4.7 Peak flow according to Log Normal three parameters distribution

Return period	Peak flow according to Log Normal 3, m ³ /s	Observed peak flow, m ³ /s	Corresponding year
2.33	69136	68565	2005
100	103059	1,03,249	1998

4.3.1.5 Determination of Flood Event for Bankfull Discharge Event

Bankfull discharge of Jamuna River at Bahadurabad station has been calculated from various empirical formulae. The bankfull discharges obtained have been enlisted in Figure 4.

Table 4.8 Comparison of different bankfull discharge predictors

Author of the Equation	Predictor	Predicted bankfull discharge (cumec)
Chang, 1979	Graphical relation	40000
Williams, 1978	$Q_b = 4 \times A^{1.21} i^{0.28}$	50000
Inglis, 1968	50% of Q_{max}	52000
Wolman and Leopold, 1957	1 to 2 year return period	67000

Based on the calculated bankfull discharges 2011 flood event was selected as bankfull event.

4.4 Morphological Analysis

4.4.1 Sediment Transport Analysis

Sediment rating curve of Jamuna have been prepared from the available historical sediment data of Bahadurabad station and Mymensingh station. The sediment discharge and corresponding flow discharge of Jamuna River have been plotted on log-log paper, shown in Figure 4.10.

From trend line analysis the following relationships have been found.

For Jamuna River the equation is as follows:

$$Q_s = 0.125 Q^{1.480} \quad (4.1)$$

Where, Q_s and Q is the sediment discharge and water discharge.

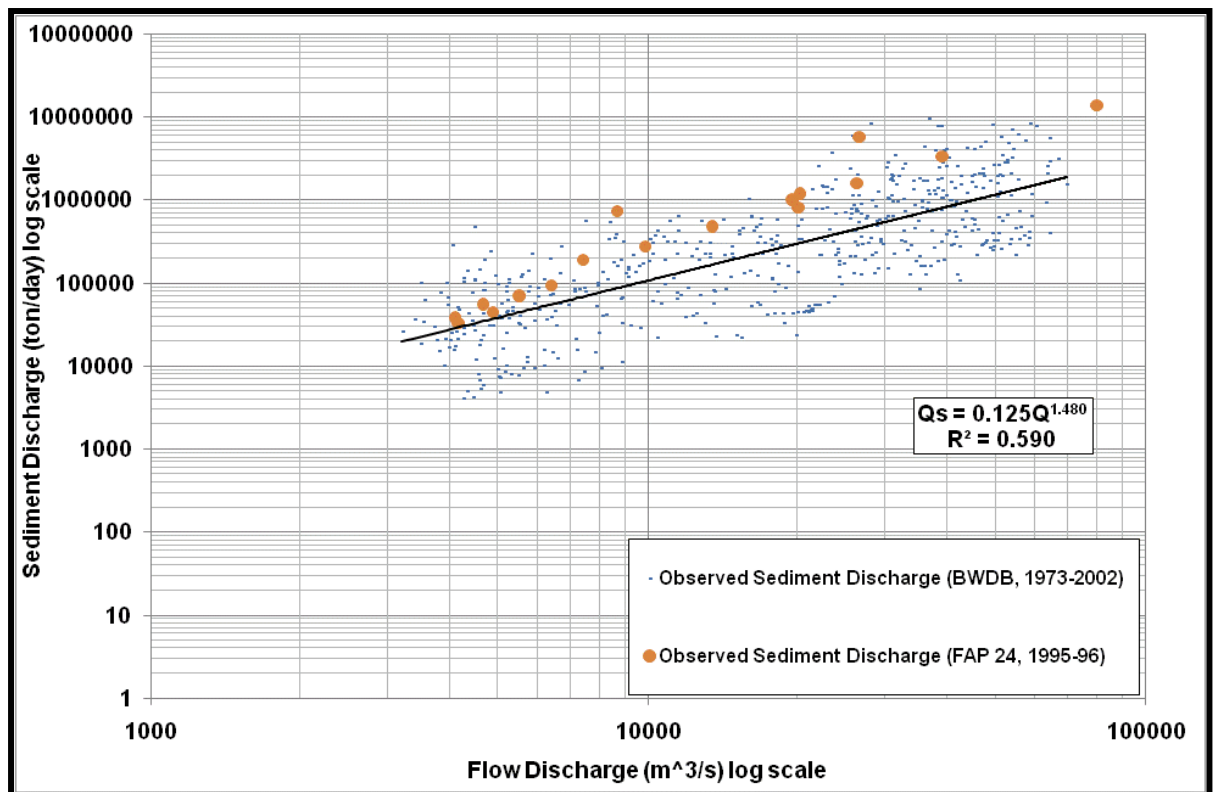


Figure 4.10 Sediment rating curve of Jamuna River at Bahadurabad station during 1968-2002

Sediment transport analysis has been done for Jamuna River by using the suspended sediment data from the period 1968 to 2002. For the Jamuna River, the combined yearly sediment transport is found 1200 million tons per year on the average (FAP 24).

4.4.2 Planform Analysis

Satellite Data Used

Time-series of satellite images were used to document historical changes in morphology and to provide the basis for the long-term bank erosion process of the Jamuna River. The time series of satellite images cover the period 1998 to 2012. Most of the images cover the entire Jamuna River starting from 6 km up from the international boundary with India and ending at 15 km down to its confluence with the Padma and the Ganges. Information about the satellite images used in the analysis is presented in Table 4.8.

Table 4.9: List of images

Image year	Image type	Image date	Resolution
1998	Landsat TM	5 Feb	30m x 30m
1999	Landsat TM	23 Jan	30m x 30m
2001	Landsat TM	28 Jan	30m x 30m
2003	IRS LISS	8 Mar	24m x 24m
2005	IRS LISS	17 Jan	24m x 24m
2006	IRS LISS	5 Feb	24m x 24m
2007	ASTER	14 Jan	15m x 15m
2009	ASTER	18 Jan	15m x 15m
2011	ASTER	12 Jan	15m x 15m
2012	ASTER	19 Jan	15m x 15m
2013	ASTER	30 Jan	15m x 15m

Image Processing and Geo-referencing

Analyses were done using time series bank lines that were delineated on geo-referenced satellite images. Each raw satellite image was transformed into a file referenced to the Bangladesh Transverse Mercator (BTM) projection. The BTM projection, described by ISPAN (1992), has the following features:

Ellipsoid	:	Everest 1830
Projection	:	Transverse Mercator
Central meridian	:	90° E
False easting	:	500,000 m
False northing	:	-2,000,000 m

The geo-referenced images were used to delineate the bank lines of the river. Bank lines are generally well defined in meandering rivers, but with regard to the very dynamically braided rivers the task is often challenging. The bank line separates the floodplains from the riverbed. spread over the floodplains during floods by overtopping the banks), are considered to be part of the riverbed. The yearly bank lines of Jamuna River are depicted in Figure 4.11.

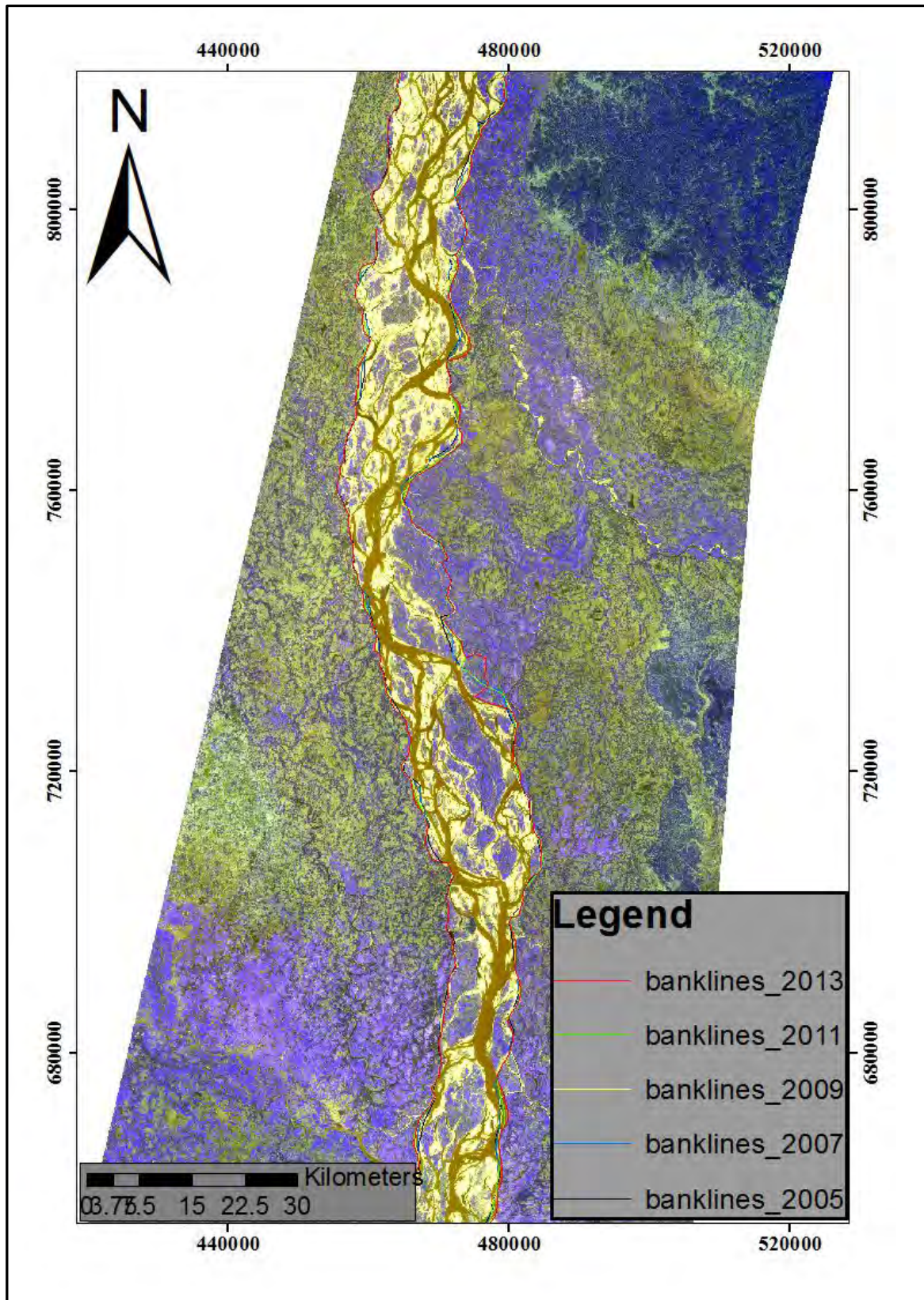


Figure 4.11 Delineated bank lines of Jamuna River for several years

4.5 Model Development for the Study Area

Mathematical modeling is an advanced technology in Water Resources Engineering for predicting variables which is tedious to find in hand calculation. To evaluate such variables which involve in the river response due to dredging, a two-dimensional morphological model, MIKE 21C has widely been used. Using this modeling software a model of Jamuna River in a selected reach has been developed. The various key steps during process the model is described below.

4.5.1 Model Setup

The model setup includes the generation of computational grids, the preparation of the bathymetry, boundary conditions and selection of calibration parameters. Followed by the set up, the model is calibrated with the tuning of hydrodynamic parameters (like Chezy's bed roughness, eddy viscosity etc.), the parameters in the sediment transport magnitude formula e.g., bed load and suspended load factors. Then the model will be simulated for different applications runs. Detail methodology for model set-up, calibration and option simulations are presented in the following sections.

4.5.2 Generation of Computational Grid

The curvilinear computational grid has been generated on the basis of bank line surveyed in post monsoon 2011. The grid has the dimension of 499 grid points along the river and 125 grid points across the river, i.e. 62325 grid points in total. Average spacing of the grid is 320m along the river while it is 62m across the river. The grid has land boundaries as well. The model simulates the hydrodynamic and morphological parameters in every computational grid point. The computational grid is shown in Figure 4.12.

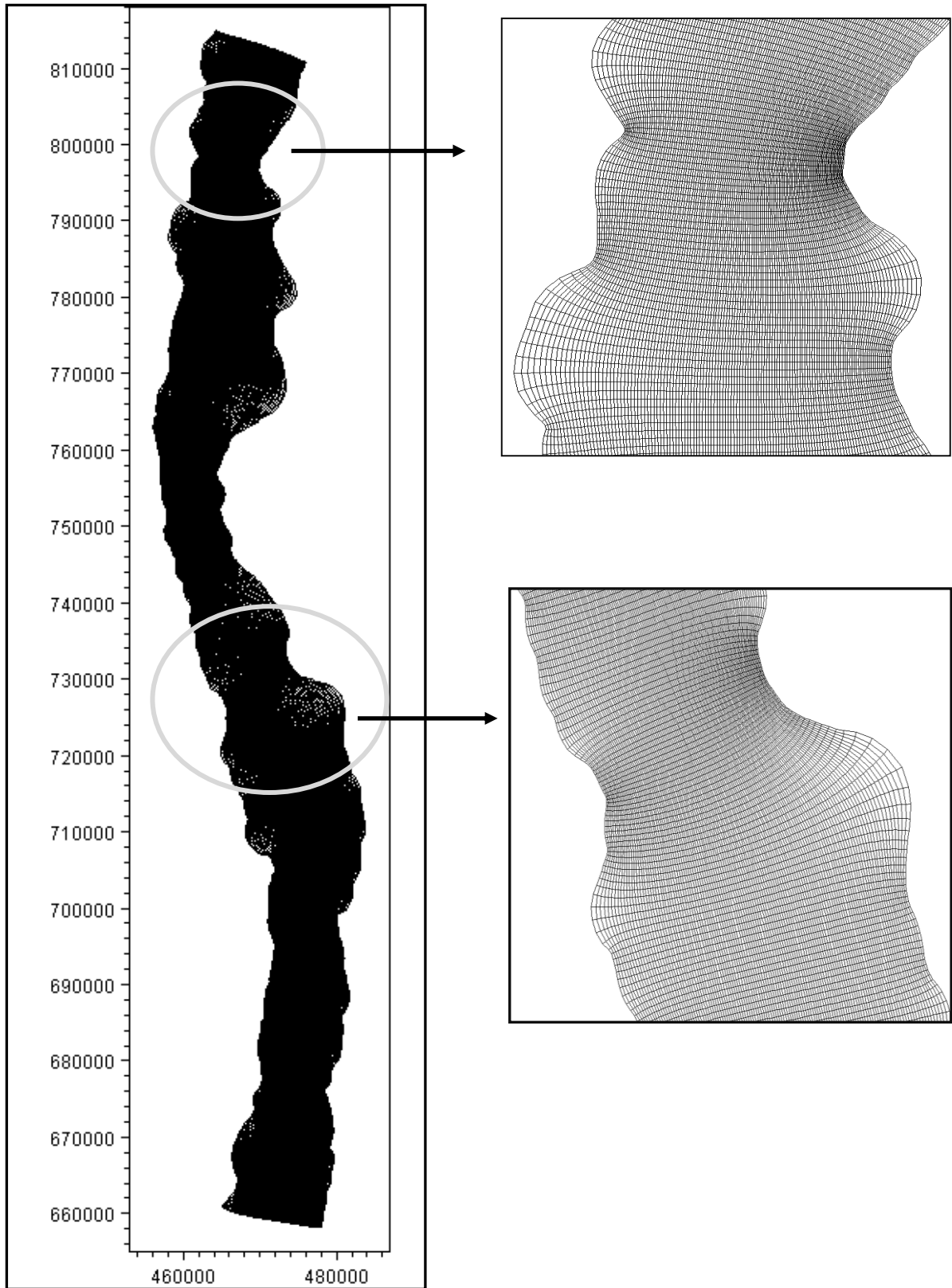


Figure 4.12 Computational grid cells in the study area

4.5.3 Generation of Model Bathymetry

The bathymetry of the model has been prepared based on data from the IWM bathymetric survey carried out during Post-monsoon 2011. A part of the initial bathymetry of the model appears in Figure 4.13. To simulate the morphological model with different hydrological events, the bathymetry data has been superimposed on the curvilinear grid (Figure 5.1). Hence every grid cell contains river cross-section data and after model simulation every grid cell produces hydrological and hydraulic parameters like, water level, discharge, water depth, velocity, bed scour and others.

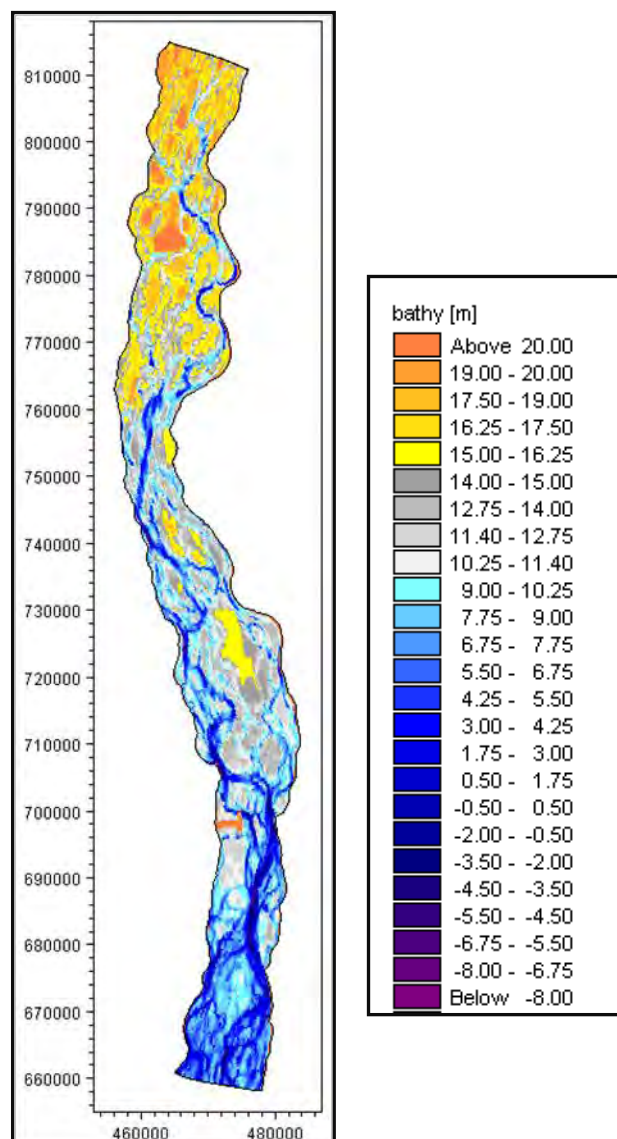


Figure 4.13 Model bathymetry of the study area for post-monsoon 2011

4.5.4 Model Calibration

It is always customary to calibrate and validate the model before making any predictions using the model, so that the reliability of the predictions can be made as much as perfect. In this study, model has been calibrated by using the boundary of 2012 as shown in Figure 4.14.

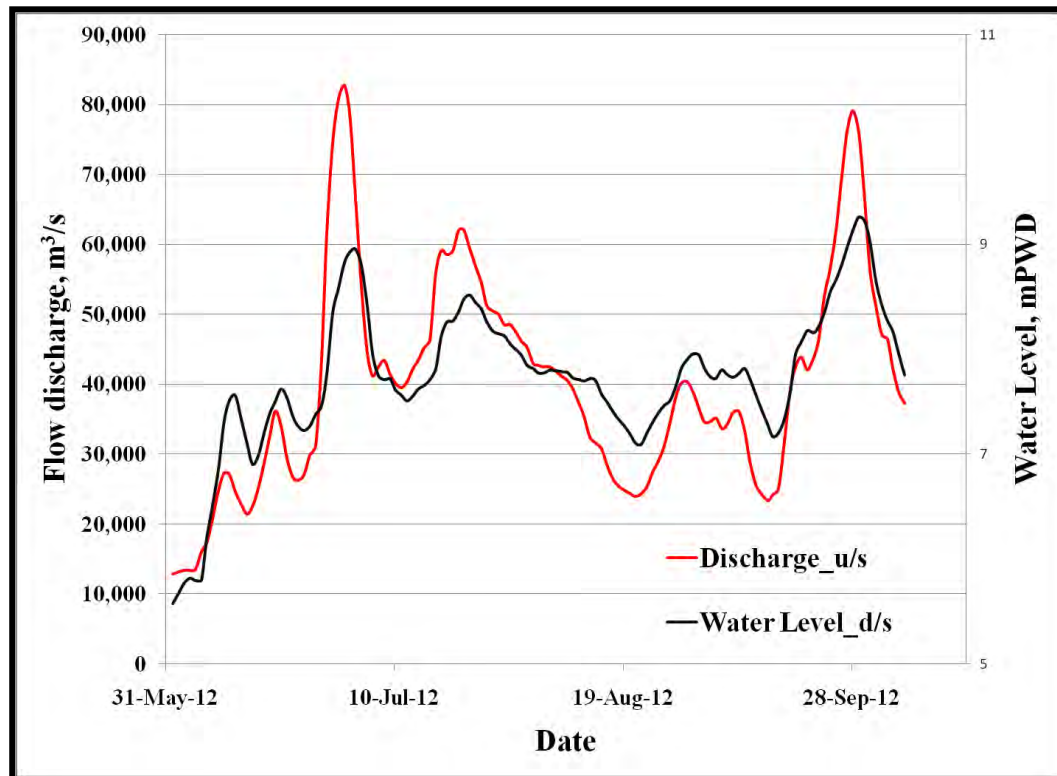


Figure 4.14 Boundary conditions for the year 2012

This section provides brief description of the hydrodynamic and the sediment transport calibration of the morphological model.

Hydrodynamic Calibration

Hydrodynamic calibration is done with the fixed bed model. Water level calibration has been done at Sirajganj station in Jamuna River. The parameters which contribute in adjusting the hydrodynamic misbalance or fine tuning the numerical models in the hydrodynamic field in MIKE21C are mainly roughness (Chezy's C), co-efficient of eddy viscosity (E) where Chezy's C influence in adjusting the water level and co-efficient of eddy viscosity used for the distribution of flow by exchanging lateral momentum of flow. The Chezy value can vary spatially and is also a function of depth. The functional

relation can be updated after each computational time step. In this model, Chezy value is updated at every time step according to the updated depth from the following formula:

$$C = a * h^b$$

Here h represents depth while a and b are alluvial resistance coefficient and exponent respectively.

Numbers of trial simulations were carried to verify the selection of the C and finally C =60 has been fixed as initial Chezy value and for the selection of the value for alluvial resistance coefficient and the exponent, as 25 and the exponent, b as 0.5 were used. So by taking these values, the equation stands in the form of $C = 25 * h^{0.5}$. The maximum limit for Chezy's factor C is considered as 95 and the minimum as 15. The reason for using the limiting value of the Chezy's factor is to control the extreme roughness of the model domain. In all the simulations, the value of eddy viscosity is 3.0 for Jamuna River. The summary of the parameters used in the model domain are shown in Table 4.10.

Table 4.10 Summary of the parameters used for the model domain

General Time Space (s)	Momentum Time space (s)	Pressure Time space (s)	Sediment transport Equation	Chezy C= $C_0 h^n$		Eddy Viscosity m^2/s
				a	b	
10	10	10	Engelund Hansen	25	0.5	3.0

The model is simulated for a specified period. Since the morphological changes and bank erosion take place primarily during the high discharges, the simulation period is selected so that it can include the main contributing part of the monsoon. On this basis the period has been chosen. So, for representing the scenario of the hydrological year total 127 days were considered starting from 1st June to the 7th October for calibration purpose. The hydrodynamic time-step has been set to 10 second for the simulation. Figure 4.15 shows the calibration results at Sirajganj station in Jamuna

River. The comparison shows more or less good agreement between the simulations.

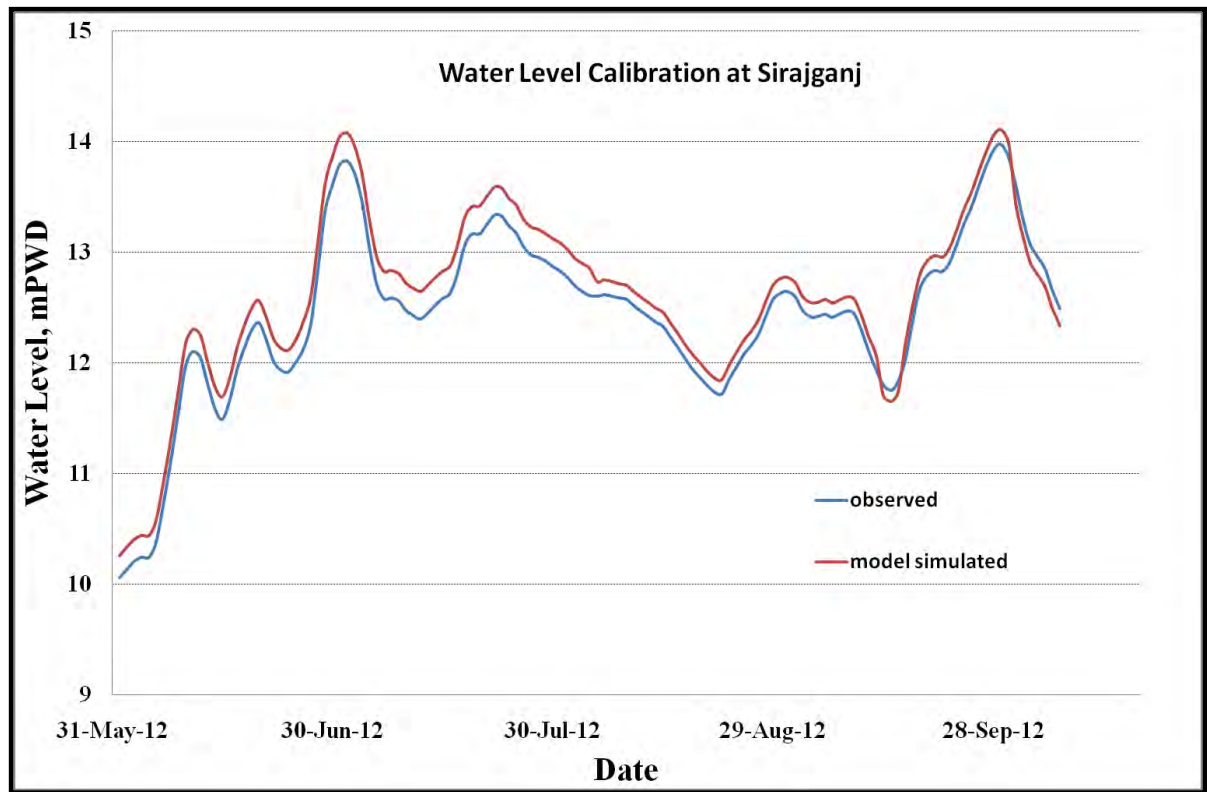


Figure 4.15 Water Level Calibration at Sirajganj Station for the year 2012

Sediment Transport Calibration of the Morphological Model

The calibration of the morphological model is basically meant in MIKE21C to deal with the sediment transport and its associated parameters, such as the grain size diameter, the selection of sediment transport formula, the helical flow strength etc. The value of grain size diameter is taken according to surveyed diameter for Jamuna River. In this study, calibration was done on the basis of the sediment transport rating curve at Sirajganj station for Jamuna River. For the application and for calibration of the model, Engelund-Hansen sediment transport formula provided better result compared to that of Van Rijn. Bed load and suspended load factors were taken as 0.4 and 1.6 respectively, The calibration of sediment transport rate is shown in Figure 4.16.

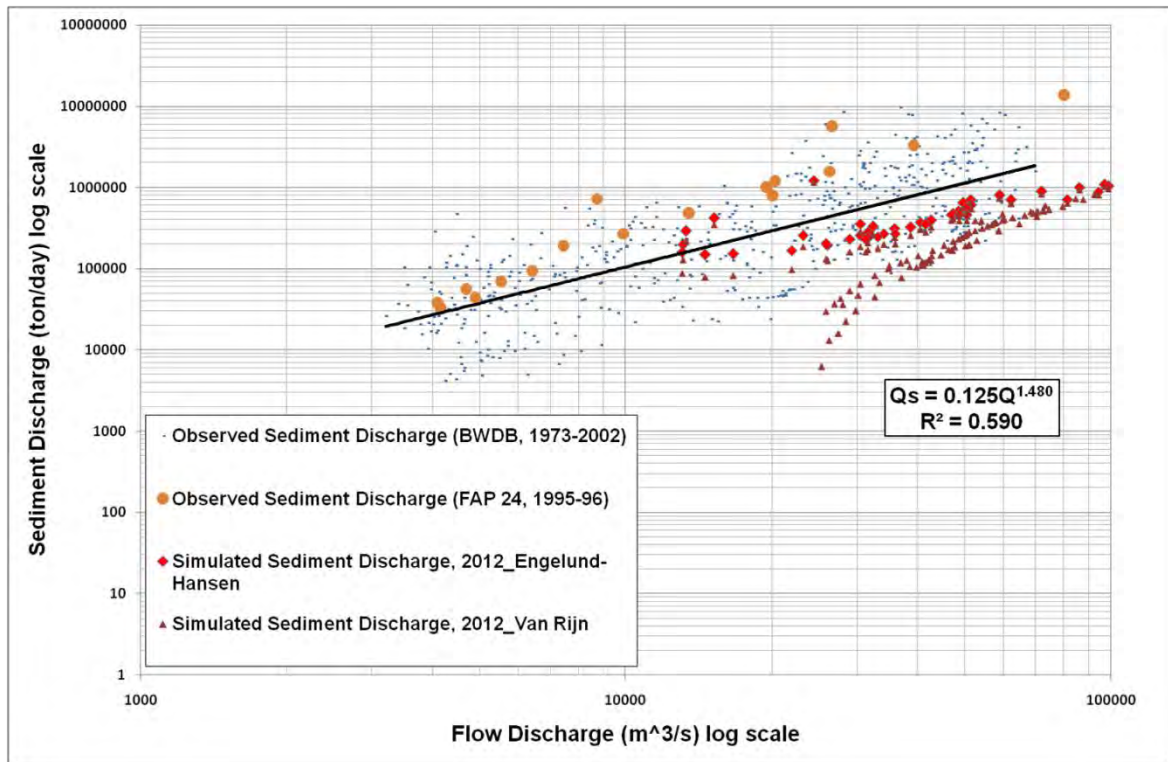


Figure 4.16 Sediment transport rate Calibration at Sirajganj Station for the year 2012

4.5.5 Model Validation

The calibrated model is validated by running for one or more simulations for which measurements are available without changing any calibration parameters. Here, model has been hydro-dynamically and morphologically validated by using the boundary of 2013. The boundary used in the model is shown in Figure 4.17.

Hydro-Dynamic Validation

Figure 4.18 shows the comparison of observed and simulated water level at Sirajganj station. It is seen that the simulated water level is almost matched with the observed one.

Morphological Validation

The model has been morphologically validated against the year of 2013. The sediment transport for 2013 is also compared with the available sediment data and presented in Figure 4.19. The simulated discharge lies within the range of observed sediment transport value.

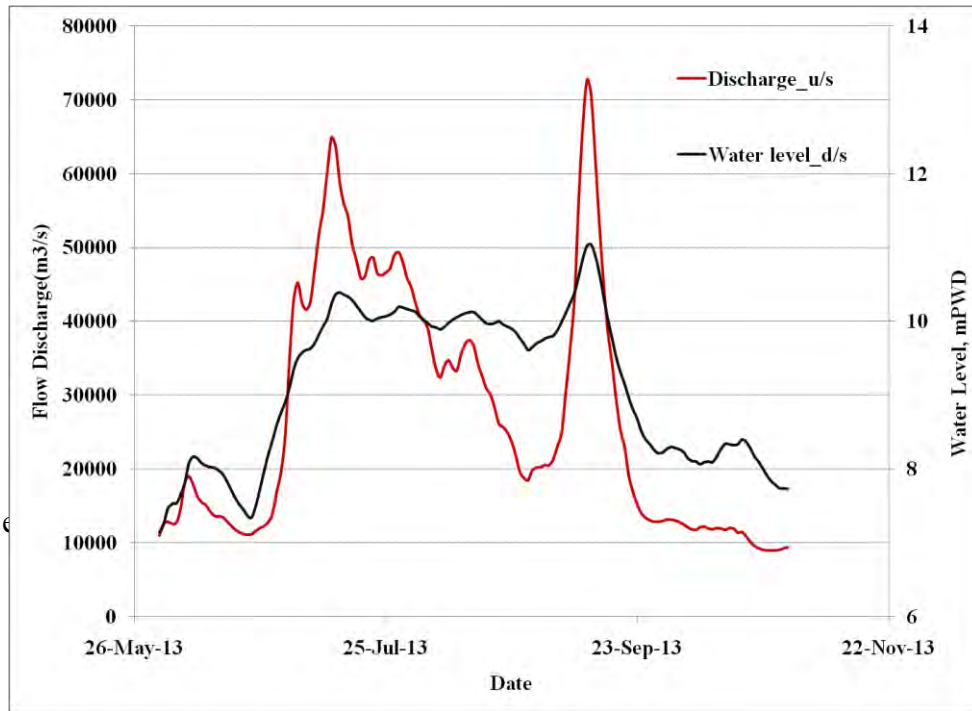


Figure 4.17 Boundary Conditions used in the model for the year 2013

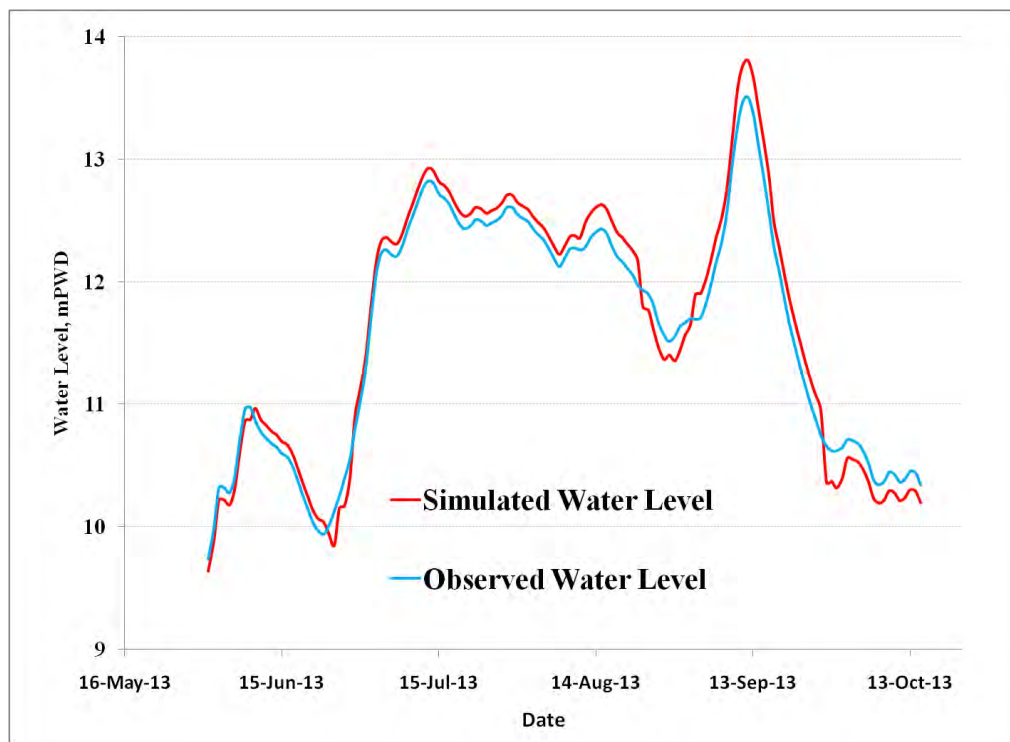


Figure 4.18 Comparison of Observed and Model simulated water level for 2013

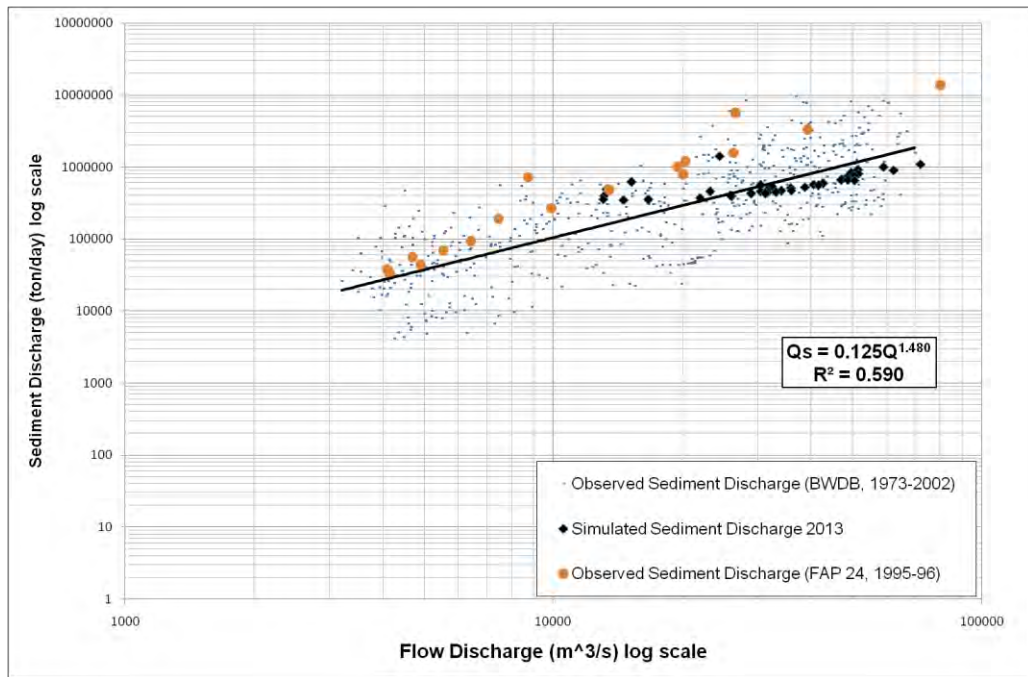


Figure 4.19 Comparison of Sediment transport rate at Sirajganj Station for the year 2013

4.5.6 Calibration of Bank Erosion

Two parameters alpha (α) and beta (β) are the calibration parameters of bank erosion module. Value of alpha was taken as 1 to 10 while value of beta was taken as 0.01 to 0.05. The trend of bank erosion of the selected reach of Jamuna River has been calibrated for the year 2012. The model simulated bank lines and digitized bank lines is illustrated in Figure 4.20 and Figure 4.21.

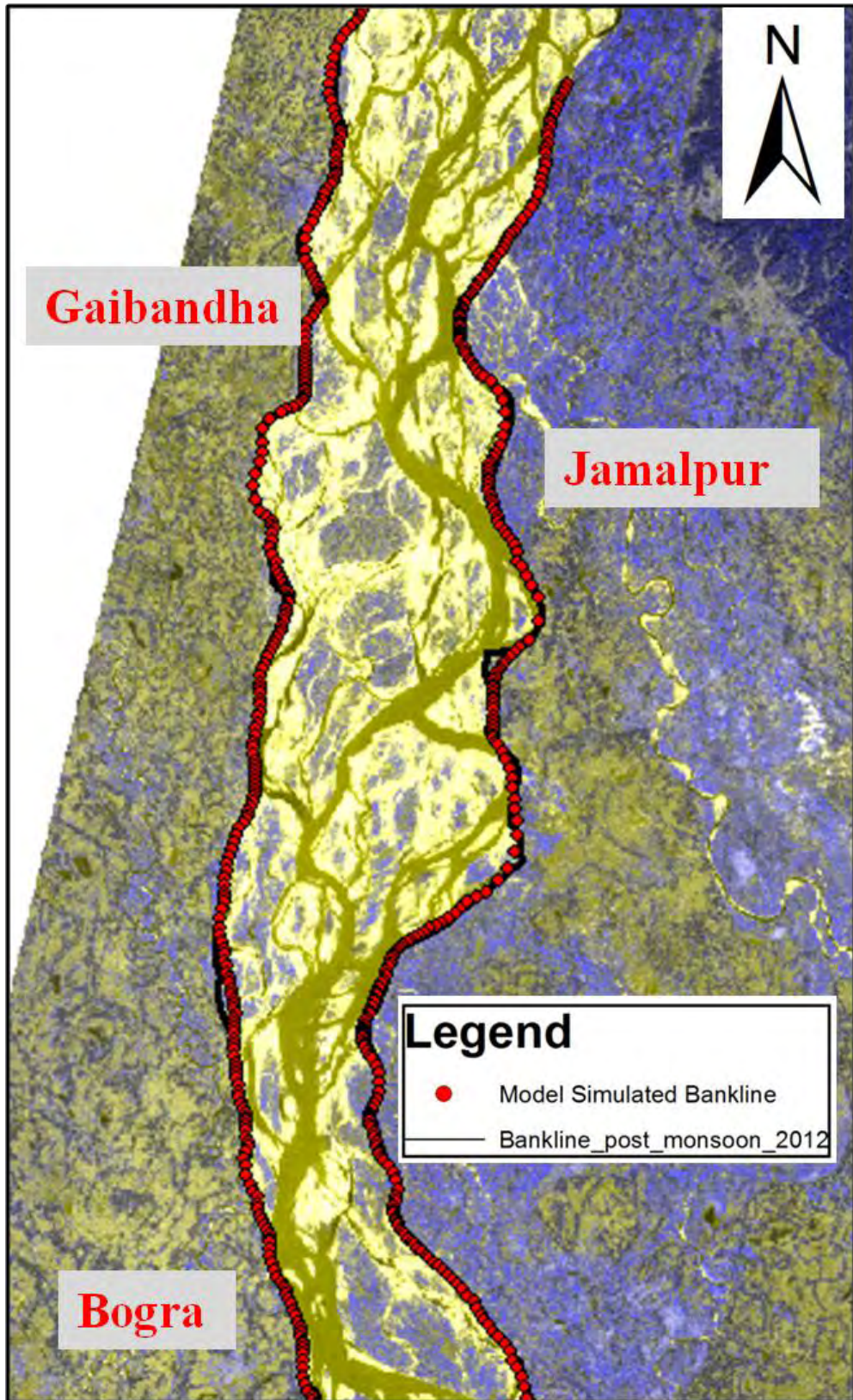


Figure 4.20: Comparison of model simulated and digitized banklines for 2012 at Gaibandha, Jamalpur and Bogra

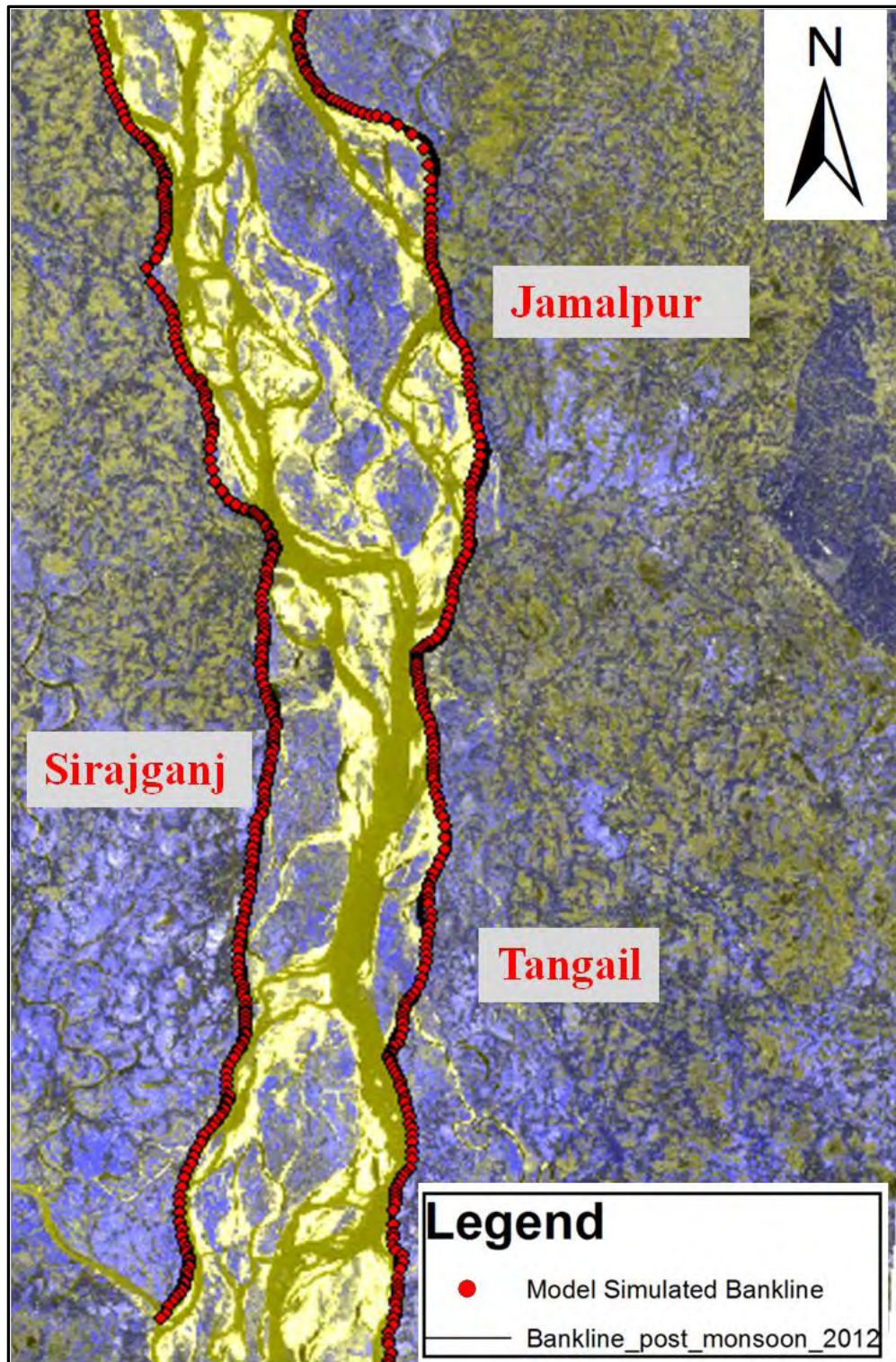


Figure 4.21: Comparison of model simulated and digitized banklines for 2012 at Bogra, Sirajganj & Jamalpur

4.5.7 Selection of Erosion Prone Reaches for Bank Protection

Five erosion prone reaches that are experiencing bank erosion each year at an alarming rate have been selected to study the impact of revetment type of bank protection works along these reaches. The selected reaches are depicted in Figure 4.22.

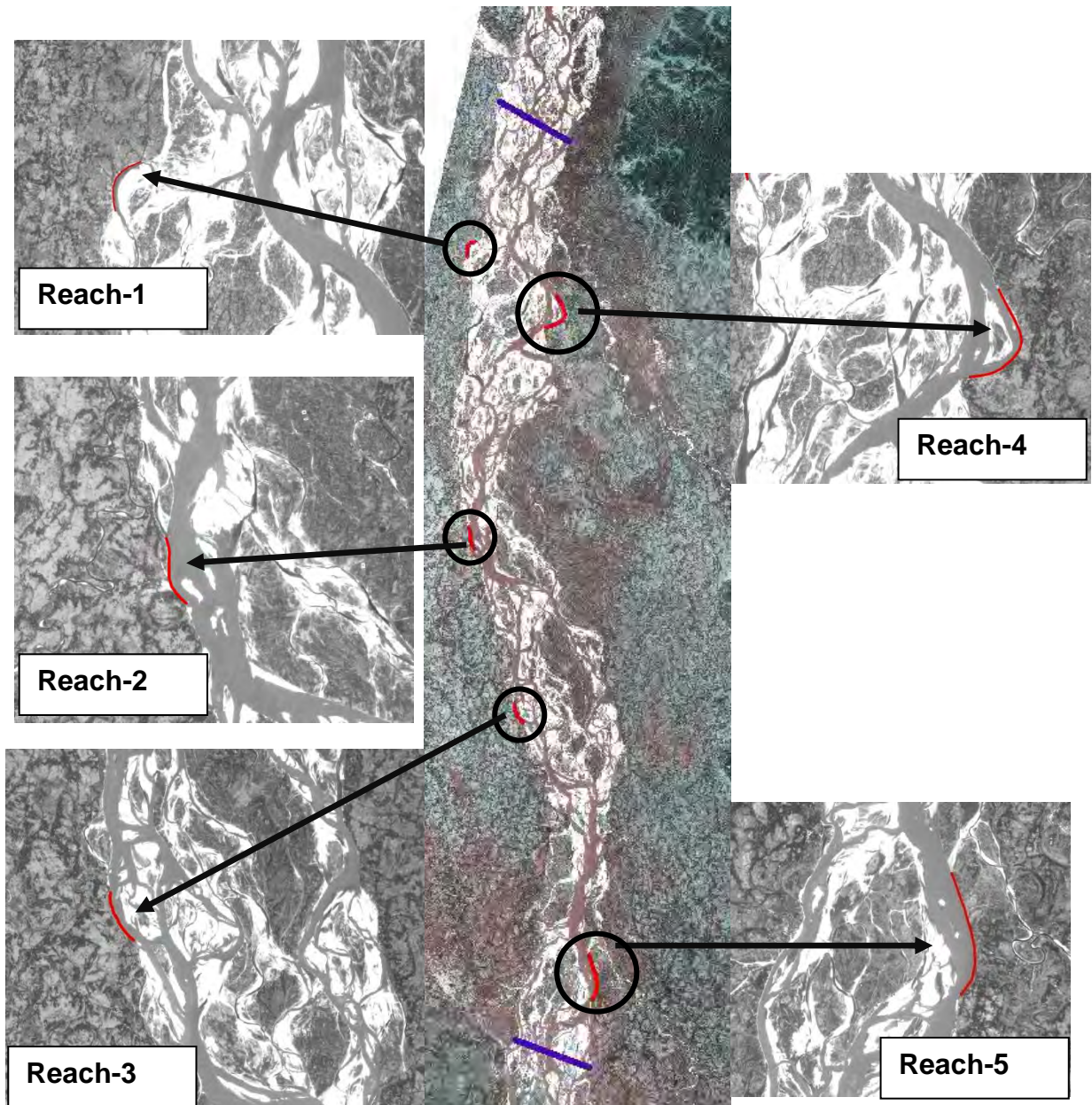


Figure 4.22 Selected Erosion prone reaches for introducing bank protection

CHAPTER 5

RESULTS AND DISCUSSIONS

5.1 General

In this thesis work various models have been simulated including the base condition and followed by structural interventions at five selected erosion prone reaches. Revetment has been selected as bank protective measure. To evaluate the impacts of these structural interventions, various outputs have been analyzed. The bed level changes near the proposed revetments have been judged by analyzing the changes in near bank velocity and bed levels. The cumulative bank erosion at the end of monsoon in the selected reaches is also analyzed. Then a correlation between average river discharge and shear stress applied by the flow was established to estimate the bank erosion of a certain reach by utilizing the average river discharge. Finally, a suggestion has been given for better erosion management in the selected reaches through these comparative analyses.

5.2 Results and Discussions

Having selected the five reaches to carry out the study the model has been simulated through two flood events; flood events with return period 2.33-year (2005 flood year), 100-year (1998 flood year) and bankfull event (2011 flood event). Response of Jamuna River in the vicinity of proposed revetments with respect to these flood events have been evaluated and compared with that from the model of the base condition. Impact assessment of these flood events have been carried out in terms of following hydraulic and morphological properties:

- Near Bank Velocity
- Change in Riverbed Level
- Bank Erosion

5.2.1 Near Bank Velocity

In order to evaluate the effectiveness of the proposed bank protection works, near bank velocity contours during peak of the monsoon from the models of base condition and

models with structural interventions for average flood event and extreme flood event, have been extracted and presented in Figure 5.1 to Figure 5.4 and Figure A.1 to Figure A.16.

Model results in terms of near bank velocity in the vicinity of the proposed revetment near Reach-1 (Figure 5.1 to 5.4) clearly reveal the reduction of flow velocity near the revetment. At the base condition this reach lying within Gaibandha district face near bank velocity 1.36 m/s and 1.47 m/s for average and extreme flood events respectively. After the implementation of revetment, this reach may experience much lower velocity than base condition for the same hydrologic events. The maximum velocities near the bank are reduced to 1.20 m/s for average flood event while it was 1.42 m/s for extreme flood event. Besides obliquity of flow was observed in the upstream portion of Reach-1 which may threaten the proposed structure at Reach-1.

In case of Reach-2 (Figure A.1 to A.4), no significant change in velocity field was observed after the implementation of revetment. Maximum near bank velocities in the vicinity of proposed revetment was 2.15 m/s and 2.20 m/s for average flood event and extreme flood event respectively, while those for base conditions were 2.05 m/s and 2.15 m/s. Flow hit the upstream portion of the Reach-2 in an oblique direction.

For Reach-3 (Figure A.5 to A.8), structural intervention brought about some changes in the flow field in the vicinity of the structure as compared to the base condition. Maximum velocities near proposed revetment in this reach were 2.25 m/s and 2.42 m/s for extreme flood event and average flood event respectively. Oblique flow was not noticed in Reach-3.

Model simulations in the vicinity of the proposed revetment near Reach-4 (Figure A.9 to A.12) clearly reveal the reduction of velocity near the revetment. At the base condition this reach situated in Jamalpur district face near bank velocities of 2.15 m/s and 2.41 m/s for average and extreme flood events respectively. After the implementation of revetment, this reach may experience much lower velocity than base condition for the same hydrologic events. The maximum velocities near the bank are reduced to 2.02 m/s for average flood event while it was 2.28 m/s for extreme flood event. Besides the model simulated flow field depict that the reach may be threatened due to obliquity of flow.

In case of Reach-5 (Figure A.13 to A.16), at Tangail obliquity of flow was not observed. Maximum near bank velocities in the vicinity of proposed revetment was 2.26 m/s and 2.58 m/s for average flood event and extreme flood event respectively.

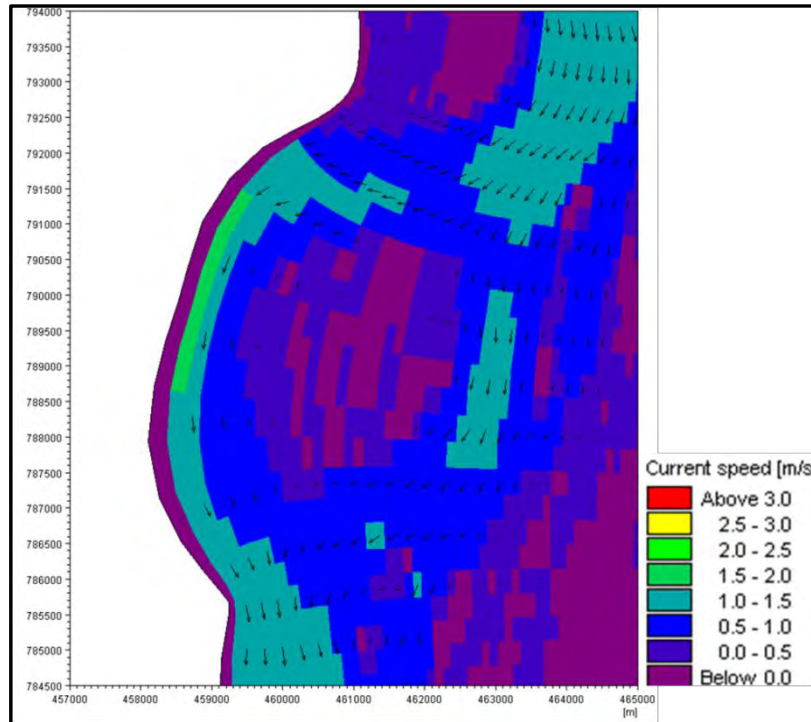


Figure 5.1 Simulated velocity contour of the Jamuna during peak of the monsoon near Reach-1 under base condition for average flood event (2005)

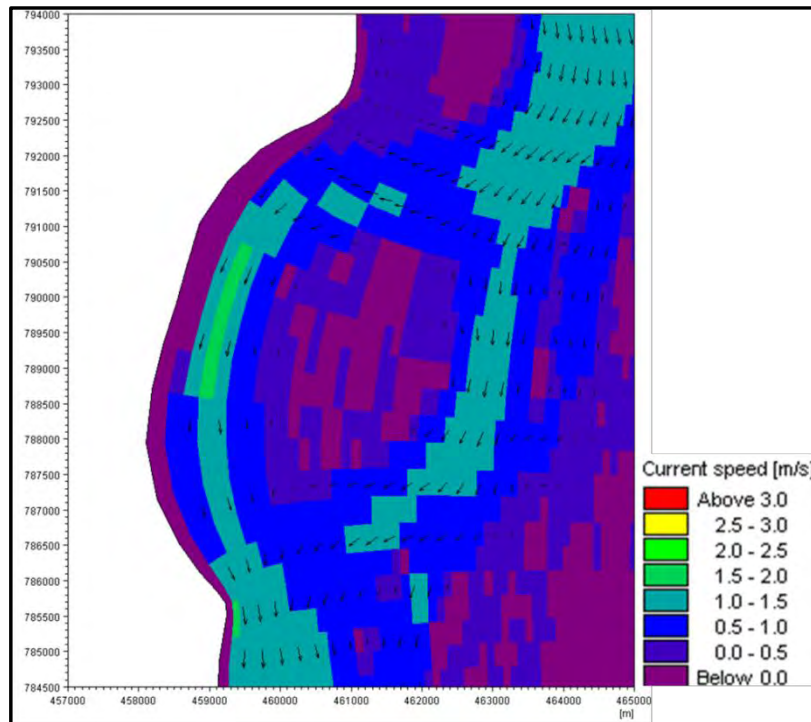


Figure 5.2 Simulated velocity contour of the Jamuna during peak of the monsoon near Reach-1 with proposed revetment for average flood event (2005)

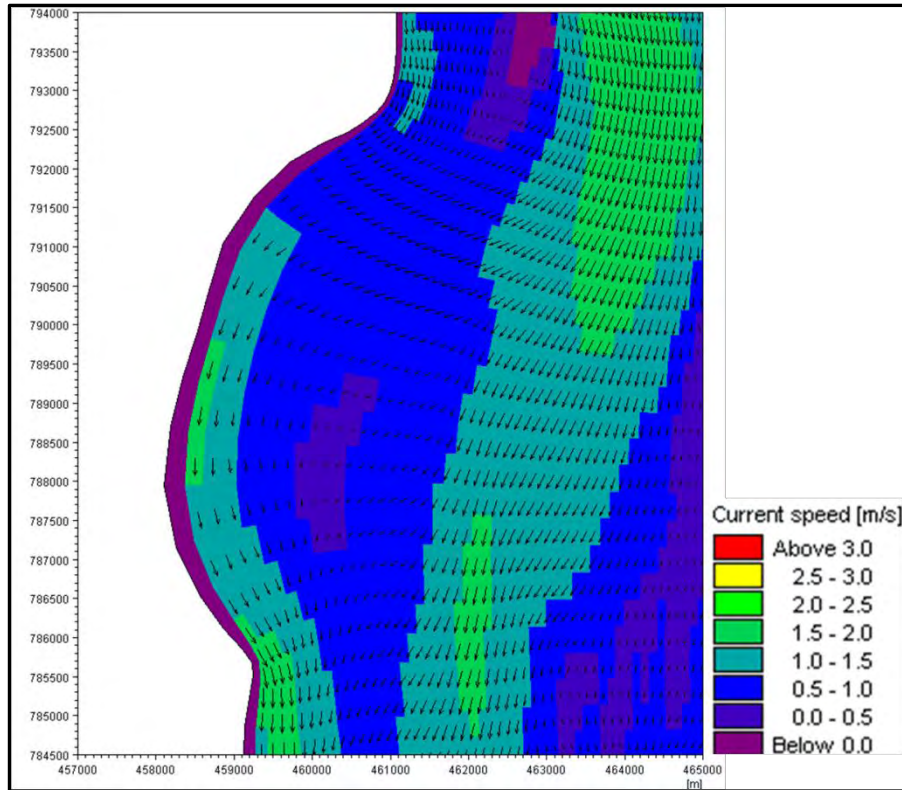


Figure 5.3 Simulated velocity contour of the Jamuna during peak of the monsoon near Reach-1 under base condition for 100 year flood event (1998)

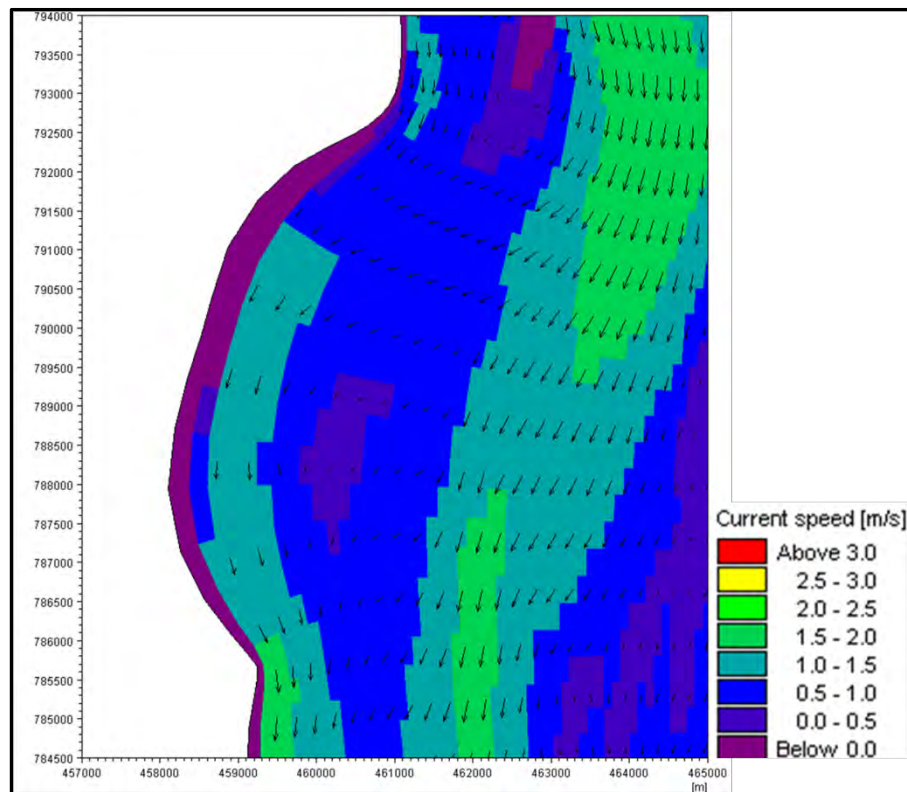


Figure 5.4 Simulated velocity contour of the Jamuna during peak of the monsoon near Reach-1 with proposed revetment for 100 year flood event (1998)

5.2.2 Changes in Bed Level for proposed revetments

In general, the impact of the proposed structures, which exactly follow the banklines, on the bed scour has been described in this section. First of all, the structures do not constrict the river since these follow the bankline. Secondly, incorporation of the structures has been made on the coarse grid that makes evaluation of impact on bed scour difficult. These structures had to be represented covering single cell, and no transverse slope and launching apron have been considered in the present model setup for obvious reasons.

Structure induced bed scour has been determined from difference of bed level during end of simulation period from “with” to “without structure” conditions. Bed scour near the structure has been assessed from few cells away from the structure.

Bed level for “with” and “without structure” condition around structure 1 is shown in Figure 5.5 to 5.8. In the vicinity of the structure at Reach-1 there are some minor changes in bed level. This is true for both extreme and average flood event; though the bed level may vary from event to event. For with structure condition, nearly 5.0 m additional bed scour might be generated within the structure due to structural intervention for extreme flood event. In case of average flood event, 0.80 m difference in bed scour is seen from with and without structure condition.

Change in bed level for “with” and “without structure” condition surrounding structure at Reach-2 has been depicted in Figure A.17 to A.20. In the vicinity of the structure at Reach-2 a moderate bed level change was observed for both of the average and extreme flood event. The scour was 1.65m for average flood event while 2.30m for extreme flood event.

Bed levels for “with” and “without structure” conditions around structure 3 have been shown in Figure A.21 to A.24. Introduction of revetment in this reach reveals that 1m of scour may take place surrounding the reach for the passage of average flood event while the same for extreme flood event is 1.80m.

Change in bed level for “with” and “without structure” condition around Reach-4 is shown in Figure A.25 to A.28. Structure induced bed scour in this reach was found to be 1.60 m for average flood event while that for extreme hydrological event was 4.0m.

Bed level for “with” and “without structure” condition around Reach-5 is shown in Figure A.29 to A.32. In the vicinity of the structure at Reach-5 significant changes in bed level were observed for both of the average and extreme flood event. Due to the passage of average flood event structure induced bed scour experienced by Reach-5 was 3.64m while the same for extreme flood event was around 10m.

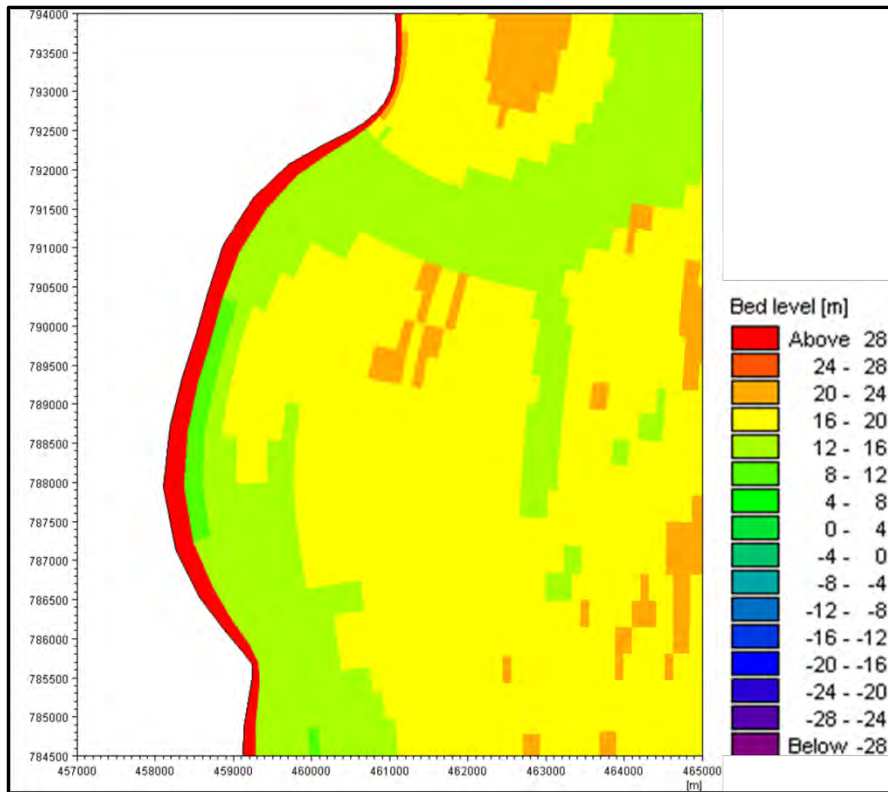


Figure 5.5 Simulated bathymetry under base condition at Reach-1 at the end of monsoon for average flood event (2005)

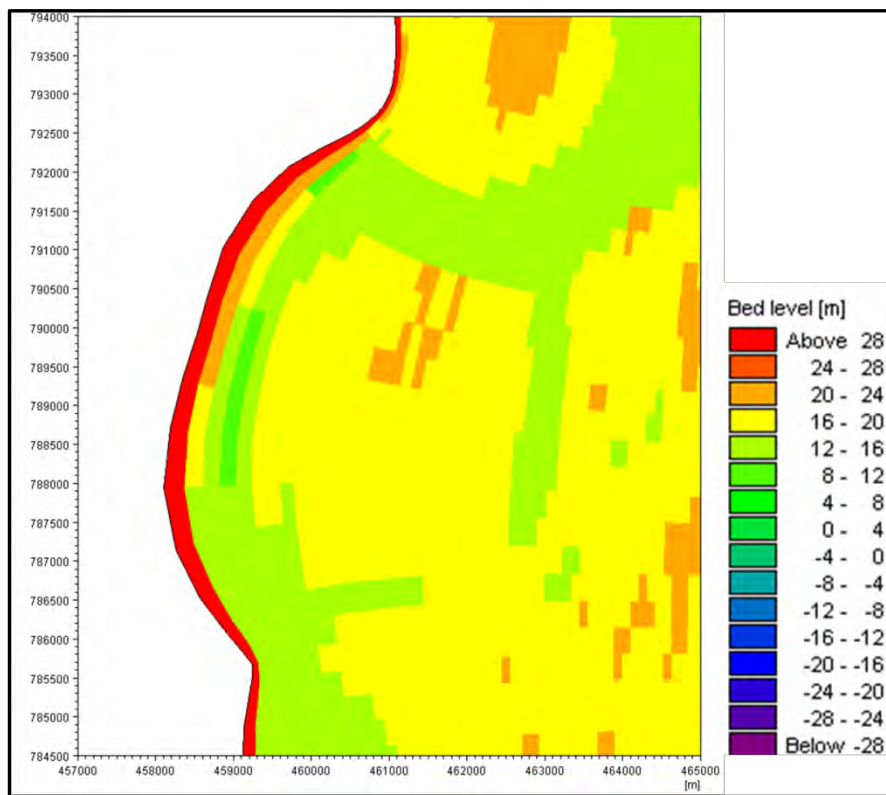


Figure 5.6 Simulated bathymetry with proposed revetment at Reach-1 at the end of monsoon for average flood event (2005)

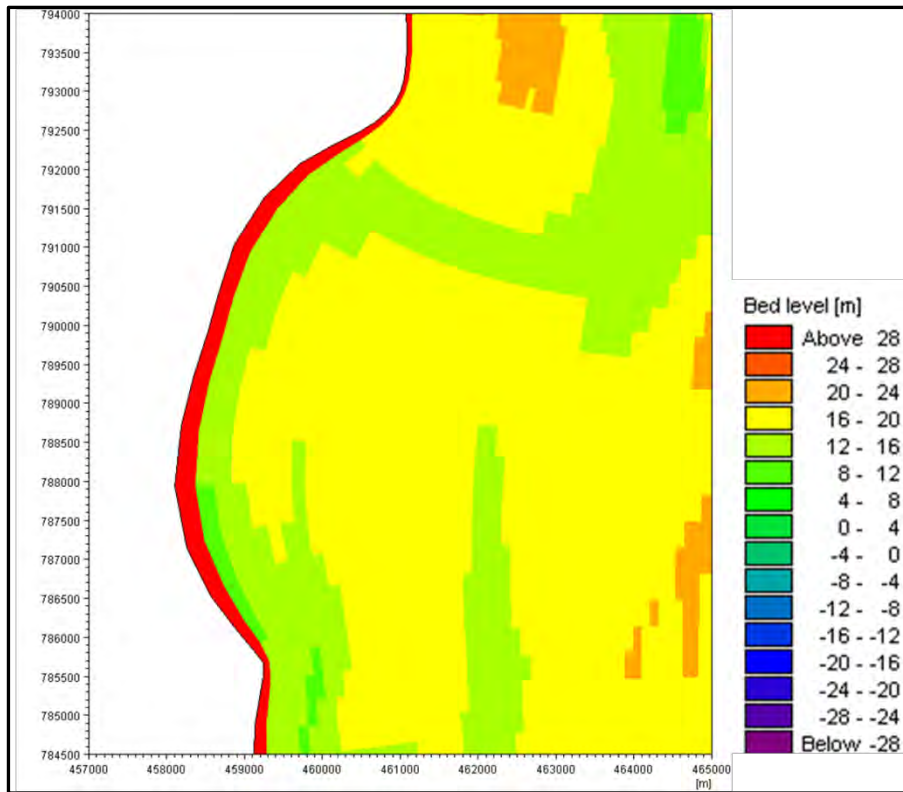


Figure 5.7 Simulated bathymetry under base condition near Reach-1 at the end of monsoon for 100 year flood event (1998)

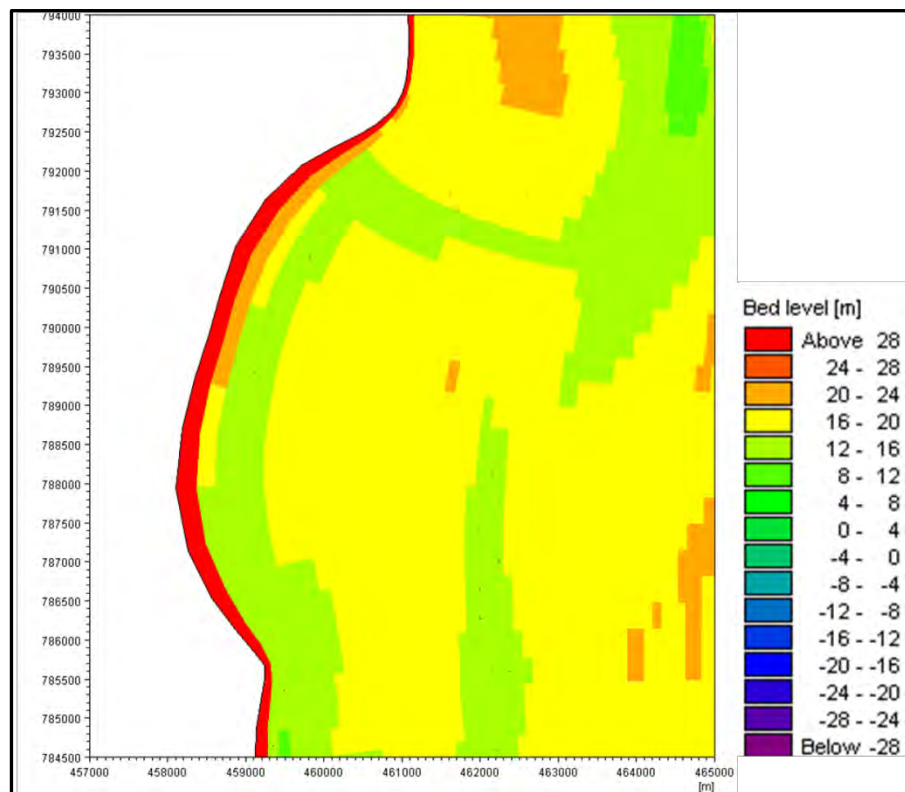


Figure 5.8 Simulated bathymetry with proposed revetment near Reach-1 at the end of monsoon for 100 year flood event (1998)

5.2.3. Bank Erosion

Model generated right bank erosion within the vicinity of introduced revetments for both flood events have been shown in Figure 5.9 to Figure 5.23. It is quite clear from the figures that the proposed structures are capable to restrain the probable bank erosion and this is true for both the flood events.

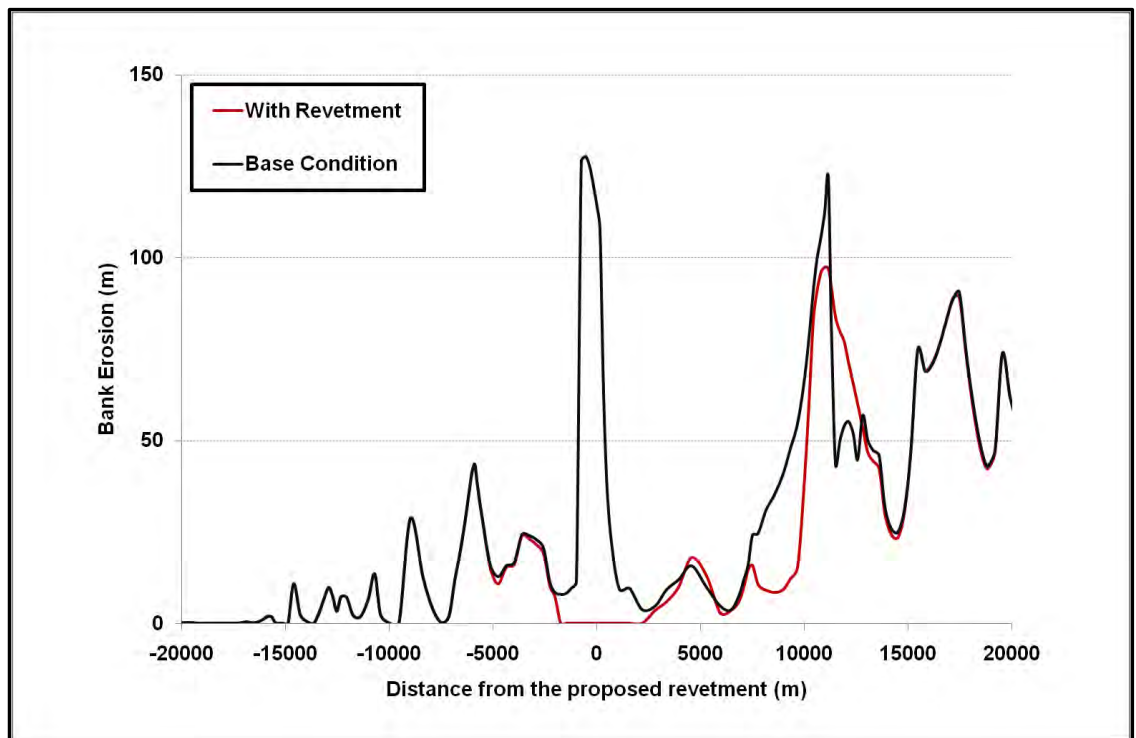


Figure 5.9 Model generated accumulated bank erosion along the right bank of the Jamuna in the vicinity of Reach-1 for average flood event (2005)

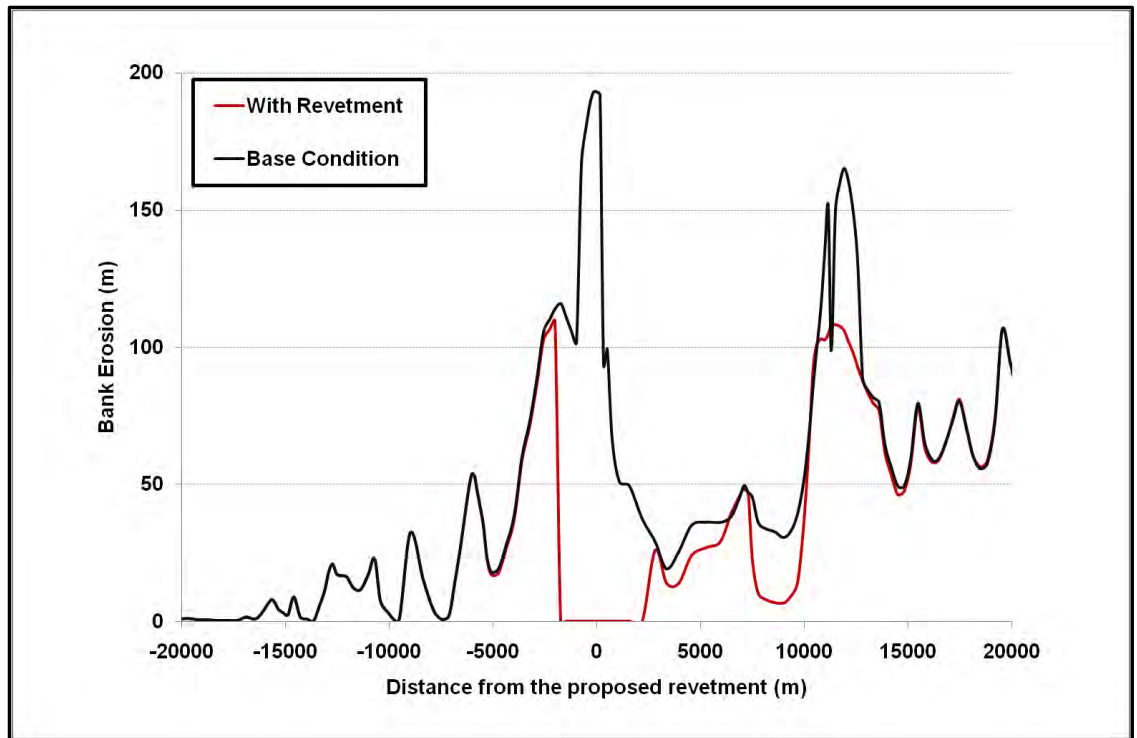


Figure 5.10 Model generated accumulated bank erosion along the right bank of the Jamuna in the vicinity of Reach-1 for extreme flood event (1998)

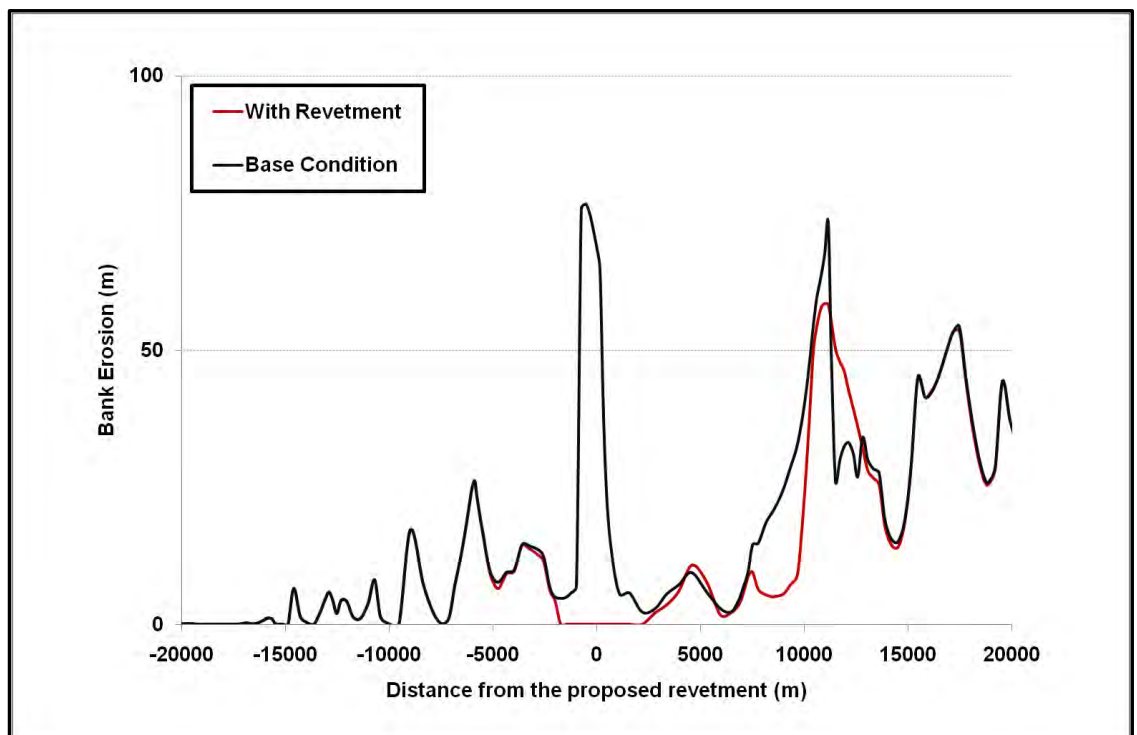


Figure 5.11 Model generated accumulated bank erosion along the right bank of the Jamuna in the vicinity of Reach-1 for bankfull event (2011)

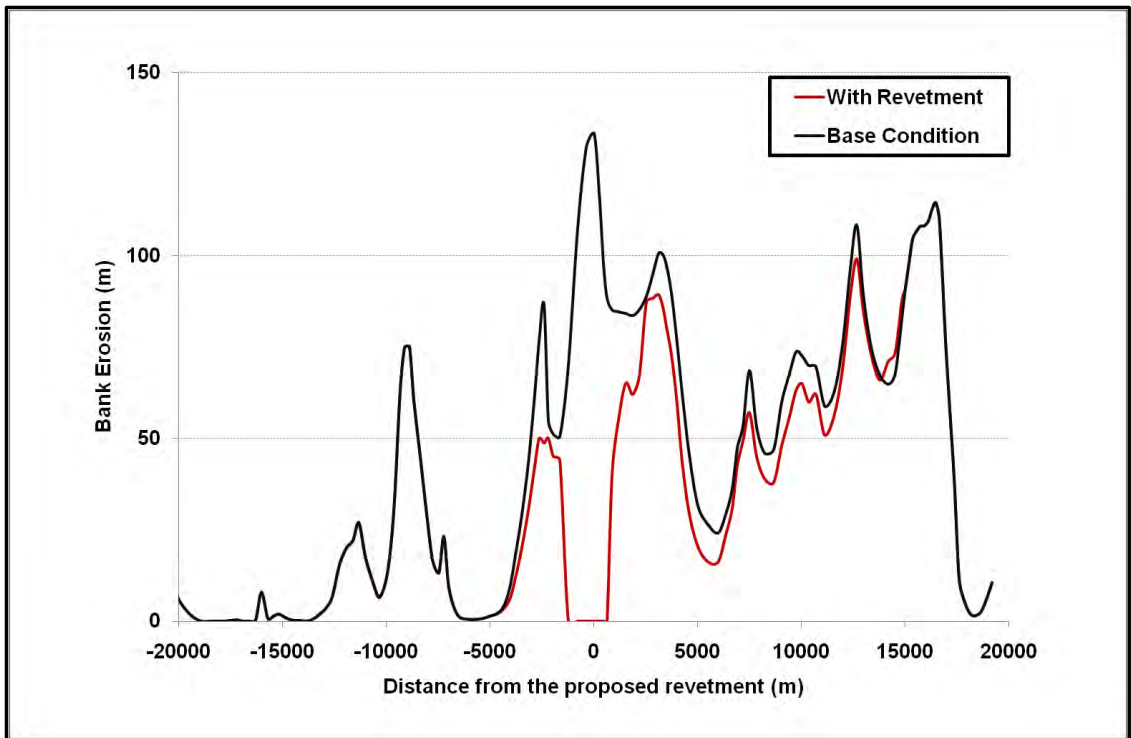


Figure 5.12 Model generated accumulated bank erosion along the right bank of the Jamuna in the vicinity of Reach-2 for average flood event (2005)

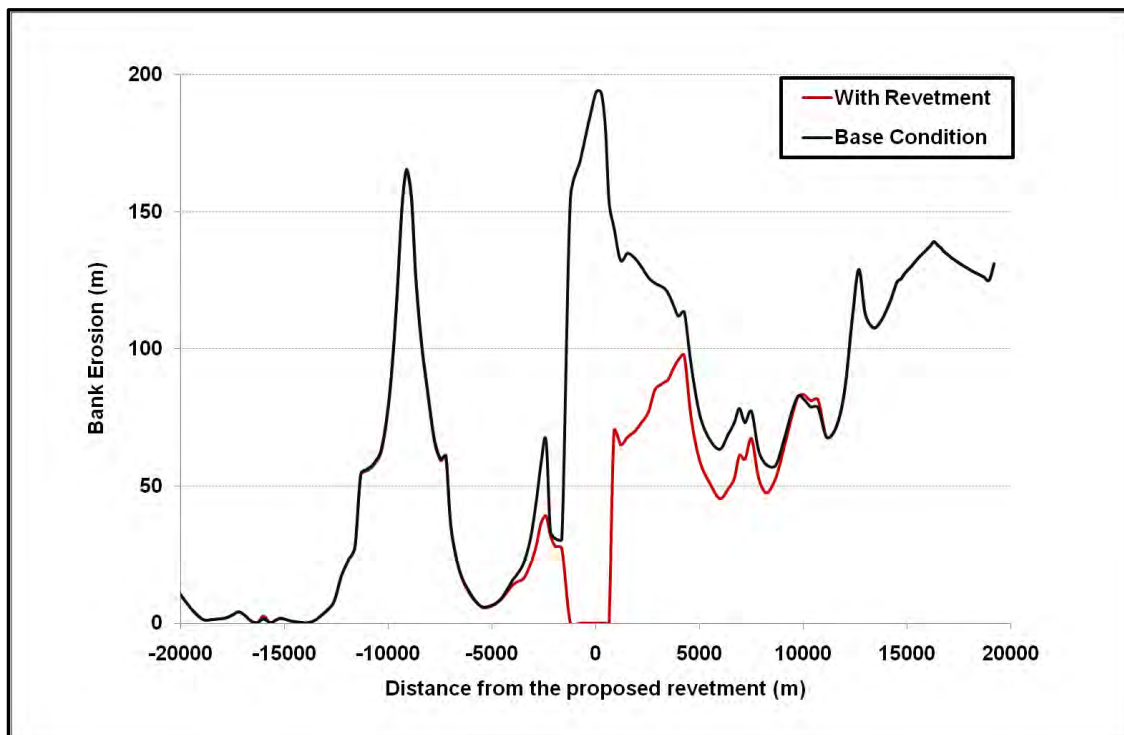


Figure 5.13 Model generated accumulated bank erosion along the right bank of the Jamuna in the vicinity of Reach-2 for extreme flood event (1998)

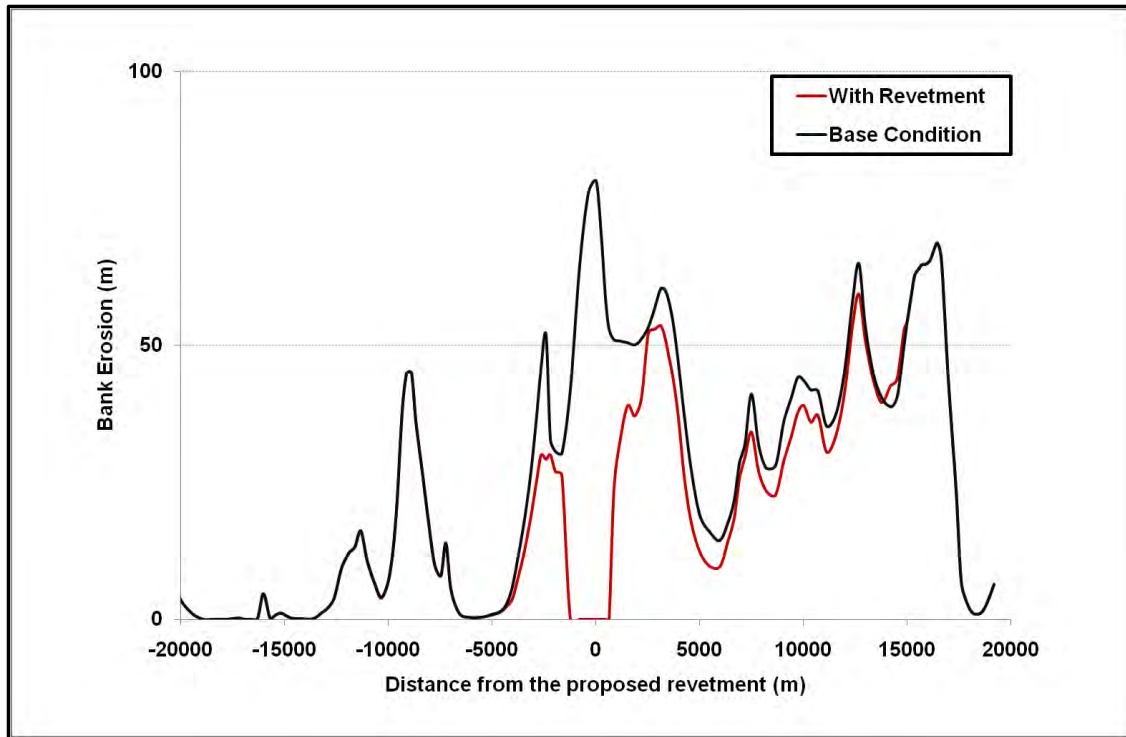


Figure 5.14 Model generated accumulated bank erosion along the right bank of the Jamuna in the vicinity of Reach-2 for bankfull event (2011)

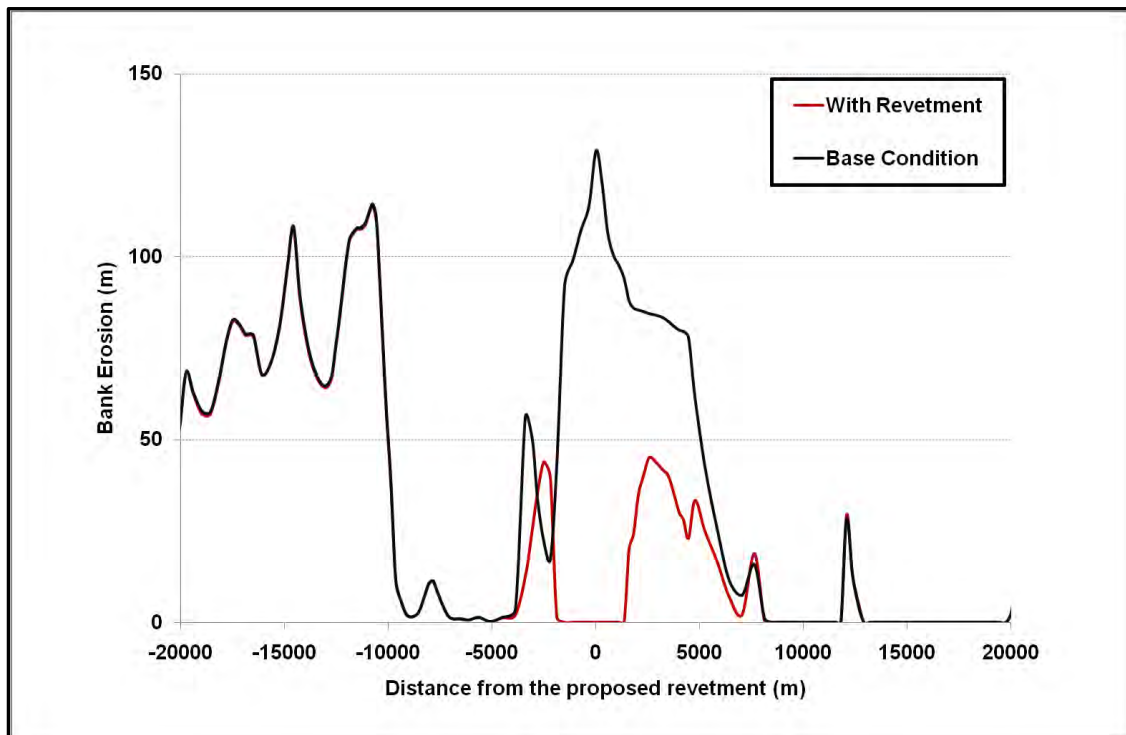


Figure 5.15 Model generated accumulated bank erosion along the right bank of the Jamuna in the vicinity of **Reach-3** for average flood event (2005)

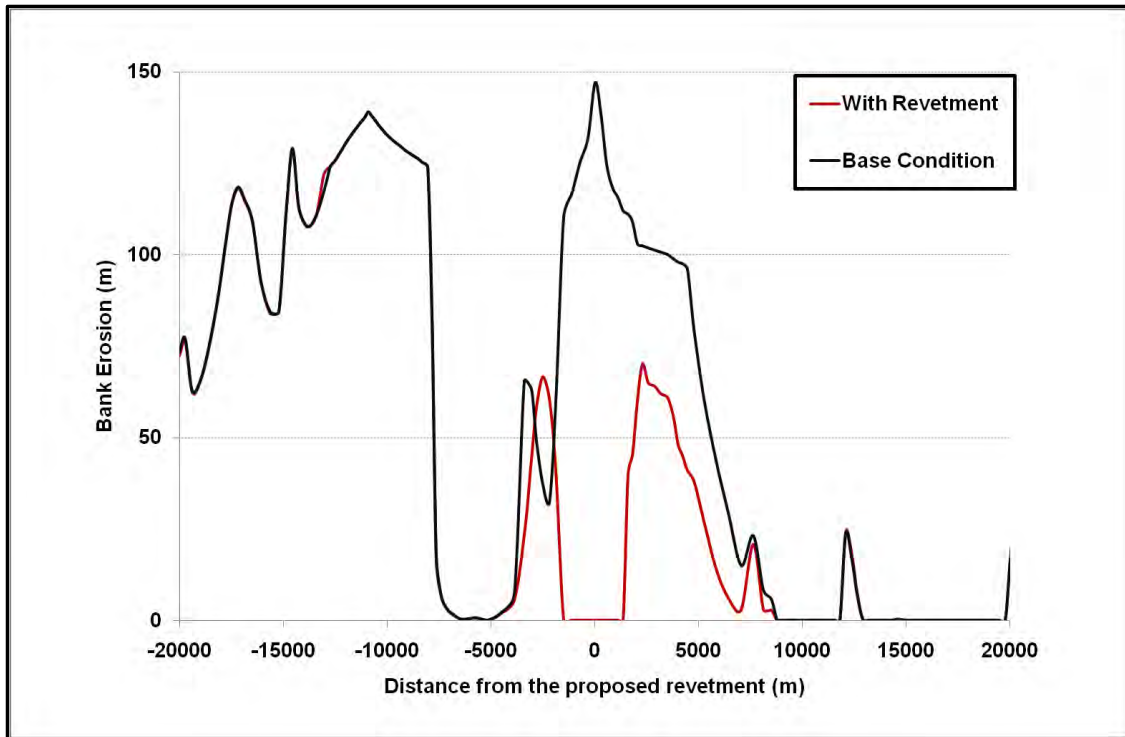


Figure 5.16 Model generated accumulated bank erosion along the right bank of the Jamuna in the vicinity of Reach-3 for extreme flood event (1998)

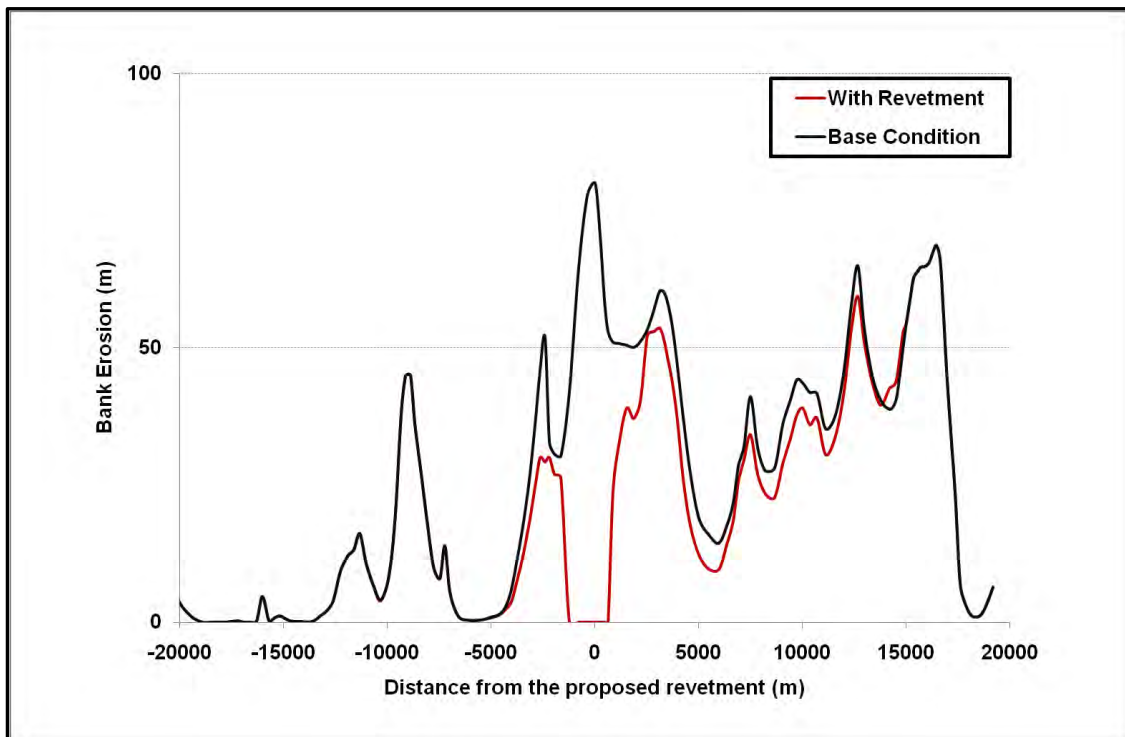


Figure 5.17 Model generated accumulated bank erosion along the right bank of the Jamuna in the vicinity of Reach-3 for bankfull event (2011)

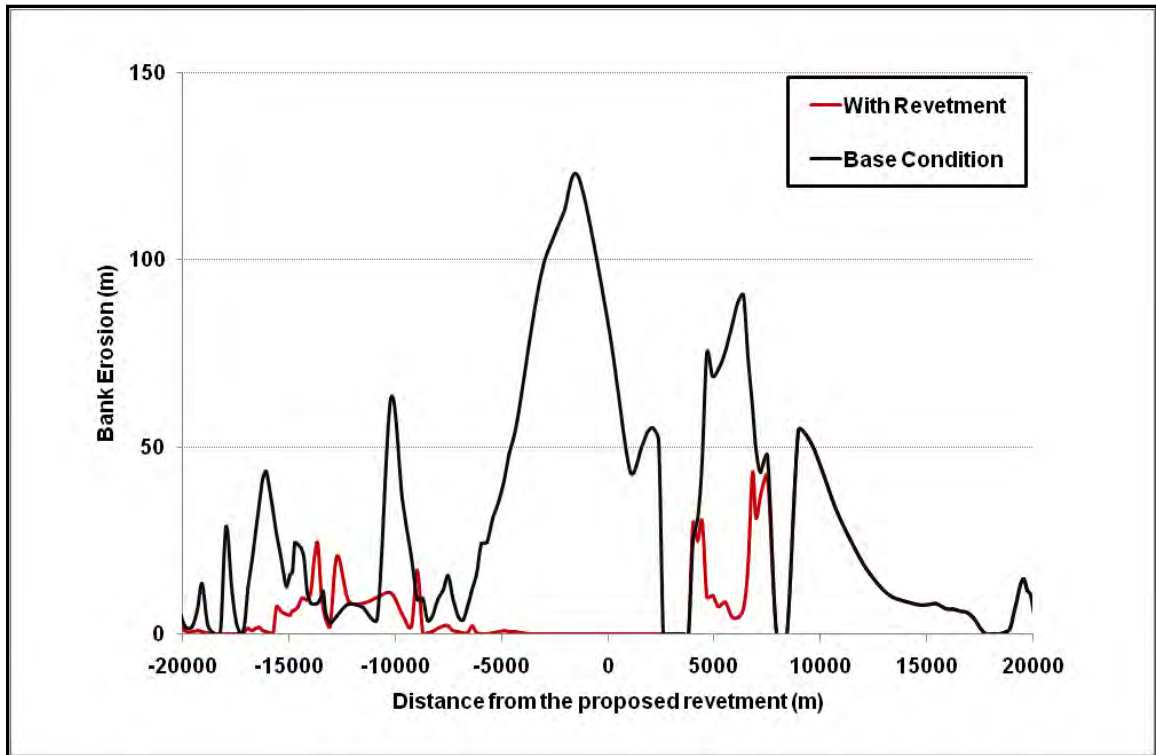


Figure 5.18 Model generated accumulated bank erosion along the left bank of the Jamuna in the vicinity of Reach-4 for average flood event(2005)

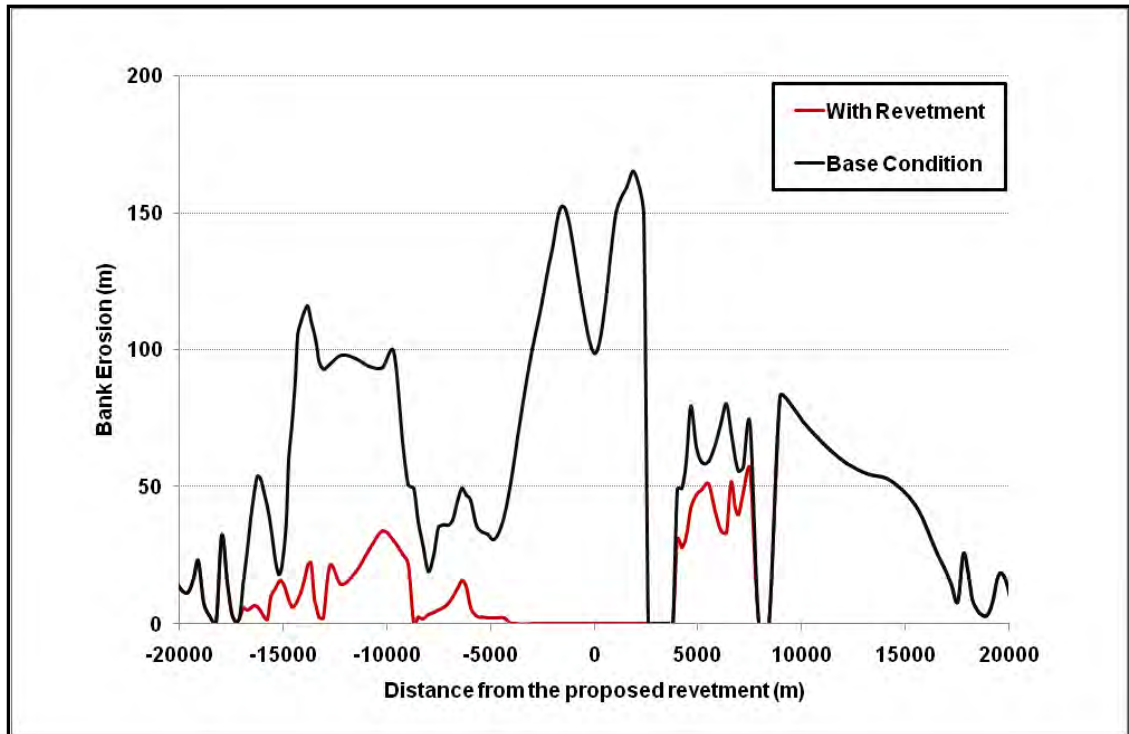


Figure 5.19 Model generated accumulated bank erosion along the left bank of the Jamuna in the vicinity of Reach-4 for extreme flood event (1998)

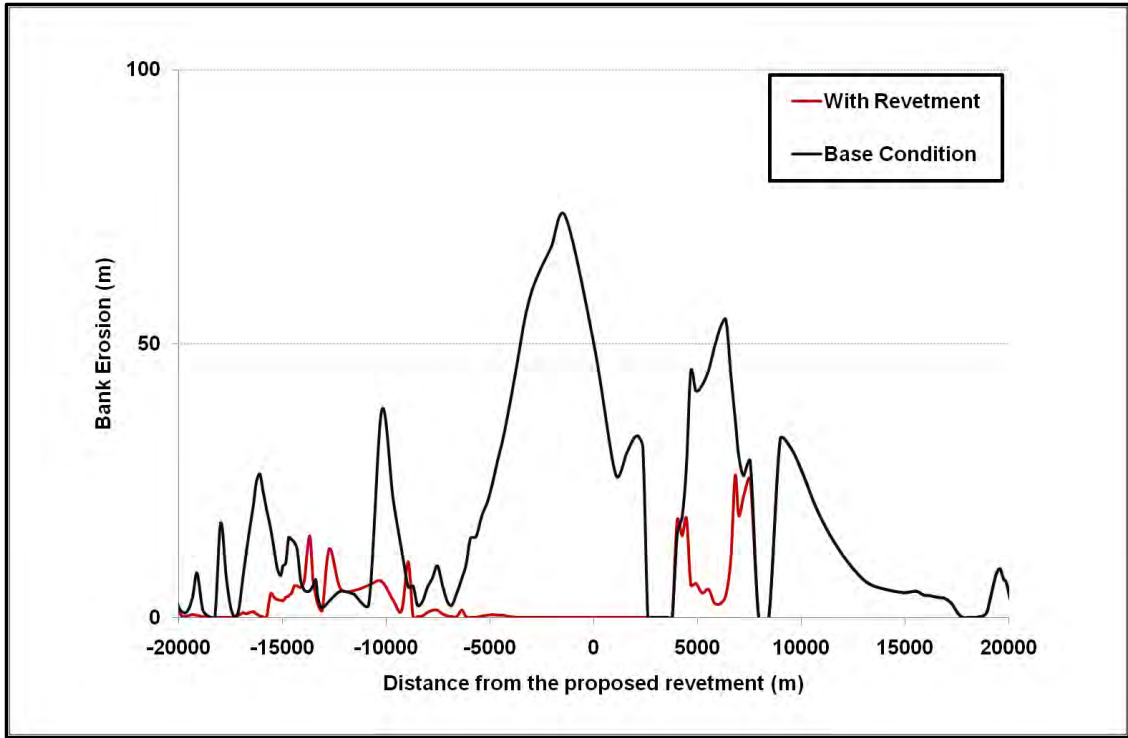


Figure 5.20 Model generated accumulated bank erosion along the left bank of the Jamuna in the vicinity of Reach-4 for bankfull event (2011)

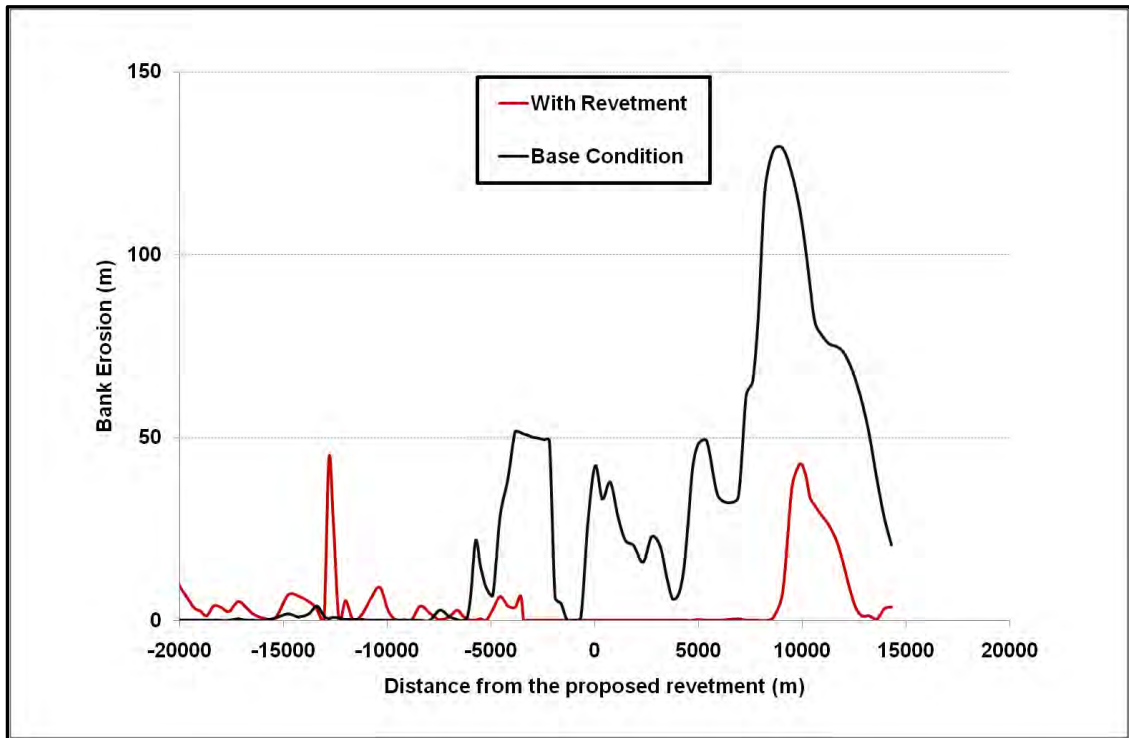


Figure 5.21 Model generated accumulated bank erosion along the left bank of the Jamuna in the vicinity of Reach-5 for average flood event (2005)

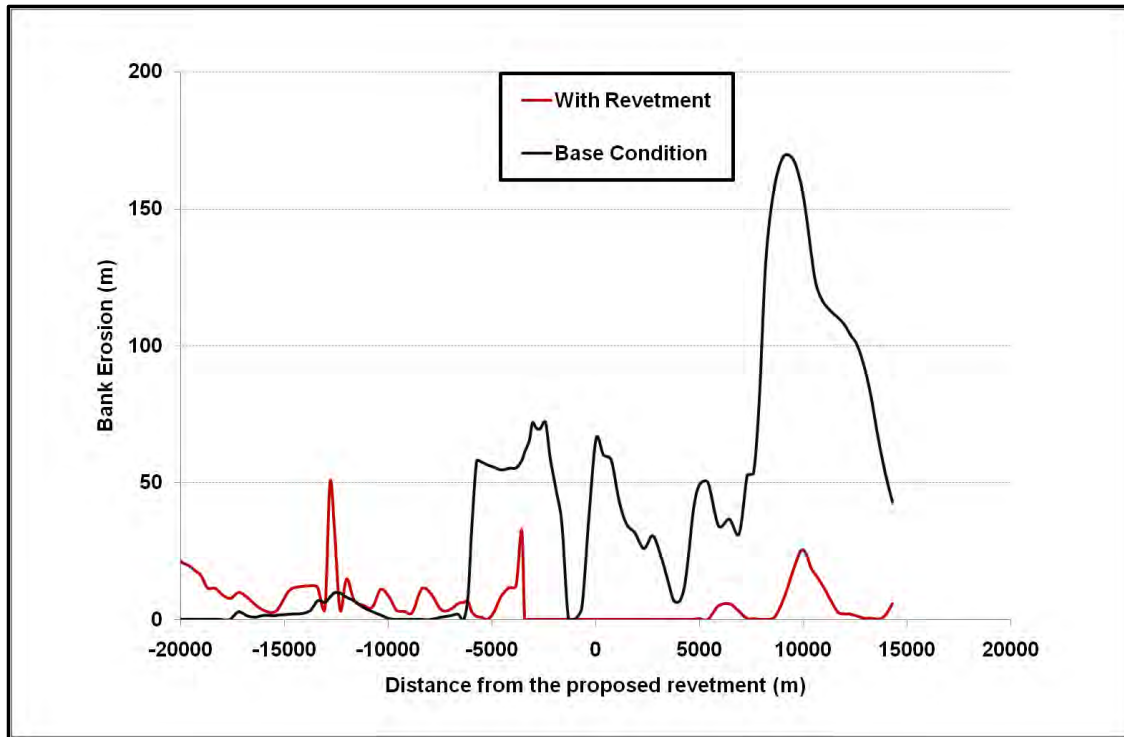


Figure 5.22 Model generated accumulated bank erosion along the left bank of the Jamuna in the vicinity of Reach-5 for extreme flood event (1998)

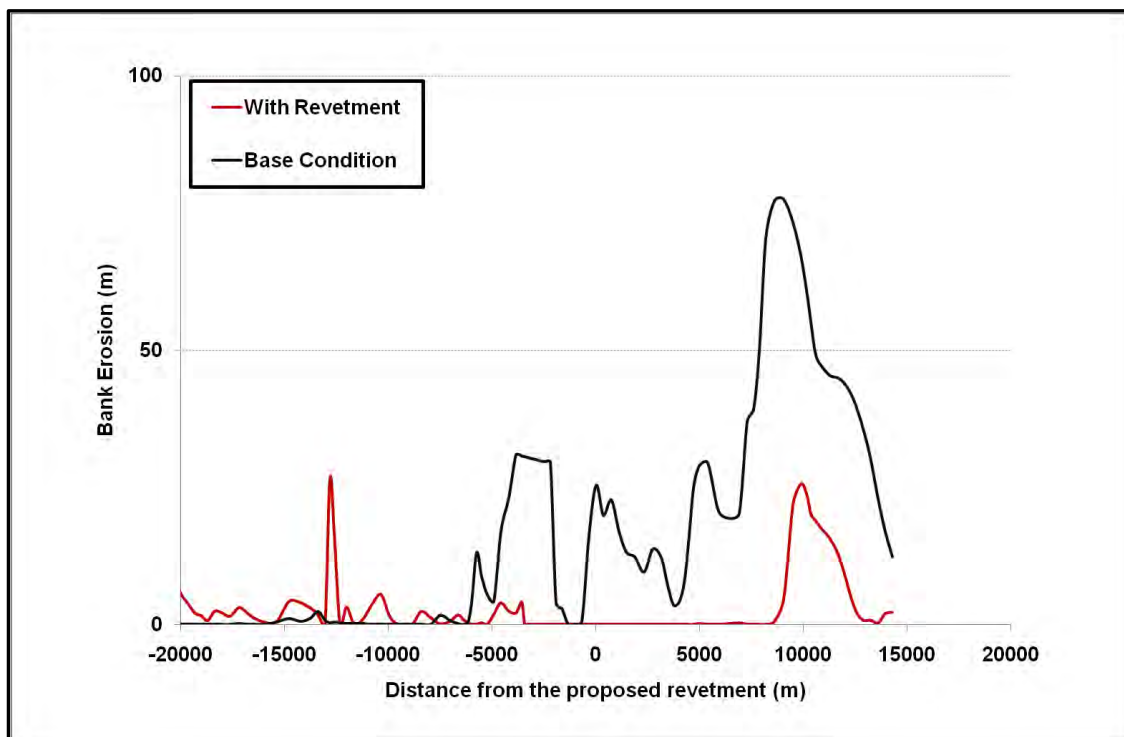


Figure 5.23 Model generated accumulated bank erosion along the left bank of the Jamuna in the vicinity of Reach-5 for bankfull event (2011)

5.3 Correlation between Average discharge and flow induced shear stress

Hansen and Simmon (2001) developed an empirical formula to quantify the erosion rates by shear stress applied by the flow and critical shear stress. The formula is given below:

$$\varepsilon = k_d (\tau_a - \tau_c)^a$$

where ε is the fluvial bank erosion rate (m/s) per unit time per unit area, τ_a is the boundary shear stress applied by the flow, k_d is the erodibility co-efficient, τ_c is the critical shear stress and a is an empirically derived co-efficient which is generally considered to be 1. An empirical relationship [5] between k_d and τ_c is

$$k_d = 2.0 \times 10^{-7} (\tau_c^{-0.5})$$

There are several approaches for determining τ_c . Critical shear stress can be determined in flume studies, estimation based on soil parameters such as particle size and soil specific gravity. For non-cohesive soils, Shields' diagram provides estimates of critical shear stress based on particle size using a representative particle diameter and assuming no interaction among the sediment particles.

The preceding formulae and 2-D model were used to establish relationship between τ_a and discharge at individual reaches. Since discharge data were not available at the desired reaches model simulated discharges at those reaches were used. Model simulated bank erosion rates for different hydrologic events (1998, 2005, and 2012) were utilized to calculate τ_a for respective hydrological events.

The calculated boundary shear stresses were then linked to model simulated average flow discharge that prevails over five months (June to October) covering the monsoon season. In all cases significant regression relationships were obtained. The best fit polynomial curves depict that simulated boundary shear stress monotonically increases with the average flow discharge. The correlations have been presented in Figure 6.51 to 6.55.

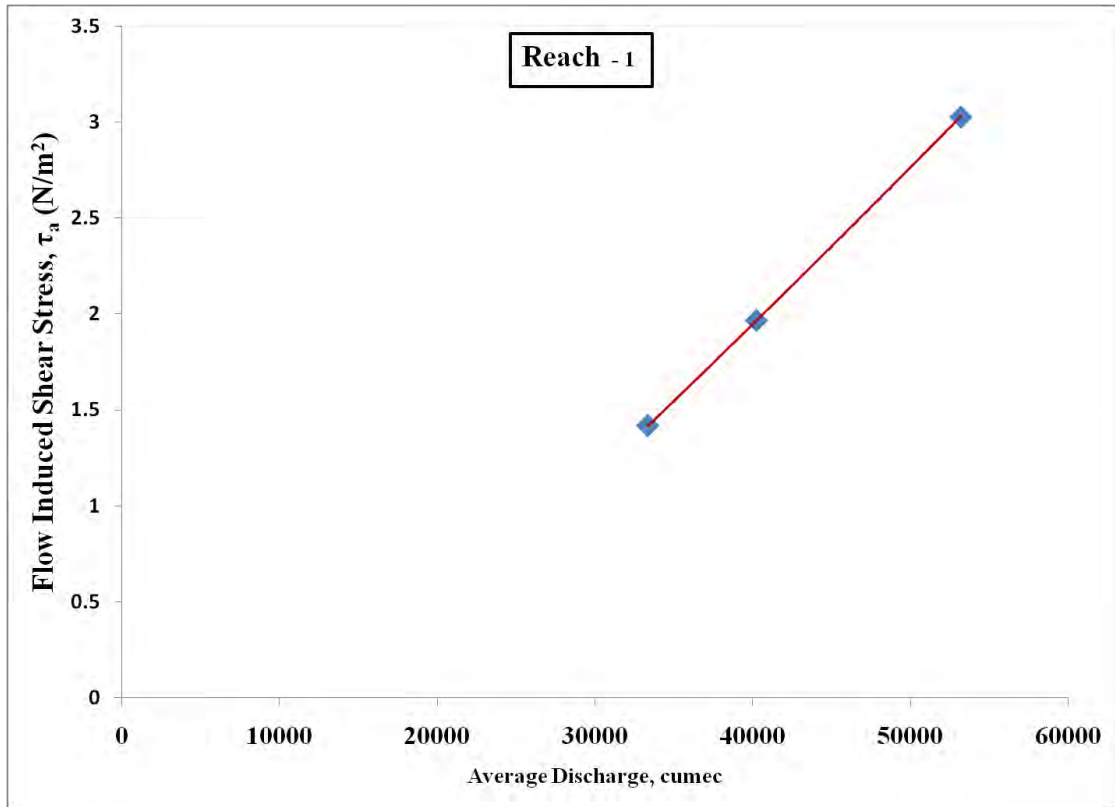


Figure 5.24 Correlation between τ_a and average discharge at Gaibandha (Reach-1)

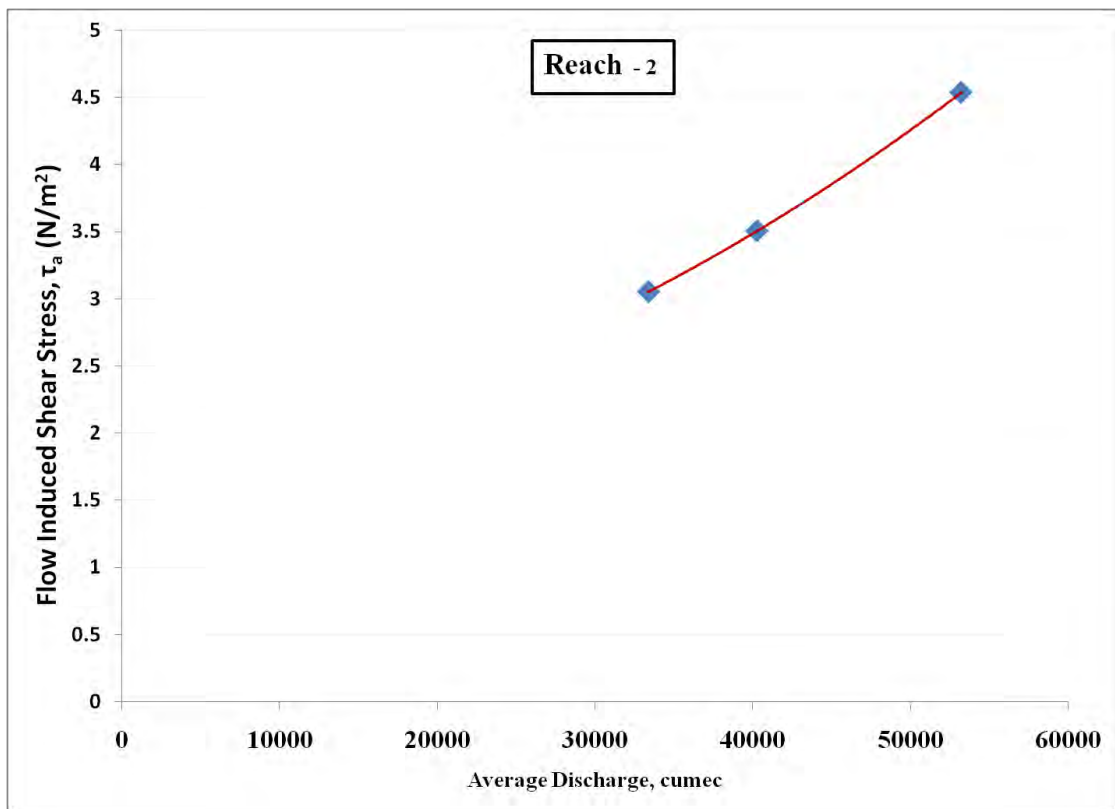


Figure 5.25 Correlation between τ_a and average discharge at Bogra (Reach-2)

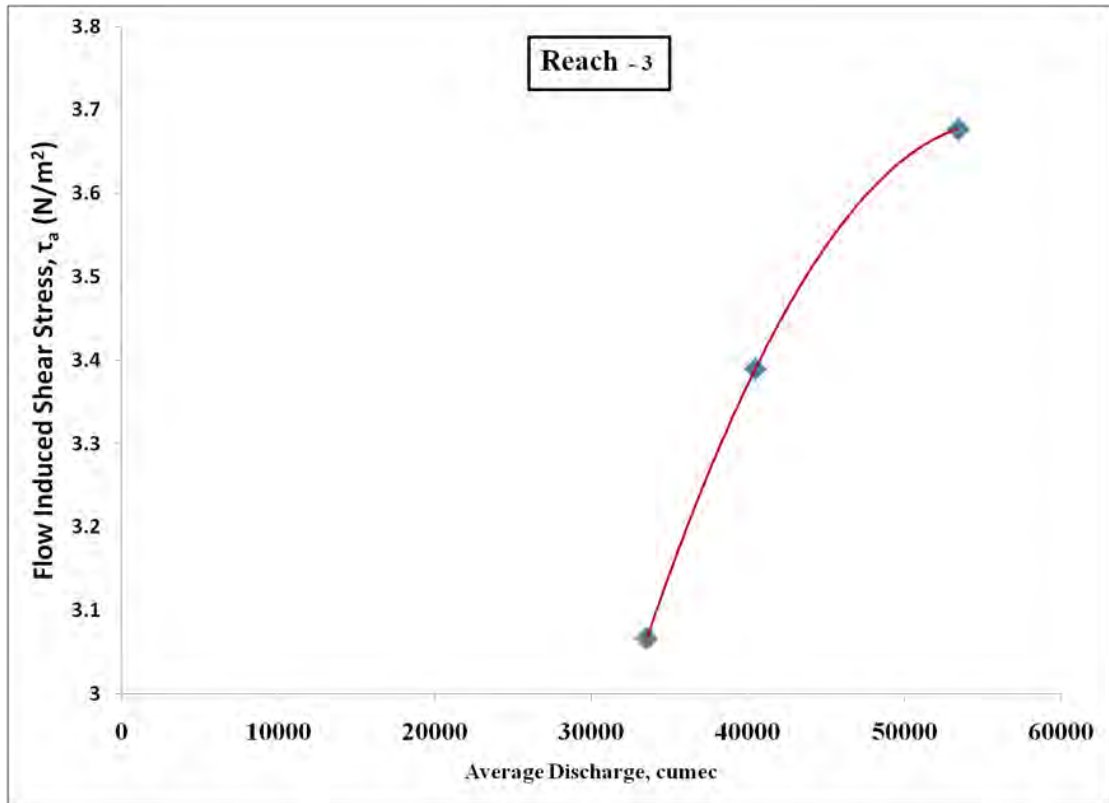


Figure 5.26 Correlation between τ_a and average discharge at Sirajganj (Reach-3)

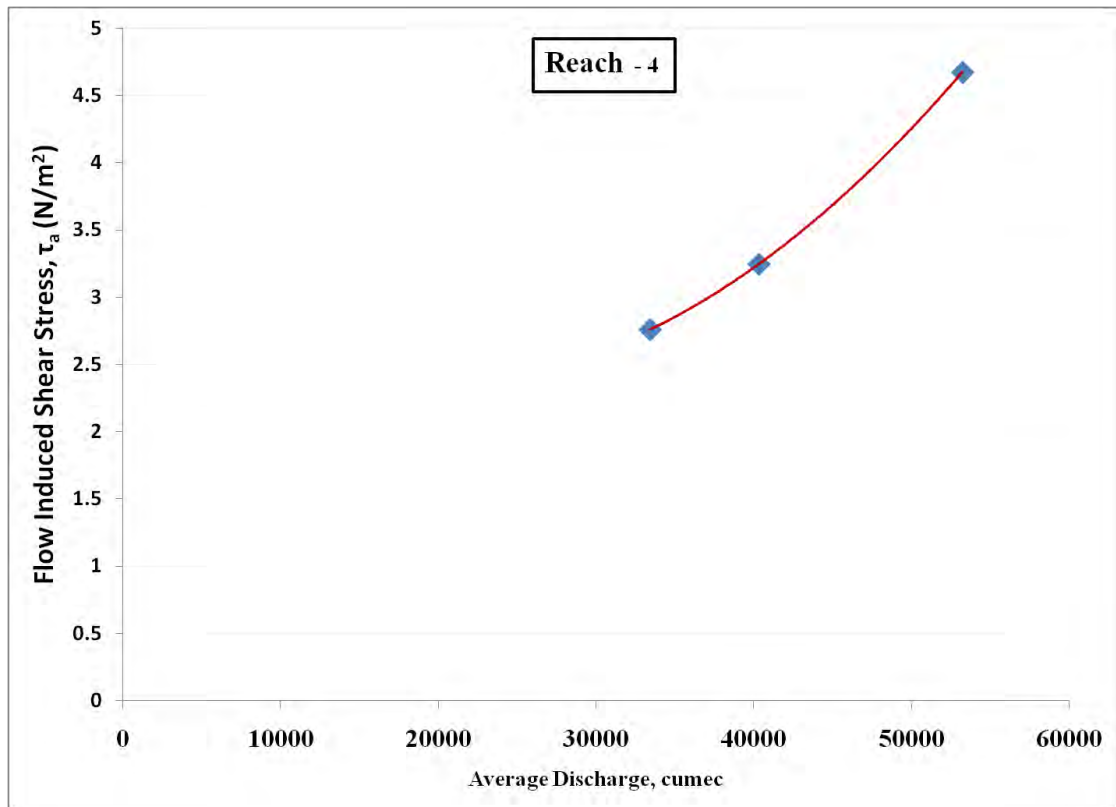


Figure 5.27 Correlation between τ_a and average discharge Jamalpur (Reach-4)

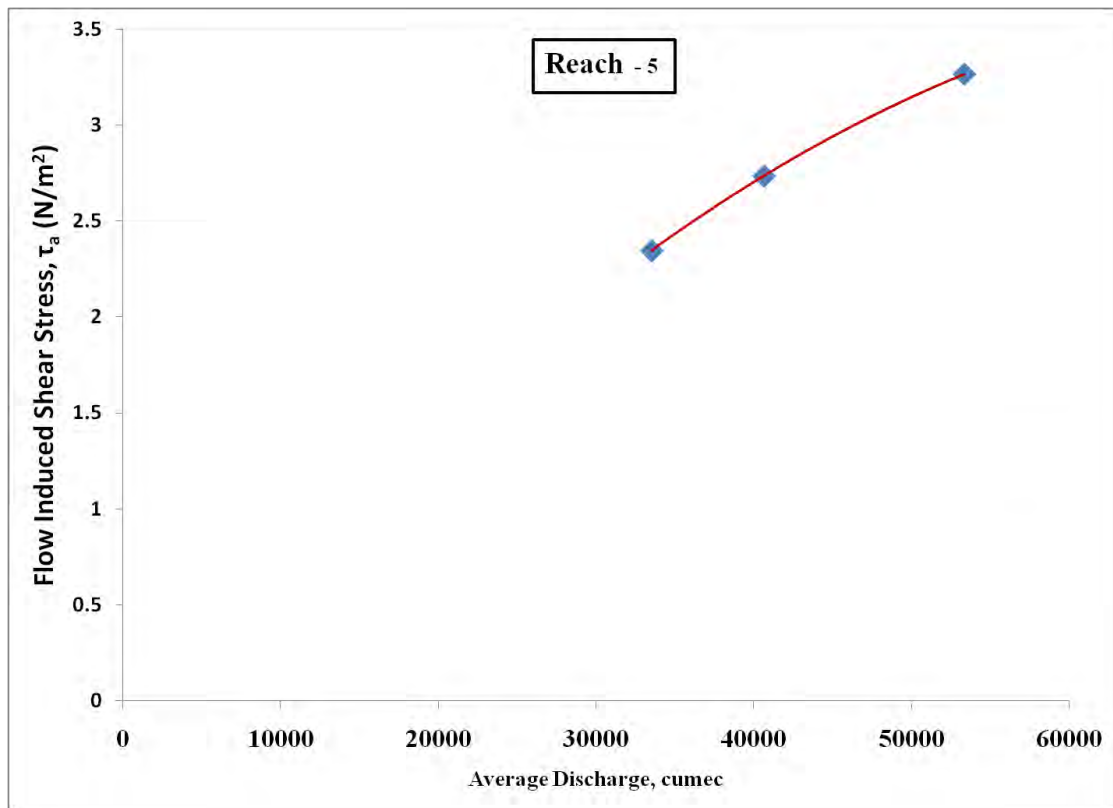


Figure 5.28 Correlation between τ_a and average discharge Tangail (Reach-5)

Furthermore, in addition to the satisfactory correlations between bank shear stress and average flow over the monsoon, it has provided a means to obtain simple bank erosion rate predictions that are linked directly to the flow discharge regime. The above illustrated relationships were next used to derive the erosion rate for the monsoon period of another hydrologic event (2013- flood event) using the developed 2-D model simulated discharge. Using the above illustrated relationships of τ_a and average flow discharge, τ_a for the respective reaches have been calculated. Then the erosion rates have been calculated using the preceding formulae. The predicted erosion rates were evaluated by comparing bank erosion rates derived from the correlation with those estimated by remotely sensed imagery. A comparison of predicted versus observed erosion rates has been presented in Figure 5.29. It is evident from the figure that observed and predicted erosion rates fall very close to the 1:1 line for four out of five erosion prone reaches.

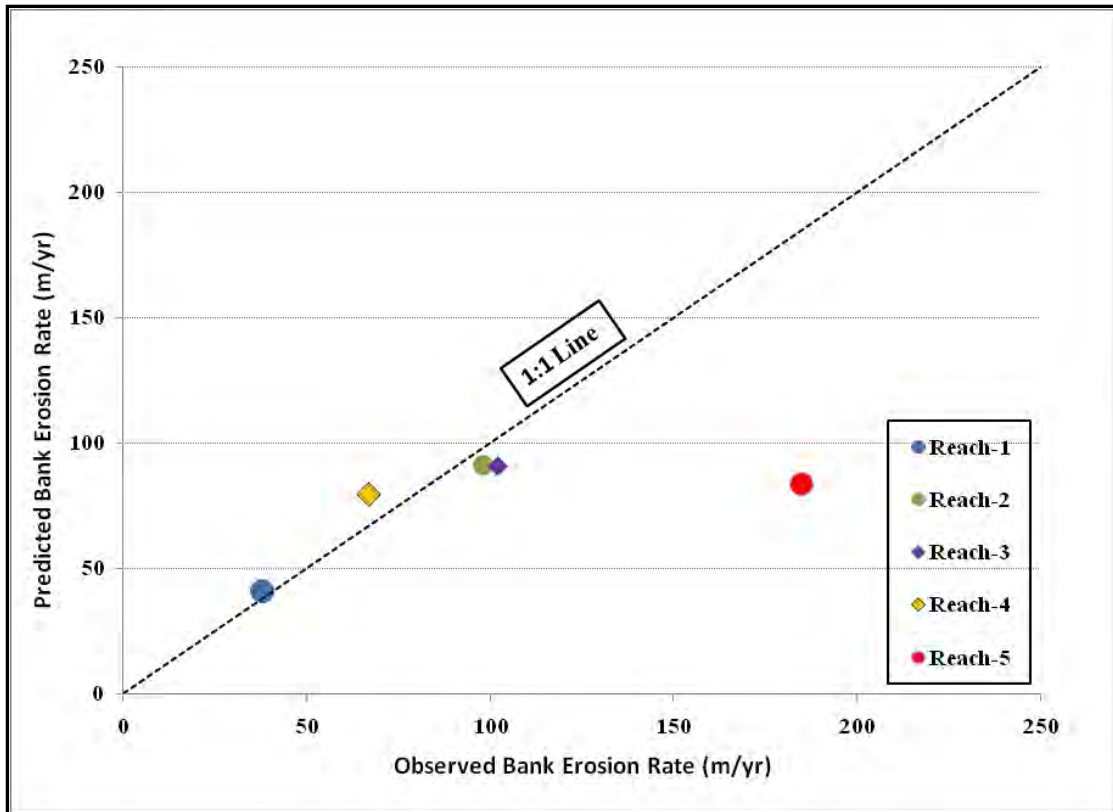


Figure 5.29 Comparison of predicted and observed bank erosion rates at the selected reaches

5.4 Summary

The summary of results extracted from different simulations has been depicted in Table 6.1.

Table 5.1 Summary results for different reaches

Reach ID	Parameters	2005		1998	
		With Structure	Without Structure	With Structure	Without Structure
Reach-1	Maximum Velocity (m/s)	1.52	1.36	1.42	1.60
	Structure Induced Scour (m)	0.80		5.0	
	Maximum Erosion (m)	-	95	-	82
Reach-2	Maximum Velocity (m/s)	2.05	2.15	2.15	2.20
	Structure Induced Scour (m)	1.65		2.30	
	Maximum Erosion (m)	-	130	-	190
Reach-3	Maximum Velocity (m/s)	2.25	2.32	2.42	2.48
	Structure Induced Scour (m)	1.0		1.80	
	Maximum Erosion (m)	-	130	-	146
Reach-4	Maximum Velocity (m/s)	2.15	2.28	2.02	2.41
	Structure Induced Scour (m)	1.60		4.0	
	Maximum Erosion (m)	-	125	-	160
Reach-5	Maximum Velocity (m/s)	2.26	2.39	2.58	2.5
	Structure Induced Scour (m)	3.64		10.0	
	Maximum Erosion (m)	-	50	-	66

CHAPTER 6

CONCLUSIONS AND RECOMMENDATIONS OF THE STUDY

6.1 General

Understanding the bank erosion processes of Jamuna River is the pre-requisite to pragmatic erosion management. To get familiar with such complex process two-dimensional morphological model has been a useful tool. In this regard a two dimensional morphological model MIKE 21C has been utilized to evaluate the feasibility of introducing revetments as structural intervention along five erosion prone reaches in five districts under the study area. Besides a correlation between average discharge prevailing during monsoon and shear stress applied by the flow has been established to estimate the erosion rate from average discharge.

6.2 Conclusions of the Study

The following conclusion can be drawn after summarizing the present study-

- a. In general magnitude of near bank velocity gets reduced after the introduction of revetments along the erosion prone reaches.
- b. Oblique flow was noticed in some of the erosion prone reaches rendering the reaches more susceptible to bank erosion.
- c. The proposed structure-induced bed scour may vary from 0.80 m to 10 m. Scour estimates have been mentioned excluding the local scour; i.e., the corresponding scours are the outcomes of structural interventions along those reaches.
- d. Based on the results of the two-dimensional morpho-dynamic model MIKE21C, the river training work structures proposed in this study do not cause significant changes in the short term (one flood season) hydro-morphology of the selected reach of Jamuna River.
- e. Revetment type of bank protection measures introduced in this study executes satisfactory performance in restraining the possible bank erosion along the Jamuna River.

Besides the extent of erosion in the adjacent reaches also gets reduced in most of the cases due to such interventions.

f. The use of correlation of river discharge and shear stress in estimating the erosion rate experienced by the reach after the passage of monsoon 2013 using average discharge was satisfactory for four out of five reaches.

6.3 Recommendations of the Study

a. Since MIKE 21C is a rigid boundary model, the banklines of the model cannot adapt with the continuously changing banklines. Therefore models using flexible boundary may be incorporated for further study.

b. Effect of revetment type of bank protection measures have been studied in this thesis work. Impact of implementing other bank protection measures like spurs, groynes may be studied in future.

c. Effect of bank protection measures on long-term morphology of river has not been studied; long term effects can be studied in further studies.

d. The correlation between flow induced shear stress and river discharge has been established for five reaches. To get a better insight more reaches may be considered for further studies.

e. Alignment of the proposed structures may not follow that of the existing banklines as it corresponds to post monsoon bankline of 2011. It is strongly recommended to use the model that corresponds to most recent field condition and assess the impact of the proposed structures prior to implementation.

f. Study on effect of human interventions like dredging, introduction of closures etc. on bank erosion process may be carried out in further studies.

References

- Andres D.M., Kamal A.R., 2014: Modelling River Bank Erosion Processes and Mass failure Mechanisms using 2-D depth averaged numerical model, *Geophysical Research Journal*, v. 16, EGU 2014-10857.
- Annandale G.W., Parkhill D.L., 1995: Stream bank erosion: application of the erodibility index model. *Proc.1stInt.Conf. on Water Resources Engineering*, ASCE, New York, 2, 1570-1574.
- Ariathurai R., Arulanandan K., 1978: Erosion rates of cohesive soils. *Journal of Hydraulic Division*, 104, 279-283.
- ASCE 2007: *Sedimentation Engineering, Part 1: Processes, Measurements, Modeling and Practice*”, ASCE Manuals and Reports on Engineering Practice No.-110.
- Azim A.F., Basak J.K., 2012: Effects of River Bank Erosion on Livelihood, Prepared for Unnayan Onneshan, p. 6-12.
- Bahar, S.M.H., Fukuoka, S. 2002: Study of Cohesive Riverbank Erosion Mechanism Through Analysis at Flow Fields Near and Inside Eroded Bank, *Annual Journal of Hydraulic Engineering, JSCE*, Vol:46, pp 749-754.
- CEGIS, 2013: Prediction of Erosion along Jamuna River, Technical Report prepared for Bangladesh Water Development Board.
- Delft Hydraulics and DHI, 1996: Morphological Processes in Jamuna River, Special Report No. 24, River Survey Project (FAP-24), Prepared for WARPO, Bangladesh, p. 35
- Eric P. 2011: Bank Erosion in Alluvial Rivers With Non-Cohesive Soil In Unsteady Flow, Institute of River and Coastal Engineering, Hamburg University of Technology.
- Formann H., Heberseck S., Schober F., 2007: Morphodynamic River Processes and Techniques for River Assessment of Channel Evolution in Alpine Gravel Bed Rivers, *Journal of Geomorphology*, v. 90, p. 340-355.
- Grissinger E.H., 1982: Bank erosion of cohesive materials. In R.D.Hey, J.C.Bathurst and C.R.Thorne (eds), *Gravel-bed Rivers*, Wiley, Chichester, 273-287.
- Hasnataye, 2013: Recent Study on Riverbank erosion on Jamuna River.

Hiroshi T., Fujita M. 2012, Numerical Model of Bank Erosion process of rivers in Wetland, 9th ISE, Vienna.

Izumi N., Kovacs A., Parker G., Leuthe D.P., 1991: Experimental and Theoretical Studies on Bank Erosion in Rivers and its Prevention by Low-cost Means, Project Report No. 320, University of Minnesota, Minneapolis, Minnesota.

Jagers B.(2003). "Modeling Planform Changes of Braided Rivers", Ph.D. thesis, Delft University.

Jagers, 2008: Modeling Planform Changes of Braided Rivers, Ph.D. Thesis, University of Twente, Netherlands.

Lawler. D.M., Coupertwaith J., Bull L.J., Harris N.M. 1997: Bank Erosion Events and Processes in Upper Severn Basin, Hydrology and Earth System Sciences, Volume-1, Issue-3, Page 523-534.

Locey D.B., 2006: Natural Processes affecting Bank Erosion, an update to Engineered Solution to Bank Erosion, Monthly Report for April, Maine Geological Survey, Department of Agriculture, Conservation and Forestry, Maine.

Mohammad F., Honarbacks F. 2012, River Channel Change Simulation of Khoshke Rud Farsan River and Bank Erosion Process Using a Numerical Depth Averaged Model, CCHE2D, Iranica Journal of Energy and Environment 3 (4): pp- 299-306.

Mosselman E., 2005: Morphological modeling of Rivers with Erodible Banks, Journal of Hydrological Processes, v. 12, p. 1357-1370

Mosselman, E. 1998: Morphological modelling of rivers with erodible banks, Hydrological, Processes, Vol.12, No.8, pp.1357-1370.

Nasreen I., Amirul H., 2003: Quantification of Erosion Patterns in the Jamuna-Brahmaputra River using GIS and Remote Sensing Techniques, Hydrological Processes, v. 17, p. 959-966.

Nazneen A., 2013: Historical Trend of Bank Erosion along the Braided River Jamuna, International Journal of Sciences: Basic and Applied Research, v. 11, no. 1, p. 173-180.

Pahlowan E., 2015: Jamuna River Erosional Hazards- A Remote Sensing & GIS Approach.

Patrick K.P., 1998: Understanding and Evaluating Erosion Problems, prepared by Woodward Clyde Consultants, Anchorage, Alaska for Department of Community and Regional Affairs, Alaska, p. 3-15

Sainath P.A., Shashikanth L., 2012: River Change Detection and Bank Erosion Identification using Topographical and Remote sensing Data, International Journal of Applied Information Systems, v. 2, p. 45-56.

Sarker M.H., Akter N., Ahmed S., Mahmud F., Akter J., 2007: Long-term Bank Erosion Processes of Jamuna River, prepared by CEGIS for Jamuna-Meghna River Erosion Mitigation Project of Bangladesh Water Development Board.

Sarker M.H., Akter N., Noor F., Bhuiyan N.M., 2010: Long-term Erosion Processes of Ganges River, Prepared by CEGIS for Jamuna-Meghna River Erosion Mitigation Project of Bangladesh Water Development Board.

Stephen D., Andre A., 2002: Numerical simulation of Bank Erosion and Channel Migration in meandering Rivers, Water Resources Research, v. 38, no. 9, p. 208-214.

Thorne, C.R. (1982). Processes and mechanisms of river bank erosion, in: Hey, R.D., Bathurst, J.C., Thorne, C.R. (Eds), Gravelbed Rivers, Wiley, Chichester, 227-271.

University of Minnesota (1991), “ Experimental and theoretical studies on bank erosion in rivers and its prevention by low-cost means “, Project Report No.320.

Watson A.J., Basher L.R., 2006: Stream Bank Erosion; A Review Process of Bank Failure, Measurement and Assessment Techniques and Modeling Approaches, Manaki Whenua Landcare Research, prepared for Stakeholders of Motueka Integrated Catchment Management Programme and the Raglan Fine Sediment Study.

APPENDIX

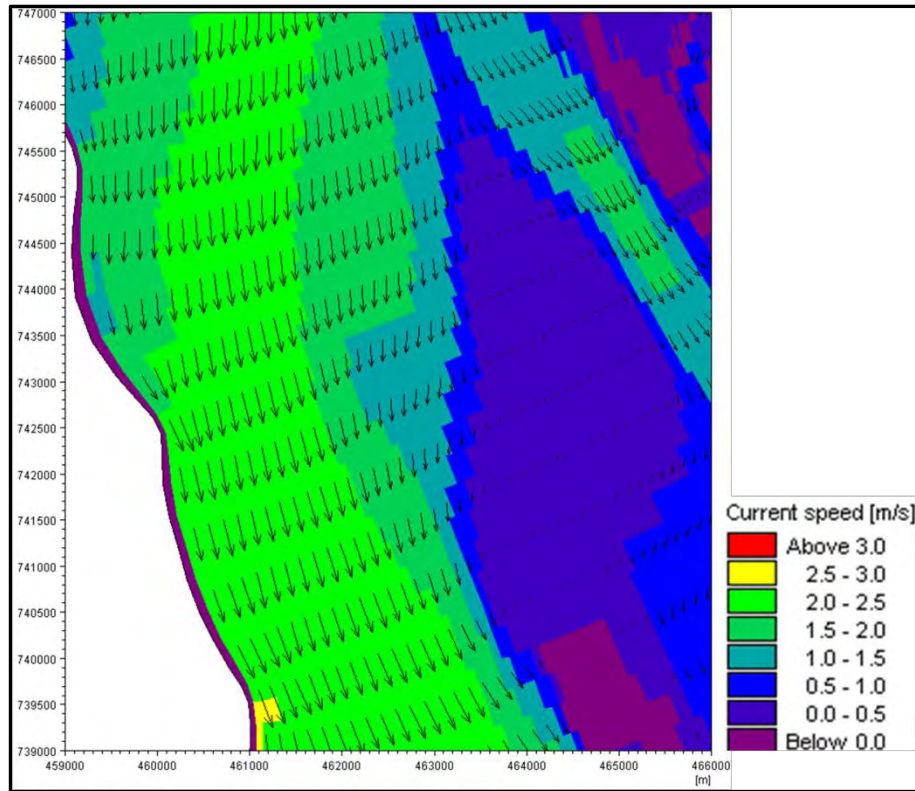


Figure A.1 Simulated velocity contour of the Jamuna during peak of the monsoon near Reach-2 under base condition for average flood event (2005)

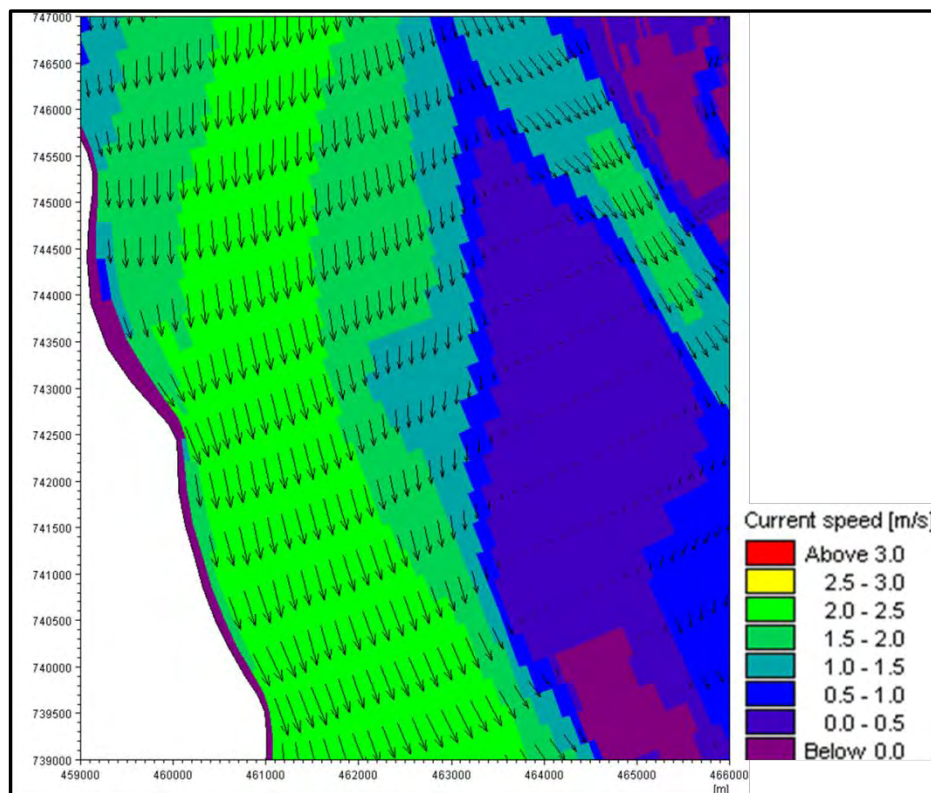


Figure A.2 Simulated velocity contour of the Jamuna during peak of the monsoon near Reach-2 with proposed revetment for average flood event (2005)

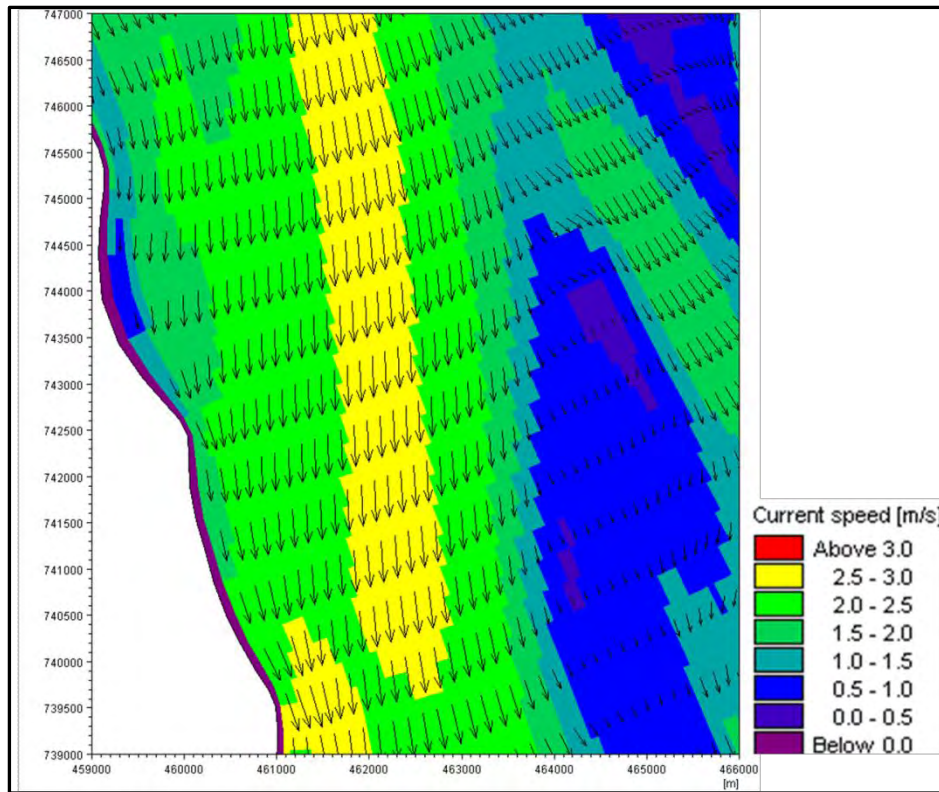


Figure A.3 Simulated velocity contour of the Jamuna during peak of the monsoon near Reach-2 under base condition for 100 year flood event (1998)

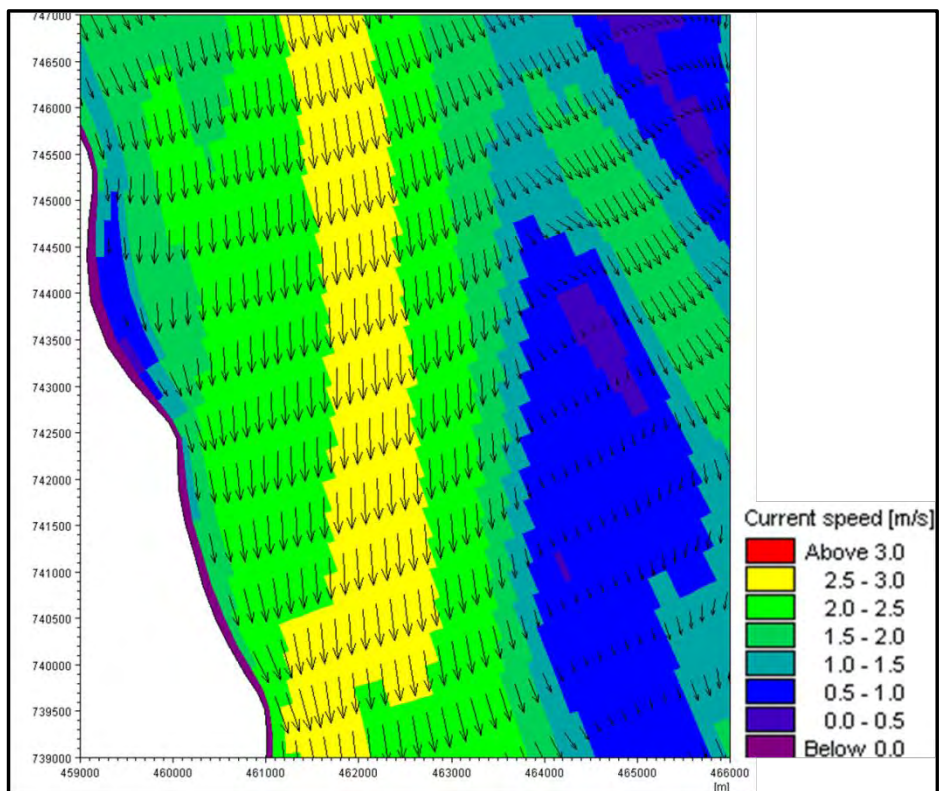


Figure A.4 Simulated velocity contour of the Jamuna during peak of the monsoon near Reach-2 with proposed revetment for 100 year flood event (1998)

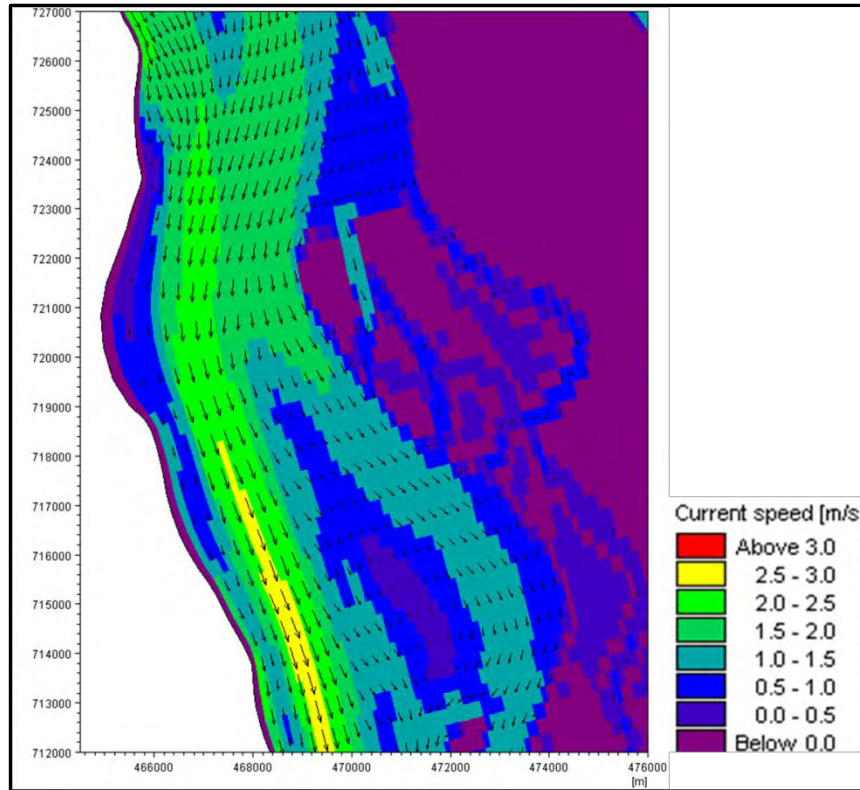


Figure A.5 Simulated velocity contour of the Jamuna during peak of the monsoon near Reach-3 under base condition for average flood event (2005)

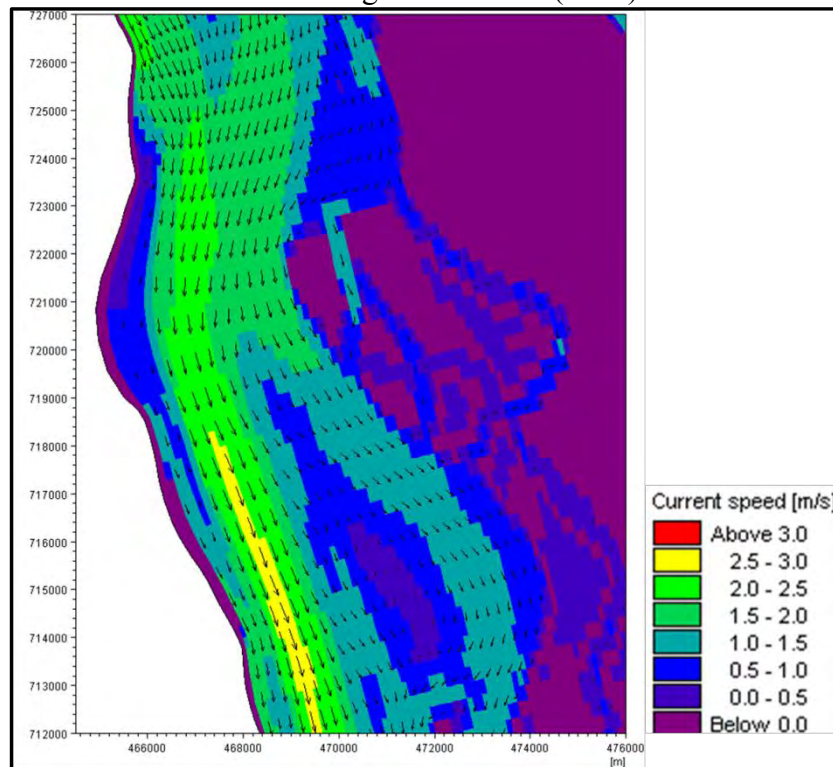


Figure A.6 Simulated velocity contour of the Jamuna during peak of the monsoon near Reach-3 with proposed revetment for average flood event (2005)

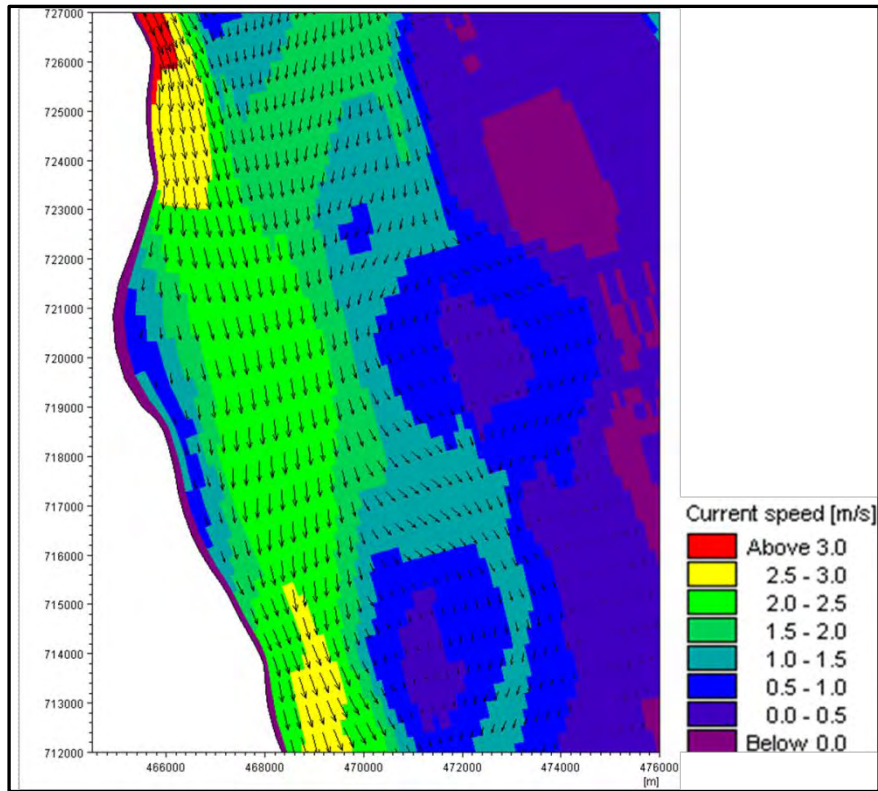


Figure A.7 Simulated velocity contour of the Jamuna during peak of the monsoon near Reach-3 under base condition for 100 year flood event (1998)

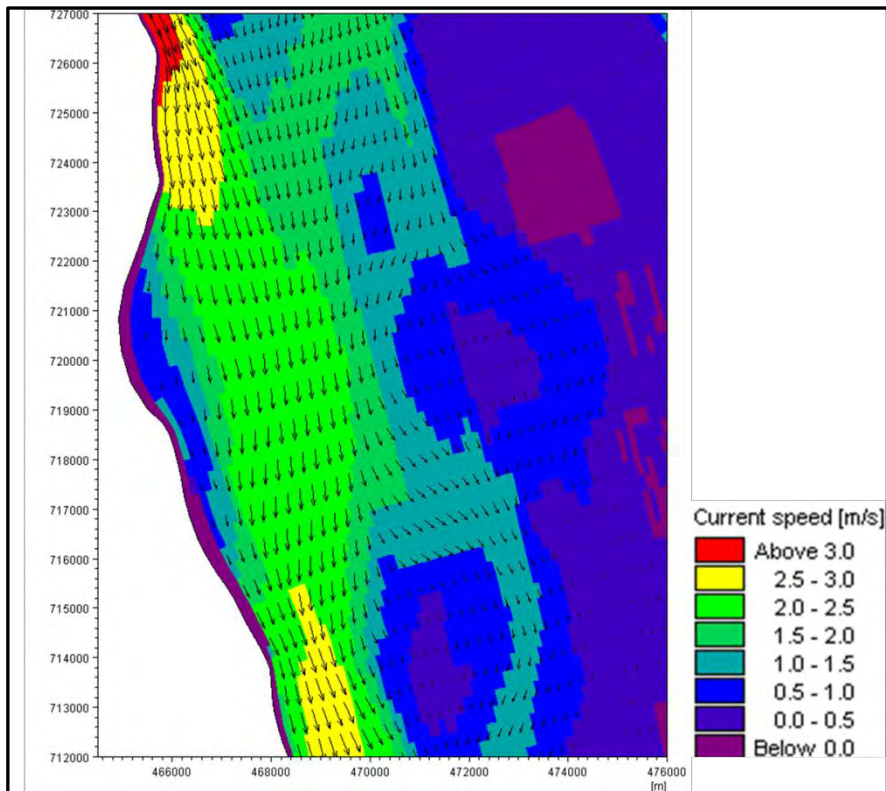


Figure A.8 Simulated velocity contour of the Jamuna during peak of the monsoon near Reach-3 with proposed revetment for 100 year flood event (1998)

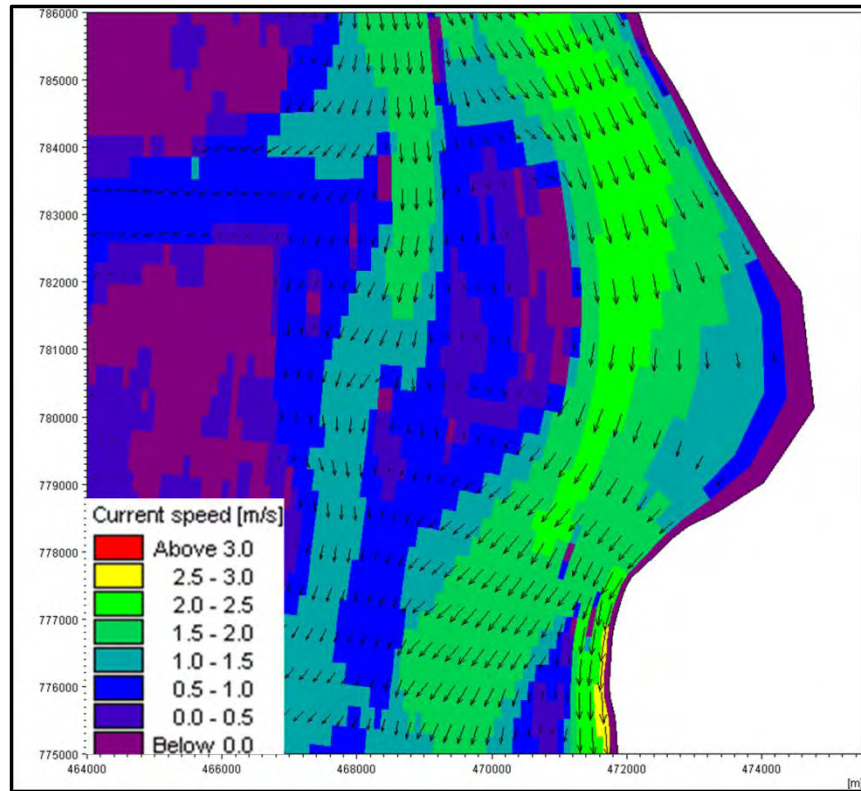


Figure A.9 Simulated velocity contour of the Jamuna during peak of the monsoon near Reach-4 under base condition for average flood event (2005)

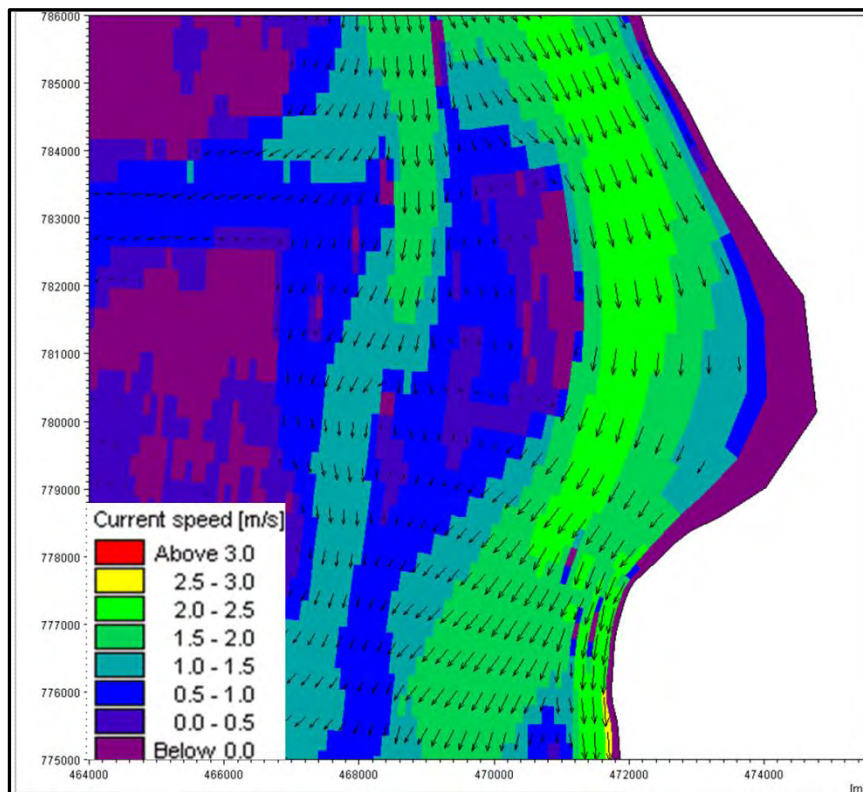


Figure A.10 Simulated velocity contour of the Jamuna during peak of the monsoon near Reach-4 with proposed revetment for average flood event (2005)

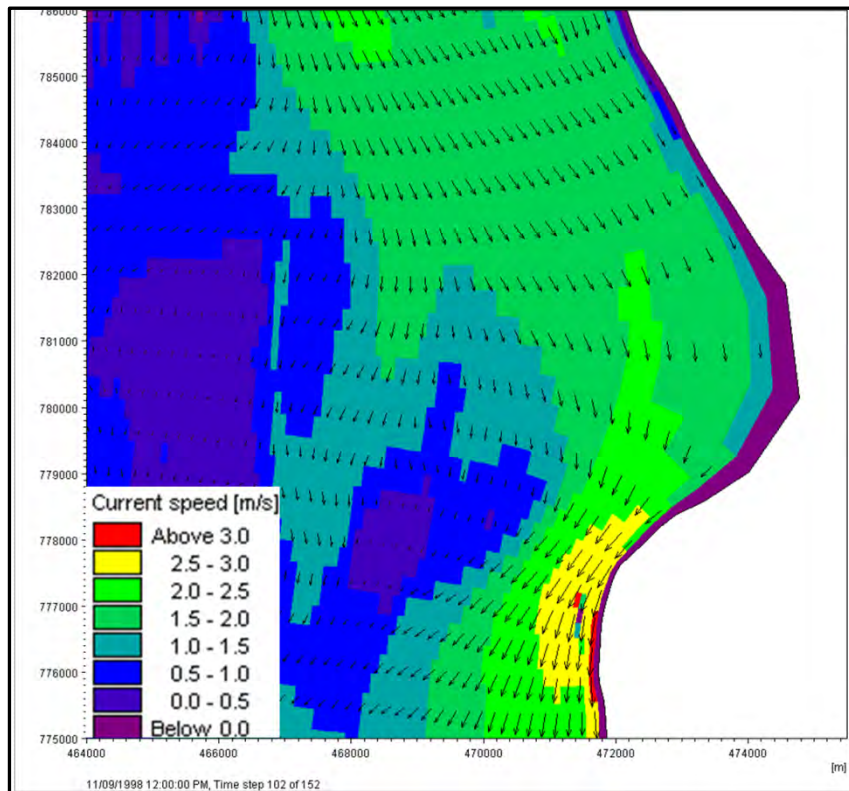


Figure A.11 Simulated velocity contour of the Jamuna during peak of the monsoon near Reach-4 under base condition for 100 year flood event (1998)

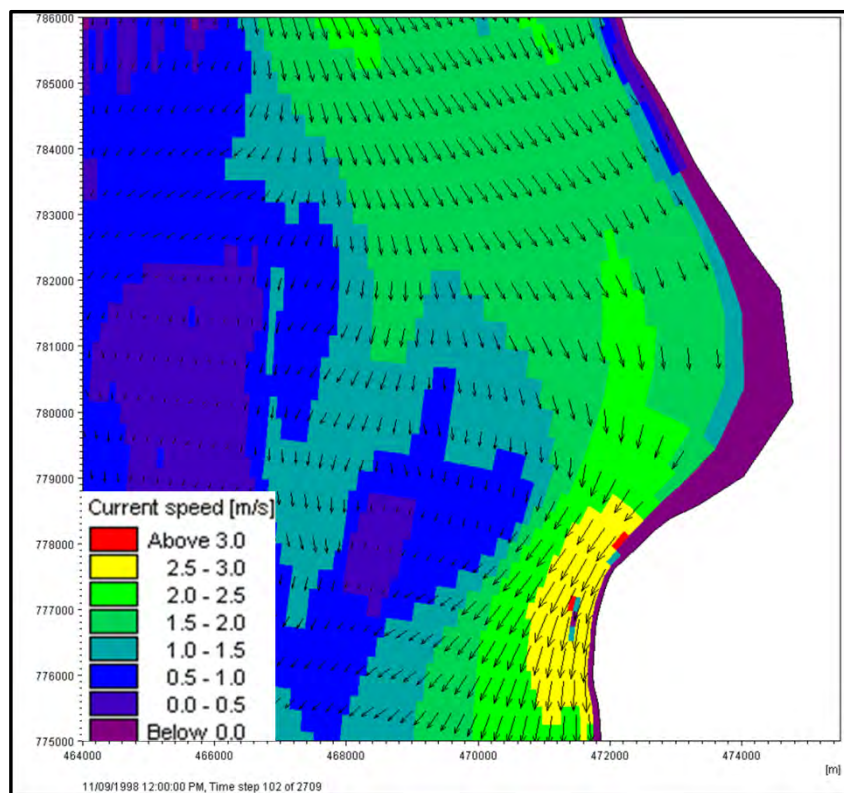


Figure A.12 Simulated velocity contour of the Jamuna during peak of the monsoon near Reach-4 with proposed revetment for 100 year flood event (1998)

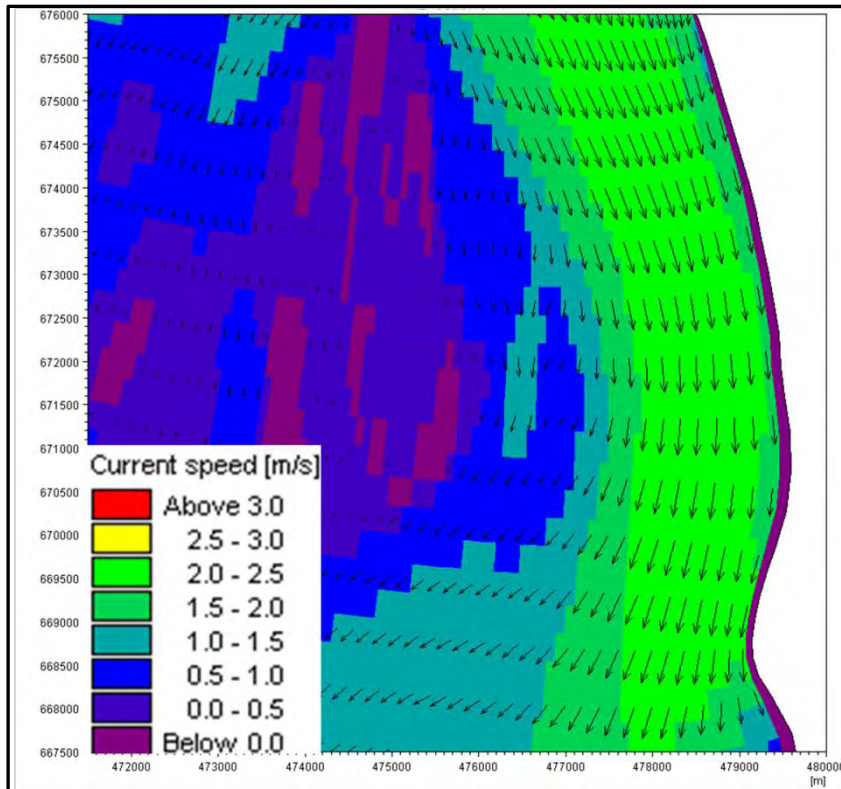


Figure A.13 Simulated velocity contour of the Jamuna during peak of the monsoon near Reach-5 under base condition for average flood event (2005)

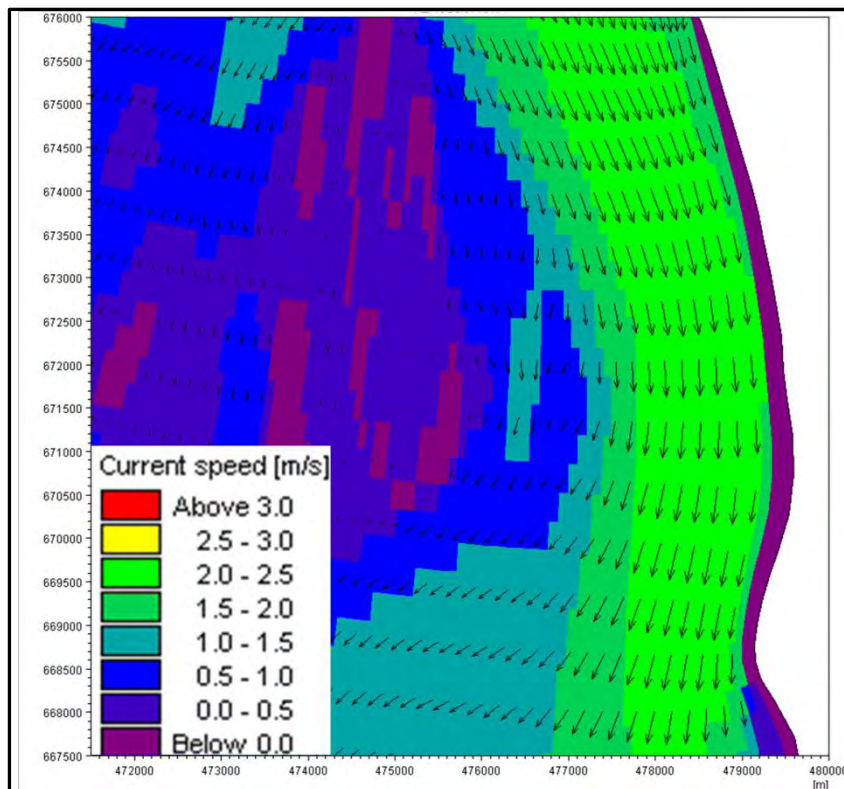


Figure A.14 Simulated velocity contour of the Jamuna during peak of the monsoon near Reach-5 with proposed revetment for average flood event (2005)

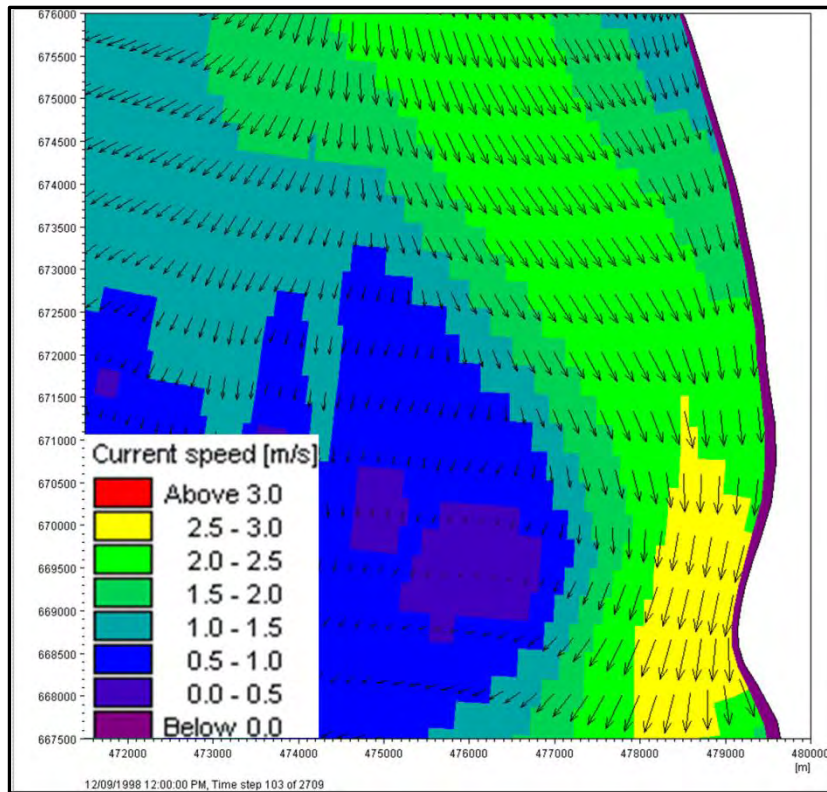


Figure A.15 Simulated velocity contour of the Jamuna during peak of the monsoon near Reach-5 under base condition for 100 year flood event (1998)

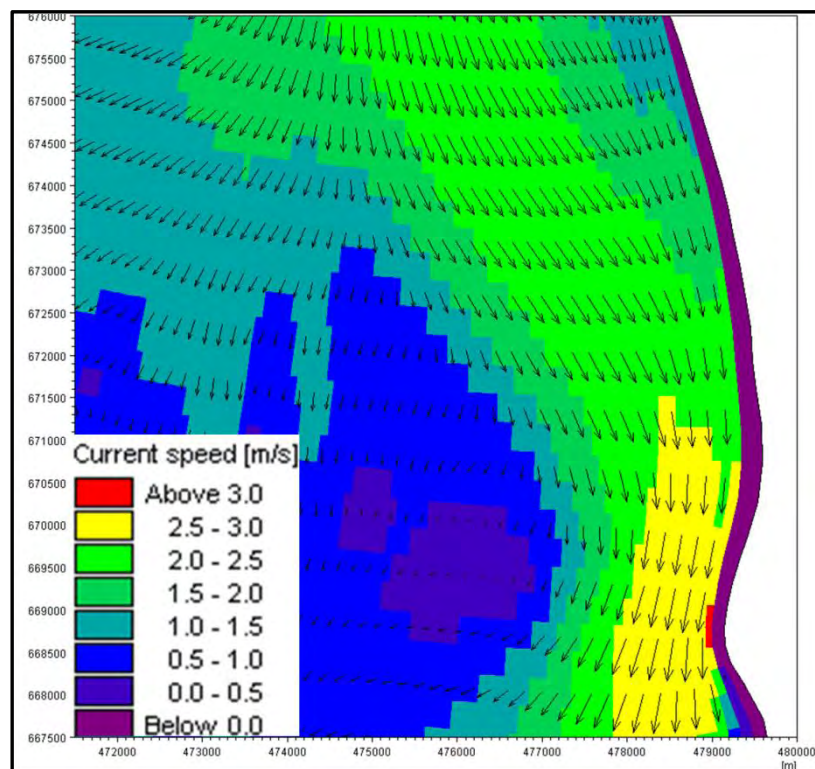


Figure A.16 Simulated velocity contour of the Jamuna during peak of the monsoon near Reach-5 under base condition for 100 year flood event (1998)

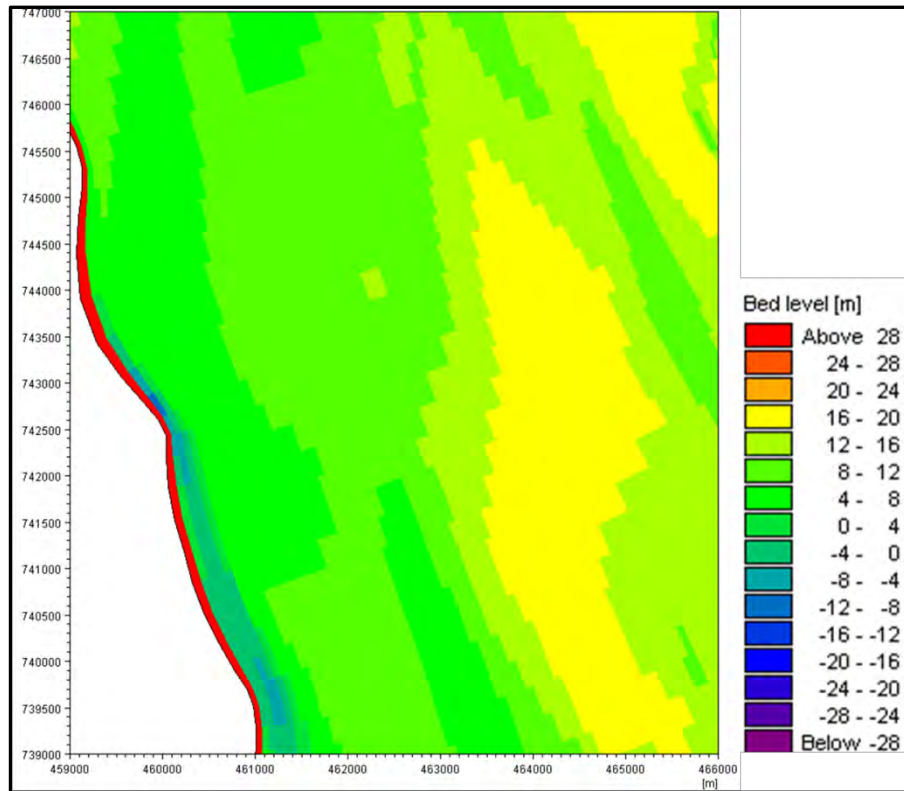


Figure A.17 Simulated bathymetry under base condition at Reach-2 at the end of monsoon for average flood event (2005)

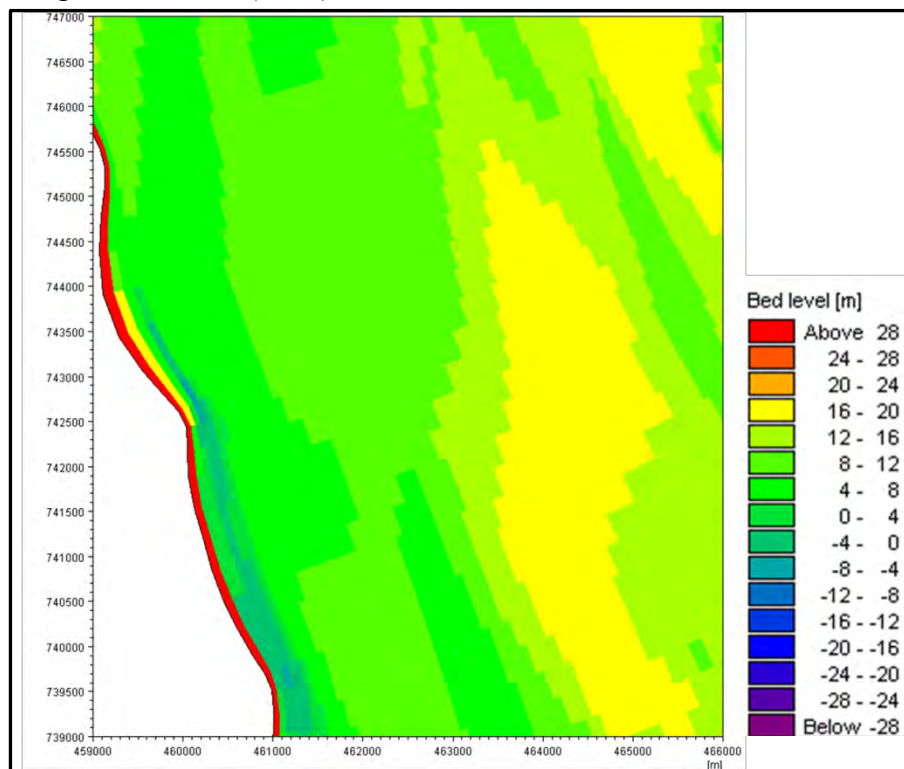


Figure A.18 Simulated bathymetry with proposed revetment at Reach-2 at the end of monsoon for average flood event (2005)

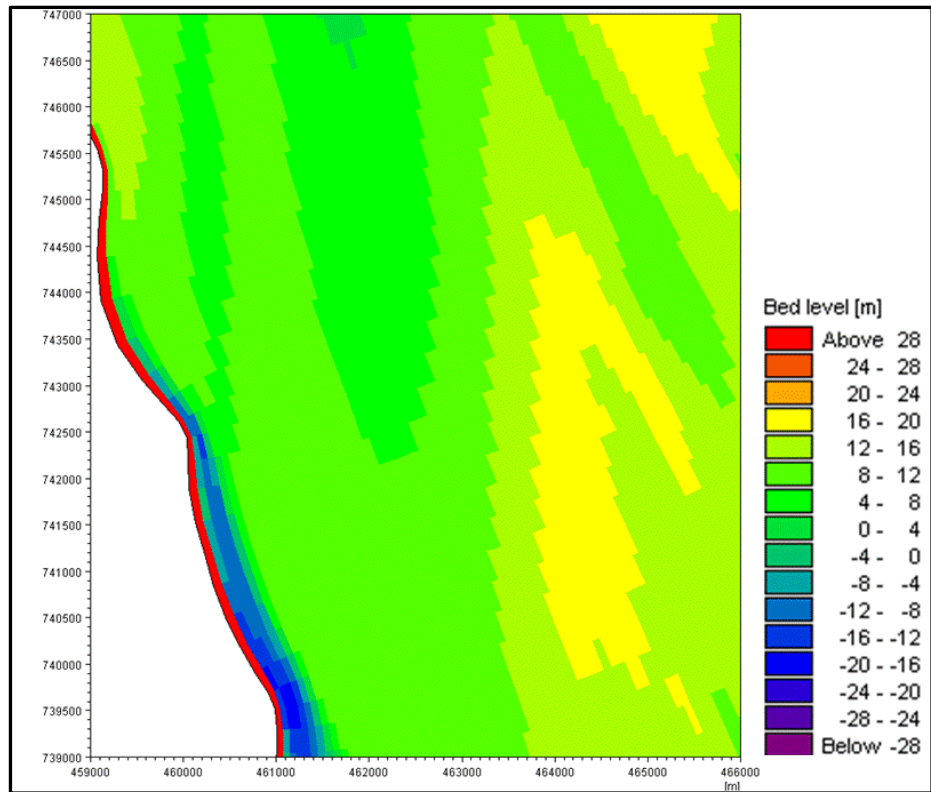


Figure A.19 Simulated bathymetry under base condition at Reach-2 at the end of monsoon for 100 year flood event (1998)

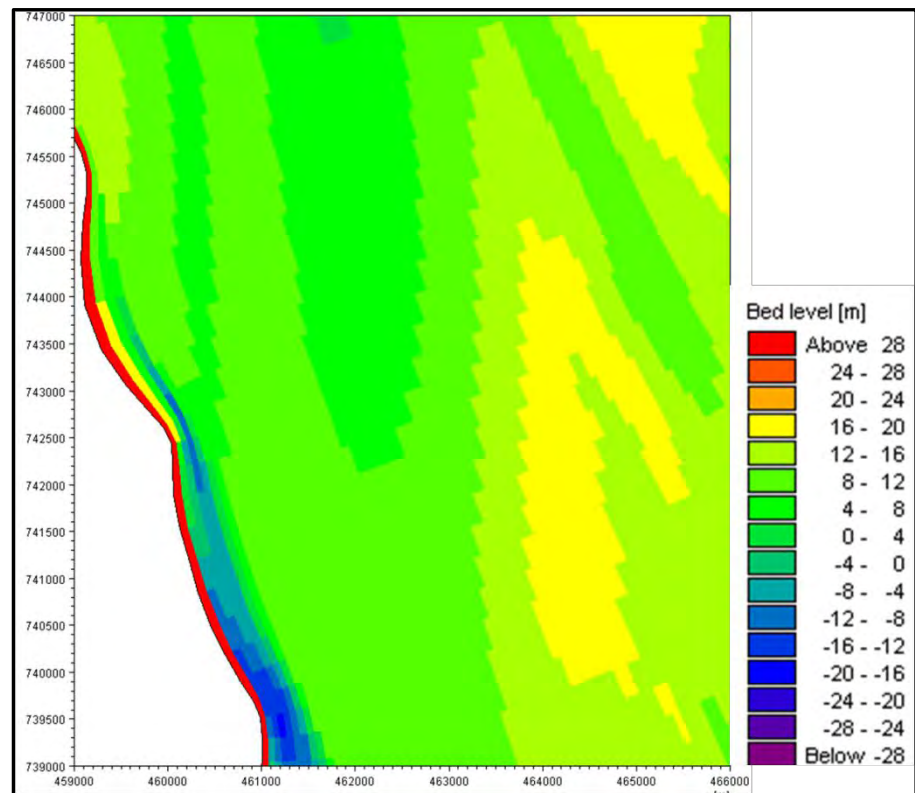


Figure A.20 Simulated bathymetry under base condition near Reach-2 at the end of monsoon for 100 year flood event (1998)

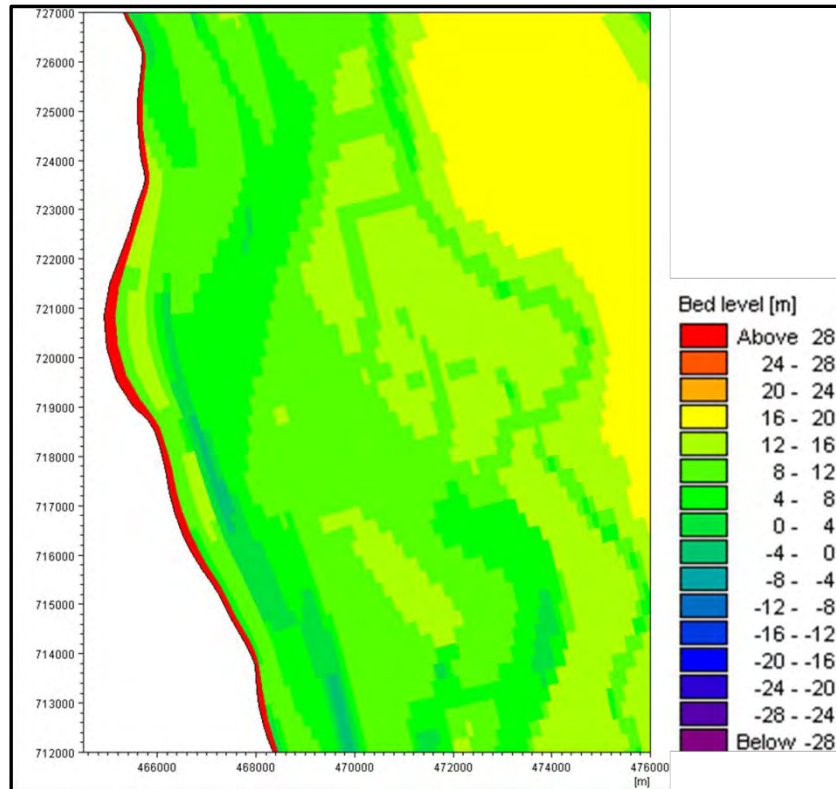


Figure A.21 Simulated bathymetry under base condition at Reach-3 at the end of monsoon for average flood event (2005)

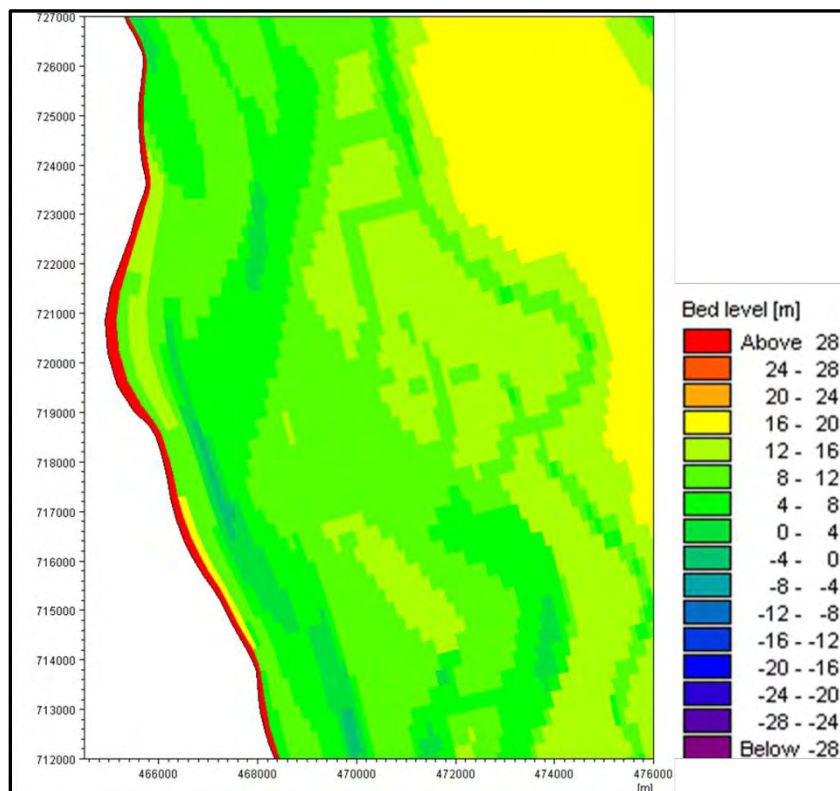


Figure A.22 Simulated bathymetry with proposed revetment at Reach-3 at the end of monsoon for average flood event (2005)

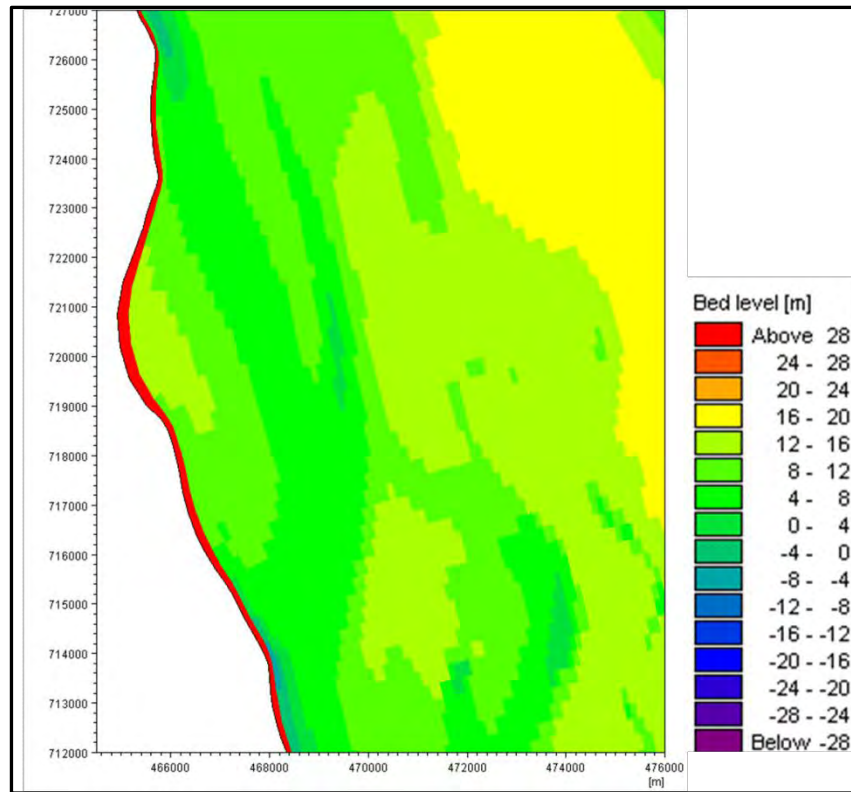


Figure A.23 Simulated bathymetry under base condition near Reach-2 at the end of monsoon for 100 year flood event (1998)

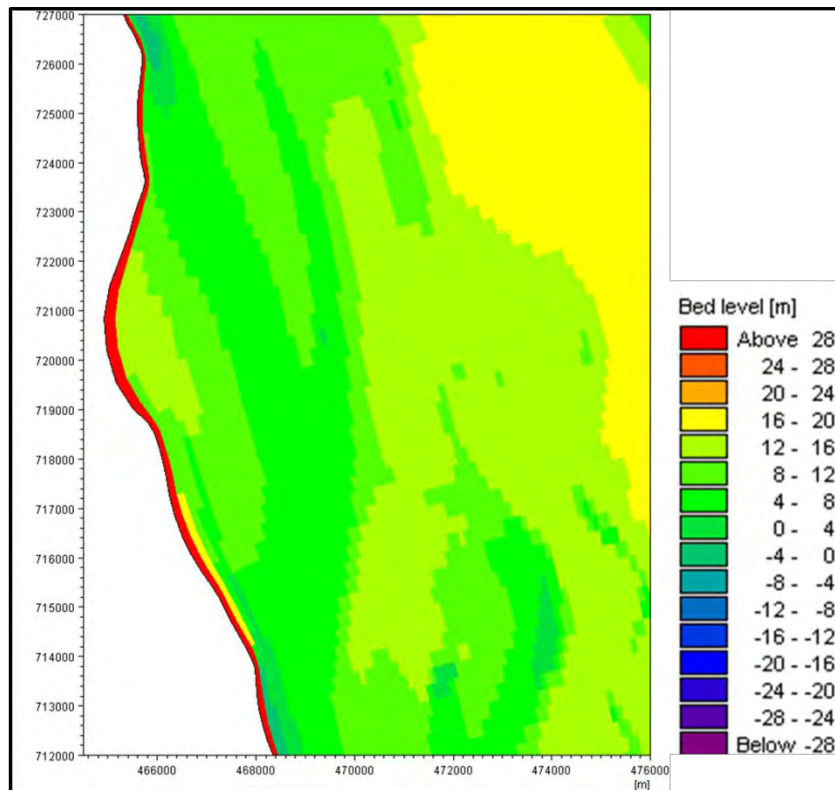


Figure A.24 Simulated bathymetry under base condition near Reach-3 at the end of monsoon for 100 year flood event (1998)

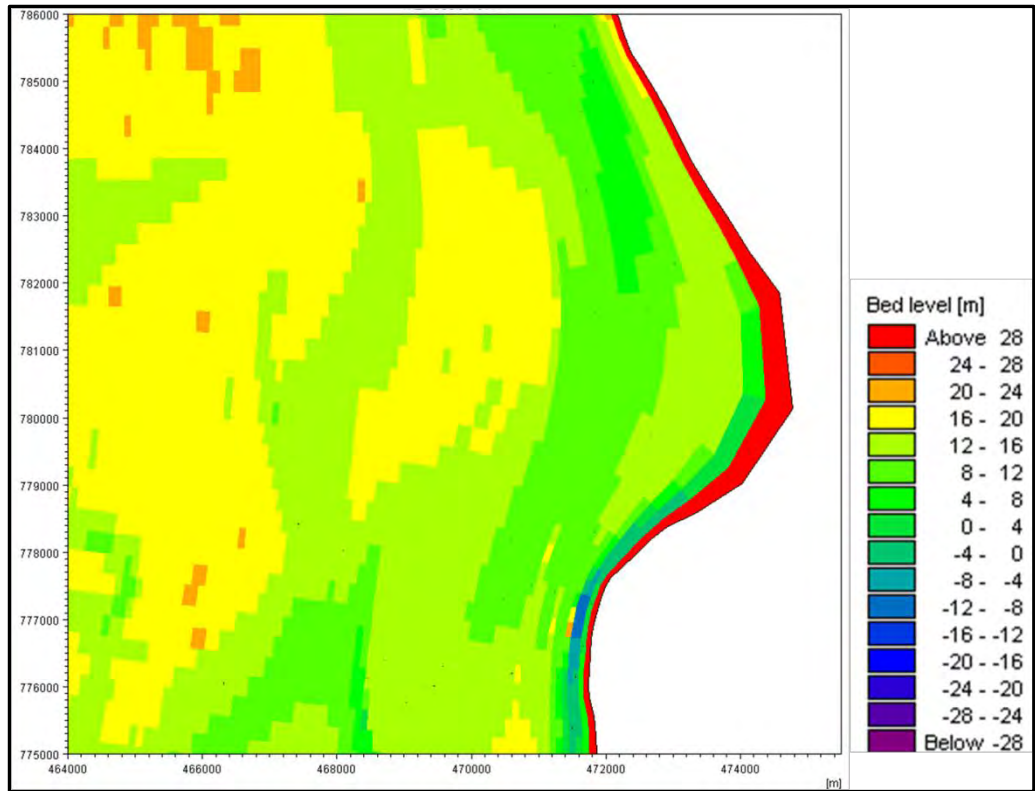


Figure A.25 Simulated bathymetry under base condition near Reacah-4 at the end of monsoon for average flood event (2005)

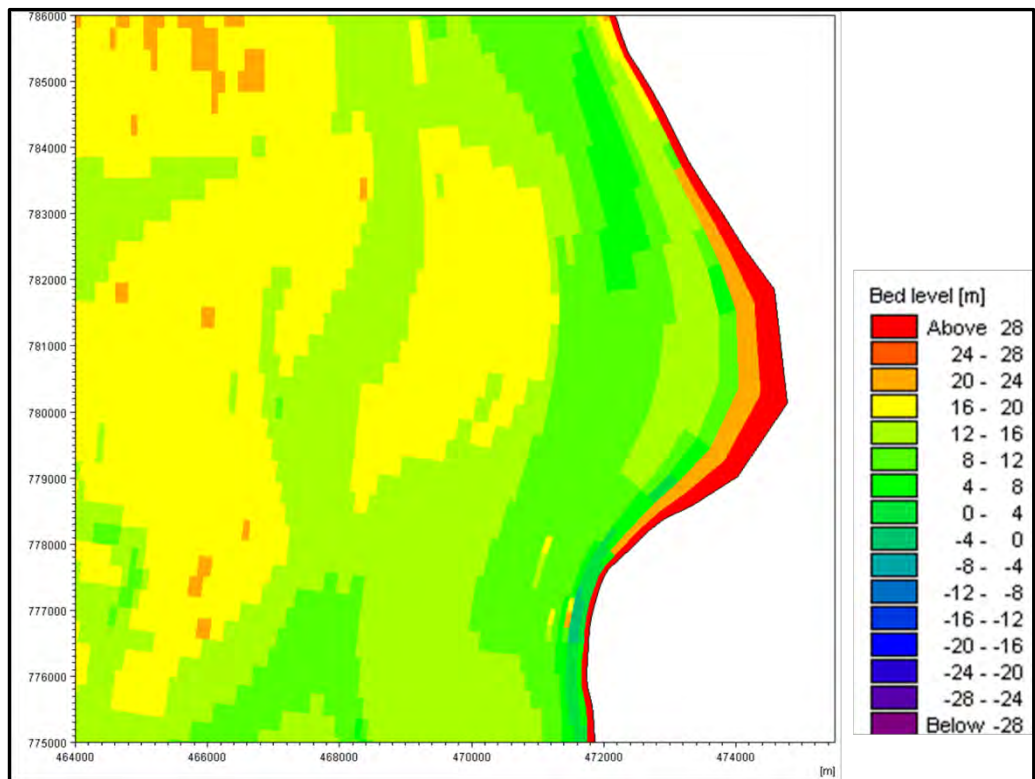


Figure A.26 Simulated bathymetry under base condition near Reacah-4 at the end of monsoon for average flood event (2005)

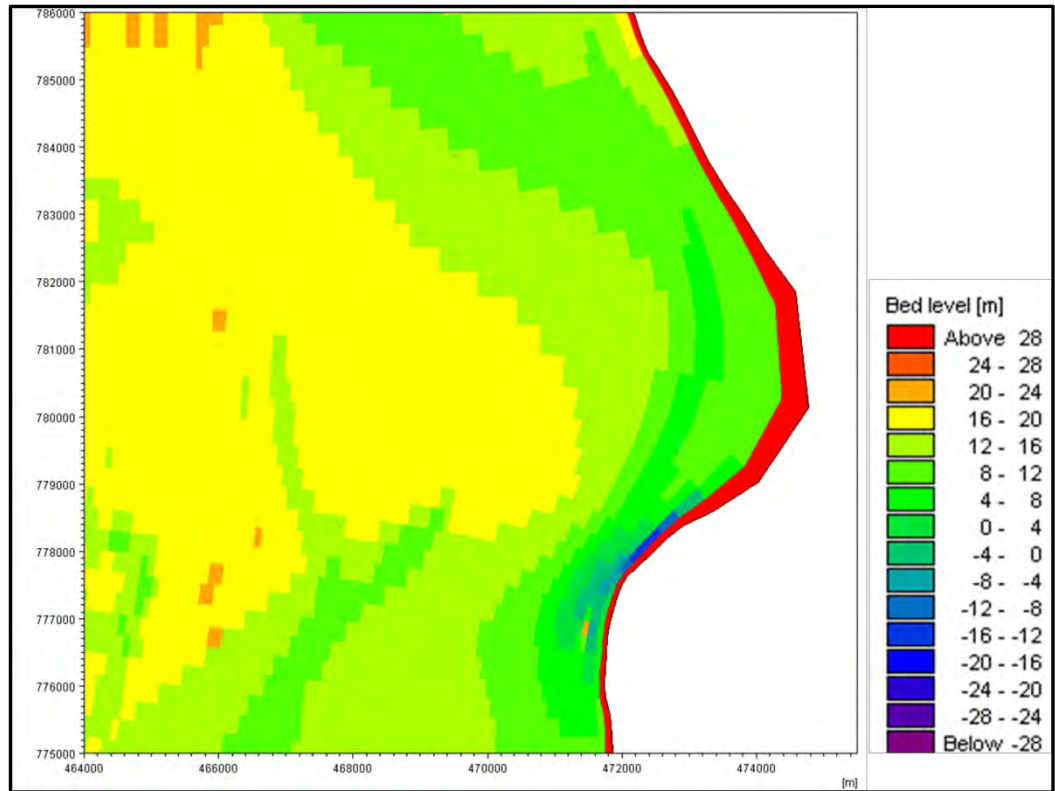


Figure A.27 Simulated bathymetry under base conditions near Reach-4 at the end of monsoon for average flood event (1998)

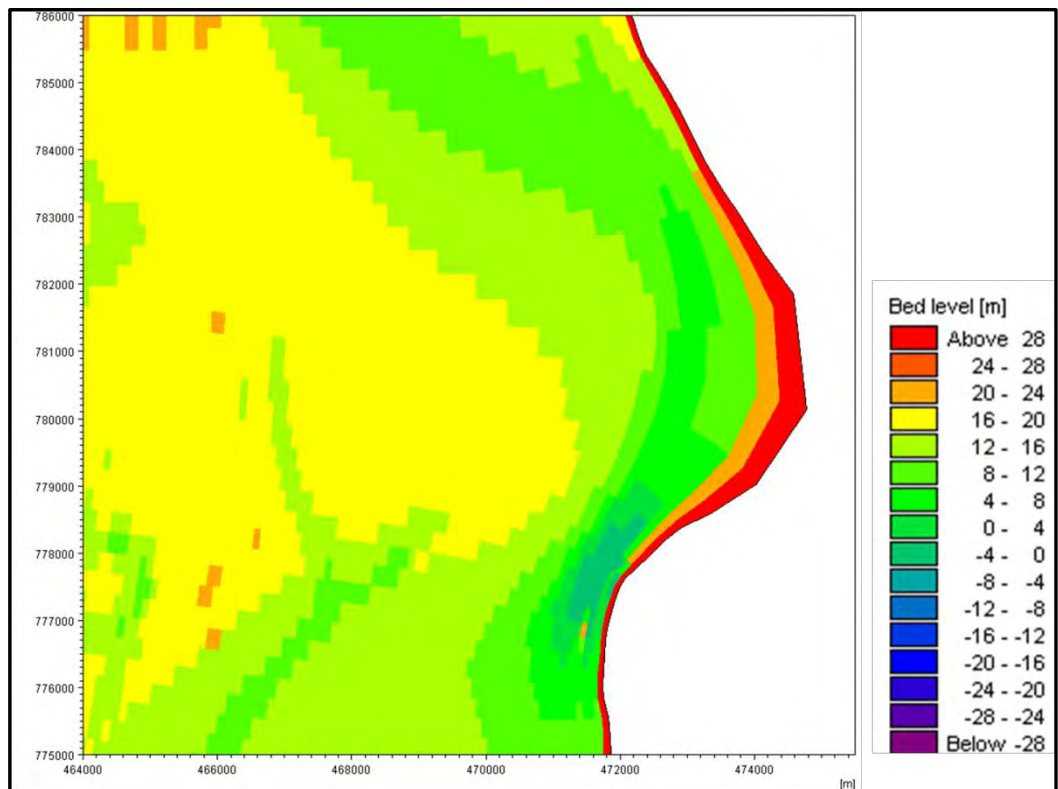


Figure A.28 Simulated bathymetry under base condition near Reach-4 at the end of monsoon for 100 year flood event (1998)

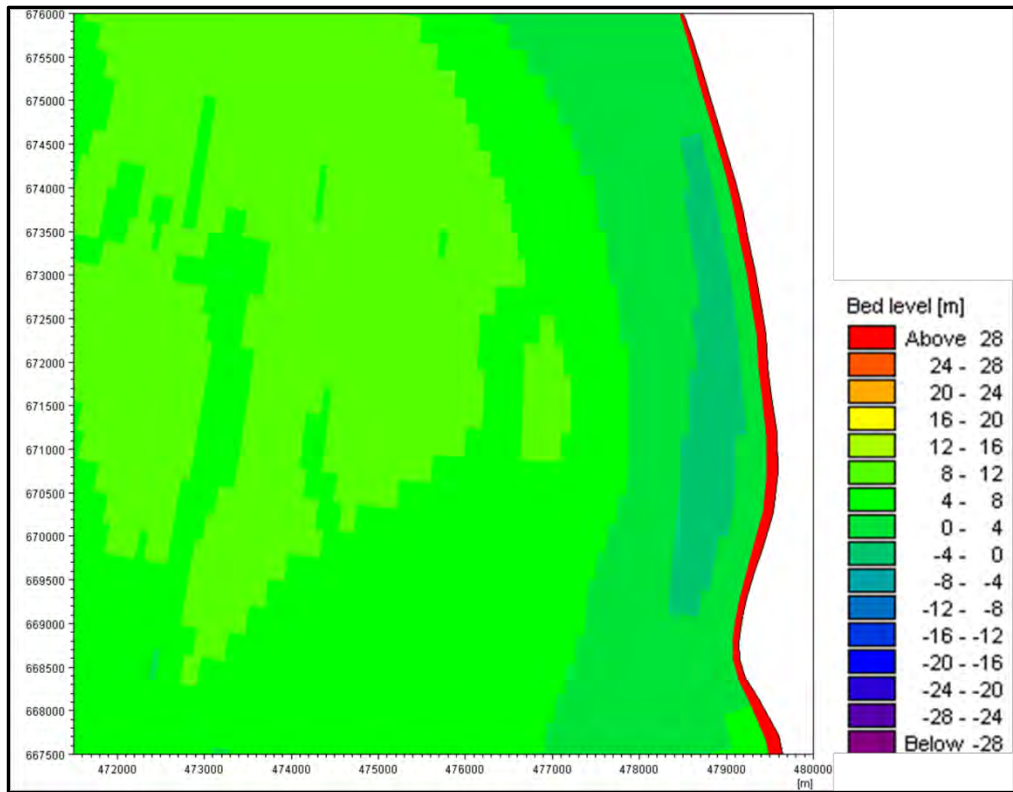


Figure A.29 Simulated bathymetry under base condition at Reacah-5 at the end of monsoon for average flood event (2005)

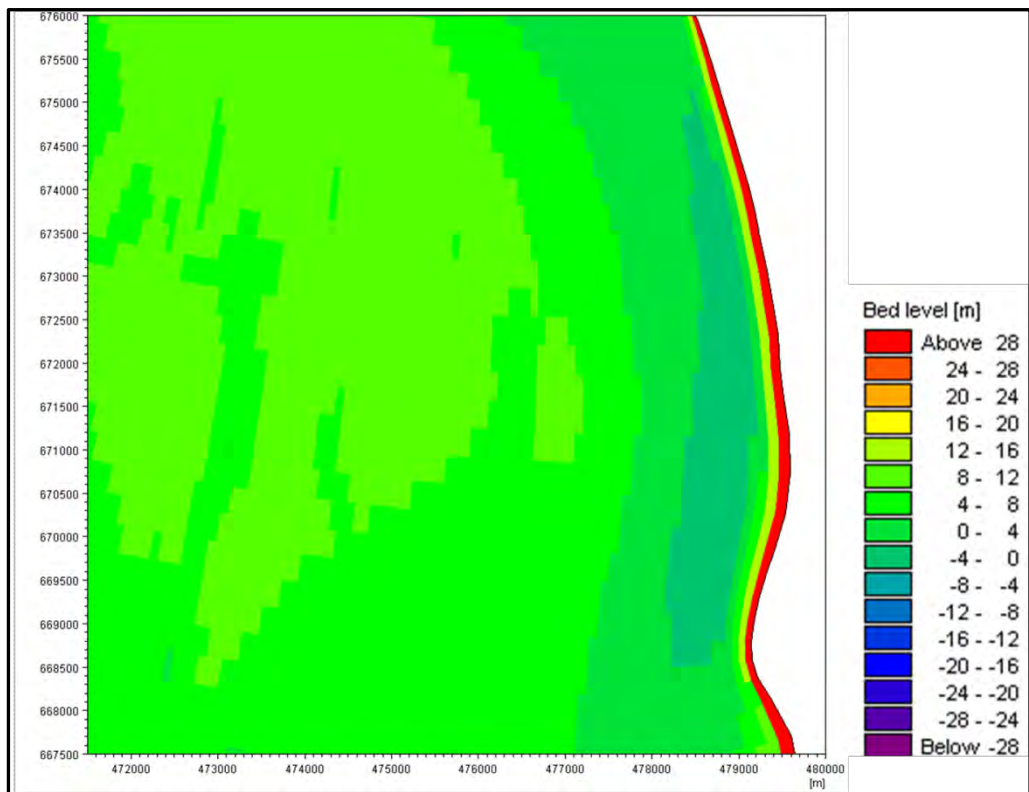


Figure A.30 Simulated bathymetry under base condition near Reacah-5 at the end of monsoon for average flood event (2005)

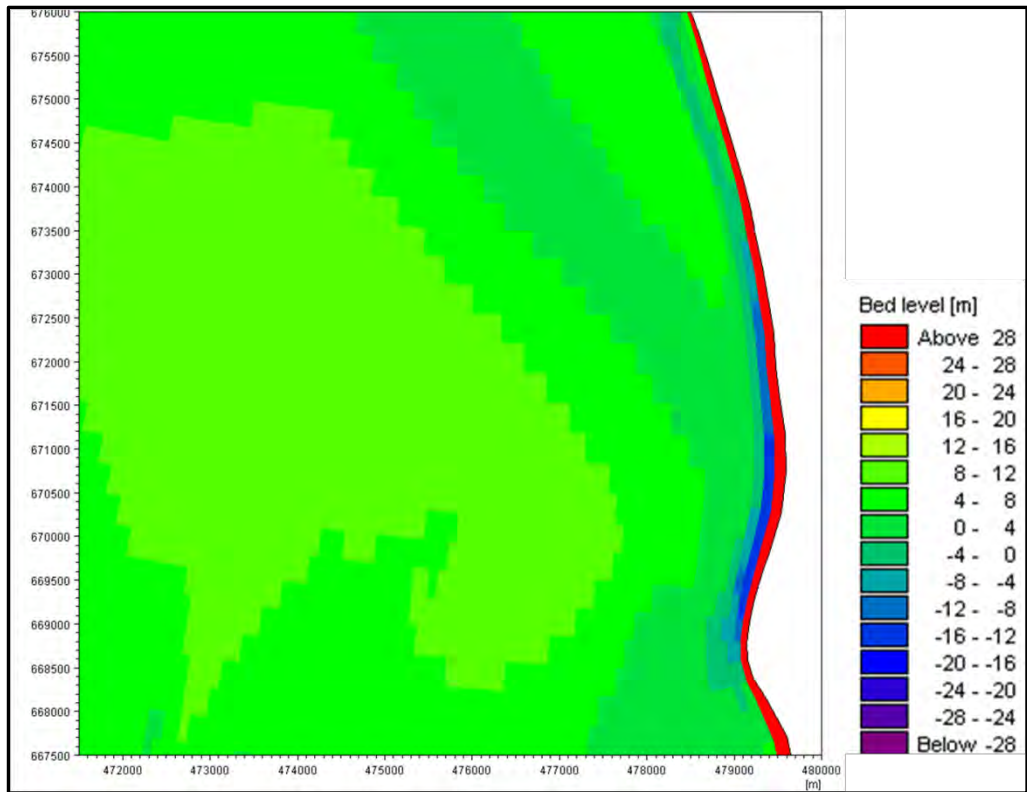


Figure A.31 Simulated bathymetry under base condition near Reach-5 at the end of monsoon for average flood event (1998)

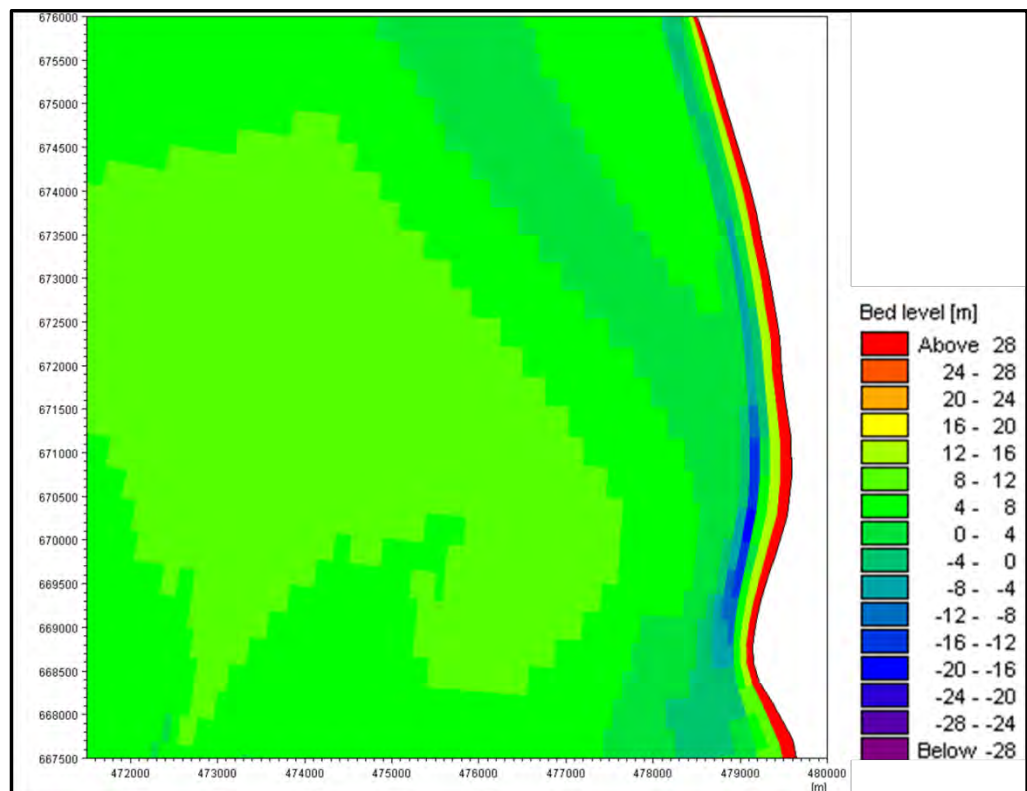


Figure A.32 Simulated bathymetry under base condition near Reach-5 at the end of monsoon for 100 year flood event (1998)